

***In vitro* Protein Engineering Approaches for the Development of Biochemical, Diagnostic and Therapeutic Tools**

Dissertation

zur Erlangung des akademischen Grades

doctor rerum naturalium (Dr. rer. nat.)

vorgelegt der

Mathematisch-Naturwissenschaftlich-Technischen Fakultät

(mathematisch-naturwissenschaftlicher Bereich)

der Martin-Luther-Universität Halle-Wittenberg

von Herrn Michael Schräml

geb. am : 08.07.1974 in München



Gutachterin/Gutachter:

1. Prof. Dr. Rainer Rudolph, Martin-Luther-Universität Halle Wittenberg
2. Prof. Dr. Johannes Buchner, Technische Universität München
3. Prof. Dr. Hans-Joachim Fritz, Georg-August-Universität Göttingen

Halle (Saale), 16.11.2005

urn:nbn:de:gbv:3-000009684

[<http://nbn-resolving.de/urn/resolver.pl?urn=nbn%3Ade%3Agbv%3A3-000009684>]

Abbreviations

aa	amino acid
µg	micro gram
µl	micro liter
ATP	adenosin triphosphate
BAP	Biotin Accepting Peptide
BCCP	<i>E.coli</i> Biotin Carboxylase Carrier Protein
BIA	Biomolecular Interaction Analysis
bioIGF-I	biotinylated IGF-I
BirA	<i>E.coli</i> Biotin holoenzyme ligase (E.C.6.3.4.15)
bp	base pairs
BSA	Bovine Serum Albumin
Camp	Chloramphenicol
<i>cat</i>	chloramphenicol acetyl transferase gene
<i>catA112/221</i>	regulatory peptide from the upstream region of the <i>cat</i> -gene
<i>cmIA</i>	regulatory peptide from the upstream region of the <i>cat</i> -gene
DNA	Desoxy Ribonucleic Acid
dNTPs	mix of dATP, dCTP, dGTP, dTTP
DSC	Differential Scanning Calorimetry
EP-PCR	Error Prone PCR
ErbB2	ectodomain of the human Her2 receptor tyrosine kinase
ErbB3	ectodomain of the human Her3 receptor tyrosine kinase
EtBr	Ethidium Bromide
FC	Flow Cell
<i>g</i>	centrifugal force
g10ε	gene 10 enhancer
GROEL/ES	<i>E.coli</i> chaperonine system
h	hour
HDACI	human Histone Deacetylase I
HTPP	High Throughput Protein Production
IGFBP-4	Insulin-like Growth Factor Binding Protein 4
IGF-I	Insulin-like Growth Factor I
IgG1FC	human IgG1 antibody FC fragment
IMAC	Ion Metal chelating Affinity Chromatography
kcal	kilo calories
K _D	equilibrium constant [M]
kDa	kilo Dalton
k _{off}	dissociation rate [s ⁻¹]
k _{on}	association rate [1/Ms]
L	litre
LEE	Linear Expression Element
min	minute

mini-BP4	IGF-binding domain of IGFBP-4
ml	milliliter
MMP	Matrix Metalloproteinase
MMP2	Matrix Metalloproteinase 2
mRNA	messenger RNA
MTP	Microtitre Plate
ng	nano gram
Ni-NTA	nitrilotriacetic acid charged with Ni ²⁺
NNK	triplet codon encoding all 20 natural amino acids
OD _{xxx}	optical density at xxx nm
OEL	Overlapping Extension Ligation
PCR	Polymerase Chain Reaction
PEX2	C-terminal hemopexin-like domain of the MMP2
pIVEX	plasmid for <i>in vitro</i> Expression
<i>Pwo</i>	<i>Pyrococcus woessii</i> DNA Polymerase
RBS	Ribosome Binding Site
rpm	resolutions per minute
RT	reverse transcription
RTS	Rapid Translation System
RU	Response Unit
RV	Reaction Volume
s	second
S	Svedberg unit
SA-HRP	streptavidin conjugated with horse radish peroxidase
SB	Stopping buffer
SecM	arrest peptide sequence from the <i>E.coli secM</i> operon
SPR	Surface Plasmon Resonance
T7P	T7-promotor
T7T	T7-terminator
TA	annealing temperature
TAE	Tris Acetate EDTA buffer
TE	elongation temperature
TFE	final elongation temperature
TIM	initial melting temperature
TIMP2	Tissue Inhibitor of Matrix Metalloproteinase 2
TM	melting temperature
tmRNA	<i>E.coli</i> <i>ssrA</i> RNA, transfer messenger RNA
tRNA	transfer RNA
U	unit
WB	Washing buffer
wt	wild type

Eidesstattliche Erklärung

Diese Arbeit wurde im Zeitraum Juli 2001 bis März 2004 bei der Roche Diagnostics GmbH in Penzberg und bei der Scil Proteins GmbH in Halle an der Saale unter der universitären Aufsicht von Prof. Dr. Rainer Rudolph und der Betreuung durch Dr. Martin Lanzendörfer (Roche Diagnostics GmbH) durchgeführt.

Hiermit erkläre ich an Eides statt, daß die vorliegende Arbeit ohne fremde Hilfe verfaßt und noch nicht anderweitig für Prüfungszwecke vorgelegt wurde.

Es wurden keine anderen Hilfsmittel als die angegebenen Quellen und Hilfsmittel benutzt. Wörtliche und sinngemäße Zitate sind als solche gekennzeichnet.

Penzberg, den 17.06.2004

Michael Schräml

Acknowledgements

Here I want to thank all those, who contributed to this work. Especially I want to thank Dr. Martin Lanzendörfer for more than four years of fantastic education and collaboration at the department of biochemical research in Penzberg. I want to thank Dr. Dorothee Ambrosius, who launched the HTPP project in 2001. I am grateful to Prof. Rainer Rudolph for supervising this work and for the opportunity to present our data to the audience at the “Halle congress of recombinant protein production” in 2002. I want to thank the team of Scil Proteins, Dr. Ulrike Fiedler, Dr. Gabriele Prötzel, Dr. Markus Fiedler, Dr. Erik Fiedler and Dr. Thomas Hey for their encouragement in our scientific collaboration. Prof. Dr. Andreas Plückthun and Dr. Michael Stumpp I want to thank for valuable advices in the ribosome display technique. Dr. Rick Engh and Dr. Tad Holak I want to thank for their help in designing the mini-BP4 protein constructs and for valuable discussion of the results. Prof. Dr. Kresse I want to thank for his support to this work. Dr. Stefan Klostermann I want to thank for his help in bioinformatics. Dr. Sabine Wizemann, Dr. Wolfgang Mutter, Dr. Erhard Fernholz, Dr. Cordula Nemetz and Dr. Manfred Watzele I want to thank for their support in questions about cell-free protein expression. Konrad Bauer I want to thank for learning tricky PCR-techniques. Ute Jucknischke and Birgit Essig I want to thank for their help in managing BIAcore sensorgrams. Dr, Christian Eckermann I want to thank for his support in refolding mini-BP4. Dr. Gunther Achhammer I want to thank for valuable discussion and advices with regard to all questions in the lab and life. Dr. Ulrich Kohnert, Dr. Frederike Hesse, Dr. Adelbert Grossmann, Dr Christian Neumann, Dr. Rupert Lang, Dr. Christian Klein and Dr. Jan Stracke I want to thank for their support to this work. Stephanie Kanzler, Lothar Driller, Georg Saalfrank, Senta Brandt, Kathrin Bohle, Jessica Stolzenberger, Max von Ruepprecht and Andreas Adelberger I want to thank for their unfailing encouragement to support this work.

Contents

1	Abstract.....	1
2	Introduction	3
2.1	Current protein research requires a High Throughput Protein Production (HTPP)...	3
2.2	Implementation of the cell-free protein synthesis into HTPP	4
2.3	The concept of a cell-free High Throughput Protein Production (HTPP)	5
2.4	Is cell-free protein synthesis able to support SPR analysis?	6
2.5	Directed evolutionary approaches complement rational protein engineering	7
2.6	Mutational study with the IGF-binding domain of human IGFBP-4	9
2.7	Using HTPP as a platform for the engineering of <i>de novo</i> binding proteins	10
3	Material and Methods	12
3.1	Devices	12
3.2	Chemicals and reagents.....	13
3.3	Kits	14
3.4	Materials	14
3.5	Proteins	15
3.6	Vectors	15
3.7	DNA-Modules.....	16
3.8	Buffers and solutions	16
3.9	<i>E.coli</i> strains.....	17
3.10	Cell culture media	17
3.11	Transformation of chemical competent <i>E.coli</i> cells	17
3.12	Cultivation and conservation of <i>E.coli</i> strains	17
3.13	Isolation of Plasmid-DNA from <i>E.coli</i> cells.....	18
3.14	Determination of the DNA-concentration and -purity	18
3.15	Agarose-gel electrophoresis	18
3.16	Isolation and purification of DNA-fragments from agarose-gels.....	18
3.17	Dephosphorylation of vector DNA.....	19
3.18	Enzymatic DNA-Ligation	19
3.19	Enzymatic restriction of DNA	19
3.20	DNA sequence analysis.....	19
3.21	Polymerase Chain Reaction (PCR)	19
3.21.1	Introduction of restriction sites	20
3.21.2	Colony PCR	20
3.21.3	Production of DNA-modules.....	20
3.21.4	Overlapping Extension Ligation PCR (OEL)	20
3.21.5	Production of the LEE T7Pg10 ϵ -HDACI- FXaAviTagT7T	21
3.21.6	Production of the LEE T7PAviTagFXa-PEX2-T7T	21
3.21.7	Production of the LEE T7PbirAT7T.....	21
3.21.8	Synthesis of the ribosome display spacers „Stalling“ and „NoStalling“	22
3.21.9	Synthesis of 32 specifically mutated mini-BP4 gene-constructs	23
3.21.10	Generation of 32 T7P(his) ₆ FXa-miniBP4-FXaAviTagT7T LEEs	23
3.21.11	Synthesis of a mini-BP4 DNA library.....	24
3.21.12	Generation of mini-BP4 ribosome display constructs.....	24
3.21.13	Synthesis of the PEX2 DNA library	25
3.21.14	PCR-mutagenesis of γ crystallin constructs	26
3.22	Cell-free <i>in vitro</i> transcription and translation.....	26
3.22.1	Site-specific biotinylation of fusion proteins	26
3.23	Ribosome Display Protocol.....	27
3.23.1	Preparation of the ectodomains erbB2 and erbB3	27
3.23.2	Coating of micro titre plates	27
3.23.3	Generation of ribosome display templates.....	28
3.23.4	Preparation of the ribosome display translation mixture	28
3.23.5	Preparation of Protein G coated magnetic beads	29
3.23.6	Purification of mRNA and removal of remaining DNA.....	29

II

3.23.7	Reverse Transcription and cDNA amplification.....	29
3.23.8	Subcloning of genes after ribosome display	30
3.24	Electrophoretic separation of proteins	30
3.25	Semi-Dry Western blotting	31
3.26	Slot Blotting.....	31
3.27	Detection of biotinylated polypeptides	31
3.28	Detection of the Flag-Epitope peptide.....	31
3.29	Configuration of the robotic pipettor.....	32
3.30	Small-scale robotic affinity purification.....	32
3.31	Spectrometrical determination of the protein concentration.....	33
3.32	Dialysis.....	33
3.33	Ultrafiltration.....	33
3.34	Fluorescence Spectroscopy.....	33
3.35	Differential Scanning Calorimetry (DSC)	34
3.36	ELISA for the detection of gamma crystallin derivatives.....	34
3.37	Expression and IMAC purification of γ crystallin derivatives.....	35
3.38	Biomolecular Interaction Analysis (BIA).....	35
4	Results.....	37
4.1	Generation of Linear Expression Elements (LEEs)	37
4.2	Preproduction of a DNA-module library	39
4.3	Generation and Quantification of Linear Expression Elements (LEEs).....	39
4.4	Development of the cell-free enzymatic <i>in situ</i> mono biotinylation.....	40
4.5	Cell-free production of mini-BP4 constructs.....	44
4.6	Activation of the IGF-I binding activity of mini-BP4	48
4.7	Robot-assisted cell-free synthesis and purification of recombinant proteins	49
4.8	SPR protein-protein interaction analysis of 32 mini-BP4 constructs.....	51
4.9	Ribosome display complements the HTPP concept.....	54
4.10	Background information: tmRNA and ribosome display.....	54
4.11	Regulatory nascent peptides reduce the PCR-product yield of ribosome display ..	55
4.12	Selection of mini-BP4 mutants with IGF-binding activity.....	62
4.13	Engineering human γ crystallin for its use in HTPP	66
4.13.1	Ribosome display of engineered γ crystallin versus erbB2 and erbB3	66
4.13.2	Ribosome display with error prone PCR generated γ crystallin libraries	68
4.13.3	Evolution of new sequence motives in γ crystallin	72
4.13.4	Expression and Purification of γ crystallin derivatives.....	73
4.13.5	Binding properties of selected γ crystallin derivatives.....	75
4.13.6	Consequences of the two domain character of γ crystallin	78
4.14	Engineering the hemopexin-like scaffold as a <i>de novo</i> binding-protein.....	81
4.14.1	Stability of the PEX2 protein	82
4.14.2	Identification of variable amino acid positions in hemopexin-like fold	84
4.14.3	Ribosome Display of wild type PEX2 versus TIMP2.....	87
4.14.4	Approach to engineer PEX2 as a binding protein	88
5	Discussion	90
5.1	Advantages of a high throughput cell-free protein production and analysis.....	90
5.2	The mini-BP4 kinetics in their scientific context	91
5.3	Regulatory peptides destabilize a ribosome display construct.....	94
5.4	Selection of mini-BP4 mutants featuring IGF-I affinity	95
5.5	γ crystallin-specific results of ribosome display.....	97
5.6	Future display strategies using the γ crystallin scaffold	98
5.7	PEX2 as a general source for affinity reagents?.....	100
6	Curriculum vitae	103
7	Publications	104
8	References	105
9	Appendix.....	112

1 Abstract

We have developed a High Throughput Protein Production platform (HTPP), which enables us to automatically generate, express and purify recombinant proteins in a small-scale. The coupled cell-free transcription and translation technology facilitates the *in vitro* expression of fusion-proteins, which are directly expressed from modular assembled linear DNA templates. A prokaryotic cell-free system was used to perform a sequence specific, enzymatic *in situ* monobiotinylation of proteins, which were genetically fused to a Biotin Accepting Peptide (BAP). These fusion-proteins were robotically purified and immobilized in an oriented manner on streptavidin-coated biosensor surfaces to determine kinetic data of protein-protein interactions using the SPR technology. In this way, 32 site-directed mutated IGFBP-4 IGF-binding domains were synthesized, assembled into LEEs, expressed in a cell-free system, purified and refolded in order to elucidate the structure-functional implication of specific amino acid substitutions on the mini-BP4/IGF-I interaction. The whole process was completely automated.

On the basis of the coupled transcription and translation system a ribosome display protocol was established, which further expanded the throughput of the system. Linear DNA templates were synthesized for their tailored application in ribosome display. We could show that regulatory nascent peptides (SecM) in the spacer sequence of a ribosome display construct negatively affected the performance of ribosome display. The ribosome display protocol was used to screen a mini-BP4 library for IGF-I binding-active mutants. The results revealed further information about the IGF-I binding-relevance of distinct amino acids in the mini-BP4-sequence.

Finally, ribosome display was used for the elucidation of proteins with *de novo* binding properties. Engineered human γ crystallin derivatives were tested for their suitability to perform in ribosome display versus the human erbB2 and erbB3 receptor ectodomains. An affinity maturation was performed using alternated mutagenesis and selection-steps. Additional amino acid substitutions besides the initial *de novo* binding patch of the γ crystallin protein templates were introduced. The proposed sequential folding and paused translation mechanism of γ crystallin was confirmed by these results and proposals for further ribosome display experiments using the γ crystallin scaffold could be made. Heading towards new protein scaffold strategies a completely new approach was made to engineer the hemopexin-like protein domain as a general source for binding proteins. We could show that the MMP-PEX2 hemopexin-like

protein-domain performs in a ribosome display selection procedure and is also amenable to be used in diverse library strategies.

On the basis of these data, future approaches will lead to the establishment of an automated platform technology for the cell-free production of tailored multi-purpose binding proteins.

2 Introduction

2.1 Current protein research requires a High Throughput Protein Production (HTPP)

In 1982 there were 606 gene sequences available at the GenBank database, two decades later, in February 2004, 32549400 sequence submissions were reported (Benson *et al.* 2004).

This clearly shows that current biotechnology research is characterized by the accumulation of vast amounts of gene sequences for which a functional description of the encoded gene-products has to be assigned. Therefore the development of approaches and instrumentation to rapidly express and purify gene-products for their structure-functional characterization is a current demand in functional genomics research.

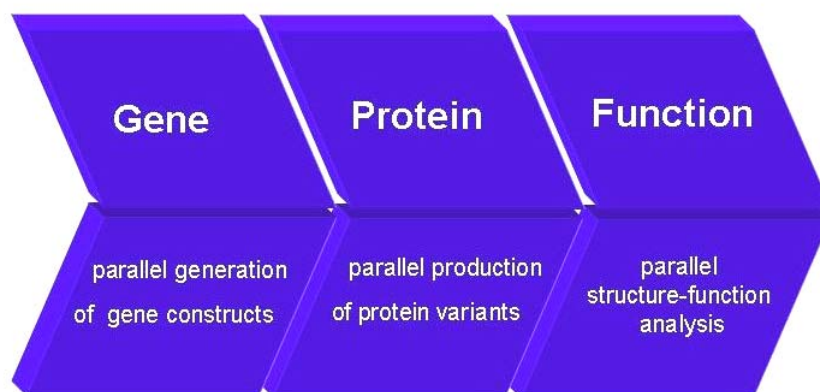


Fig.1: A current challenge in protein research is to rapidly assign function to gene-products using parallel technological approaches

To make these encoded polypeptides available to diverse analyses the identification of suitable protein constructs is a prerequisite, which mostly necessitates the engineering of mutated, truncated, labeled or post-translationally modified proteins. These circumstances further multiply the number of tailored protein-constructs to be generated and to be analyzed. In order to accelerate such a protein production and analysis process all necessary steps, inclusively the process of the gene engineering itself, must be performed in parallel (see fig. 1).

2.2 Implementation of the cell-free protein synthesis into HTPP

In this study the intention was to contribute to these actual demands. In contrast to conventional cell-based protein expression systems the strategy was to use the cell-free protein expression technology to meet the requirements of a high throughput protein production platform (Sawasaki *et al.* 2002).

Today cell-free protein synthesis is performed with prokaryotic (Zubay 1973) (Chen *et al.* 1983) eukaryotic (Royall *et al.* 2004) and even archaeal (Suzuki *et al.* 2002) cell extracts. Novel ATP regeneration systems (Dong-Myung Kim *et al.* 2000; Jewett *et al.* 2004; Sitaraman *et al.* 2004) and the Continuous Exchange Cell Free (CECF) technology (Spirin *et al.* 1988; Kigawa *et al.* 1991) improved the long-term protein synthesis. In the meantime, there are also reports about the successful cell-free production of glycosylated proteins (Duszenko *et al.* 1999), of membrane-proteins (Klammt *et al.* 2004) and of proteins containing multiple disulfide-bonds (Kim *et al.* 2004). The *in vitro* protein synthesis system has the potential not only to produce cellular proteins, but also to synthesize cytotoxic, regulatory or unstable proteins that cannot be expressed in living cells (Stiege *et al.* 1995).

The most tremendous advantage of the cell-free technology is the expression of recombinant proteins directly from PCR-generated DNA-templates (Horton *et al.* 1989; Henkel *et al.* 1993; Barik 1996; Martemyanov *et al.* 1997; Nakano *et al.* 1999). For this purpose coupled *in vitro* transcription and translation systems are used, which contain an mRNA-generating transcriptional sub-system. This is mostly driven by bacteriophage RNA polymerases (Chen *et al.* 1983). For example, in the RTS 100 *E.coli* HY System the T7 phage mRNA polymerase transcribes a linear DNA-template, which contains transcriptional promotor and translation control sequences, into mRNA. The mRNA is *in statu nascendi* translated into protein by the prokaryotic ribosomes. Nanomolar quantities of recombinant protein can be rapidly synthesized, giving rise to a higher throughput protein production application.

2.3 The concept of a cell-free High Throughput Protein Production (HTPP)

The aim was to develop a rapid DNA transcript generating method to supply various cell-free transcription and translation reactions with parallel generated, linear DNA transcripts (see fig. 2).

Strategy of High Throughput Protein Production

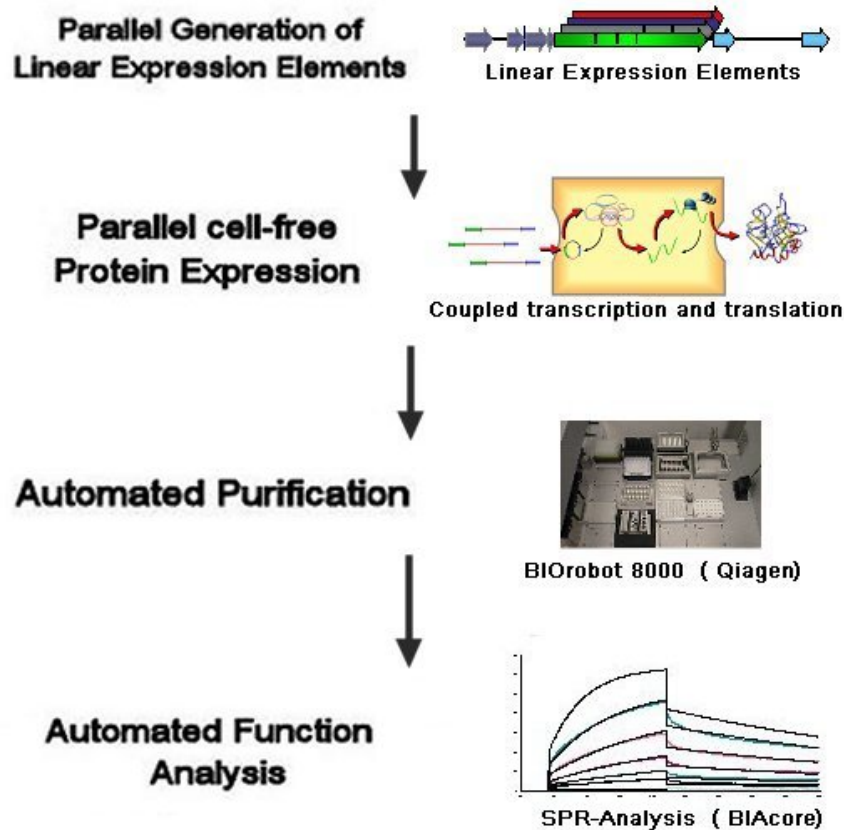


Fig. 2: Strategy of a high throughput protein production: Parallel produced Linear Expression Elements are transcribed and translated in a cell-free system. The gene-products are robotically purified to supply fully automated SPR-measurements.

Cell-free protein synthesis is highly suited to be implemented into an automated protein production process, since processes occurring during the manipulation of cellular systems, like the cloning of a gene-construct into an expression vector system, cell transformation, cell culturing, cell lysis and the removal of cellular compartments are simply bypassed.

Here the second aim was to automate the process of the gene engineering, the cell-free protein synthesis, the protein purification and the subsequent structure-functional analysis in one robotically assisted, streamlined process.

2.4 Is cell-free protein synthesis able to support SPR analysis?

Biomolecular Interaction Analysis (BIA), based on the principle of *Surface Plasmon Resonance (SPR)* (Granzow *et al.* 1992) is a sensitive method to determine protein-ligand interactions in real time analysis.

Small amounts of protein, like they are typically obtained from a cell-free batch production of recombinant proteins are already sufficient to perform SPR analyses (Alimov *et al.* 2000). SPR measurements require the stable immobilization of one of the interacting binding partners on the surface of a sensor matrix.

Here, the aim was to establish a rapid protein-labeling and immobilization method to perform SPR protein-protein interaction measurements directly supplied from a cell-free protein synthesis.

Since the interaction of biotin with streptavidin is one of the strongest non-covalent interactions known in nature ($K_D = 10^{-14}$ M), this high affinity binding couple is widely used to immobilize biotinylated proteins on streptavidin-coated surfaces such as microtiter plates, beads, sensor chips and other matrices (Bayer *et al.* 1990). This strong affinity also provides an opportunity to use this interacting couple for the presentation of biotinylated proteins on the surface of streptavidin-coated SPR sensors.

In nature, Protein Biotin Ligases (BPLs) catalyze the transfer of a single biotin moiety to specific lysines in biotinyl-protein domains, which are recognized as a substrate (Fall 1979). The best characterized BPL is the *E.coli* biotin holoenzyme synthetase BirA (Wilson *et al.* 1992), which catalyzes the transfer of biotin to the epsilon amino group of a specific lysine residue of the Biotin Carboxyl Carrier Protein (BCCP) subunit of acetyl-CoA carboxylase (Beckett *et al.* 1999).

There are also shorter peptide sequences, which are recognized by BirA as a substrate, not resembling the consensus sequence of common BirA biotinylation sites (Reddy *et al.* 2000). These peptide sequences are the product of *in vitro* selection processes using peptide libraries (Beckett *et al.* 1999). When fused to a recombinant protein, these Biotin Accepting Peptide (BAP) sequences are specific enzymatically biotinylated by BirA during the *in vivo* expression in *E.coli* (Verhaegen *et al.* 2002).

In this study a cell-free, *in situ* enzymatic protein monobiotinylation was established to rapidly supply SPR analyses with sufficient amounts of specifically biotinylated fusion proteins.

2.5 Directed evolutionary approaches complement rational protein engineering

The cell-free production and analysis of rationally engineered protein variants can be automated, but the library size of rationally designed protein-constructs to be processed remains always limited by the technical throughput of each system. Therefore the analysis of the binding-properties of a vast multitude of gene-products demands for further efforts.

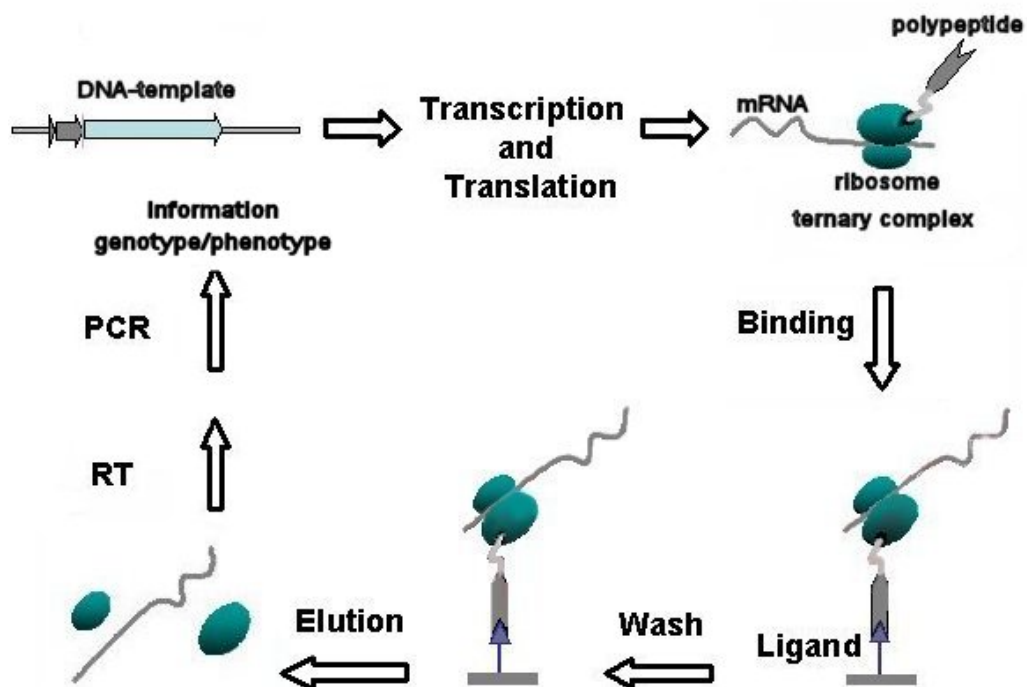


Fig. 3: Schematically, one ribosome display cycle is shown. A specific ribosome display DNA-template is transcribed and translated *in vitro* to generate functional ternary complexes. These complexes perform in an affinity selection procedure (Binding, Wash). Messenger RNA from tightly bound ternary complexes is isolated (Elution) and reversely transcribed (RT). DNA sequencing of the subcloned ribosome display PCR-products reveal information about phenotypes, which had bound to the presented ligand molecule.

Directed evolutionary techniques are well suited to complement the technical capability of a high throughput protein production platform. Based on the cell-free

protein synthesis, ribosome display is an excellent method to extend a high throughput protein production and analysis process (see fig. 3).

The aim of ribosome display is the generation of complexes, in which the genotype (mRNA) is physically linked by the ribosome to its encoded phenotype (polypeptide). A linear DNA-template, which can encode a gene-library is transcribed and translated *in vitro*. Downstream of the gene-sequence a spacer sequence is fused, where the predominant feature is the lack of a translational stop codon. This spacer domain facilitates the display of the nascent translated and cotranslationally folded polypeptide, which remains tethered to the ribosome. These complexes are subjected to a panning procedure, in which the ribosome-displayed polypeptide is allowed to bind to a presented ligand molecule. The mRNA from tightly bound complexes is isolated, reversibly transcribed and amplified by PCR. Subcloning of the PCR products into a vector system and consecutive DNA sequencing reveals information about the phenotype of the bound polypeptide. It is reported that repeated cycles of ribosome display efficiently select a pool of similar specific protein-binders from libraries in the range of up to 10^{14} members (Mattheakis *et al.* 1994; Hanes *et al.* 1997; Lamla *et al.* 2003). The handling of large libraries makes ribosome display superior to phage display (Smith *et al.* 1997), where the library size is restricted by the vector transformation efficacy of the cells used in the experiment.

The aim was to establish a ribosome display protocol in order to integrate this technology into the HTPP assembly line. Ribosome display should extend the protein production process towards the selection of binding proteins from larger libraries than it would be tractable by the conventional automated approach.

The overall stability of ternary complexes produced for the ribosome display selection procedure crucially influences the performance of the selection process (Hanes *et al.* 1997). The aim was to increase the PCR-product yield of a ribosome display selection procedure. Regulatory nascent peptides (Lovett *et al.* 1996; Nakatogawa *et al.* 2002) were examined. These peptides were implemented into the spacer sequence of a ribosome display DNA construct in order to elucidate their impact on the stability, expression rate and yield of a ribosome display construct.

2.6 Mutational study with the IGF-binding domain of human IGFBP-4

The establishment of the automated protein production and analysis assembly line enabled us to perform a mutational study with the pharmaceutically relevant human serum protein IGFBP-4. The most likely function of IGFBP-4 is the high-affinity binding of secreted Insulin-like Growth Factors (IGFs) to prevent their interaction with IGF receptors (see fig. 4) (Mohan *et al.* 1996; Miyakoshi *et al.* 1999). *In vivo* and *in vitro* studies suggest that IGFBPs play an important role in the growth regulation of a variety of tumors (Khandwala *et al.* 2000). This particularly resembles the high relevance of IGFBPs as potential anti-proliferation drugs for cancer treatment.

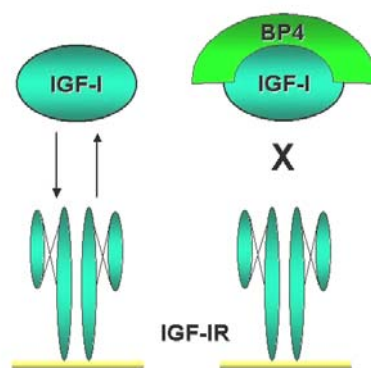


Fig. 4: human IGFBP-4 binds to IGF-I and inhibits the IGF-interaction with its receptor IGF-IR. The distant N-terminal-region of IGFBP-4 is mainly responsible for IGF-binding. The 7.5 kDa IGF-I binding domain of IGFBPBP-4 was examined for its binding affinity towards IGF-I. In order to modulate the IGF-I interaction 9 amino acid positions of mini-BP4 were substituted at positions, which are reported to mediate the interaction to IGF-I.

Mutational analyses indicated that the IGF-binding activity of IGFBPs is mainly determined by their N-terminal region (Chernausek *et al.* 1995) (Wetterau *et al.* 1999) and to a less extent by their C-terminal sequence (Qin *et al.* 1998). The IGF-binding-site of IGFBP-4 is located in the distant N-terminal region, where it is supposed to comprise a hydrophobic motive (Byun *et al.* 2001), which mediates a core IGF-I binding function.

Based on these information and data of the homologous IGFBP-5 (Kalus *et al.* 1998), a short mini-BP4 IGF-binding domain of 50 amino acids in length was engineered. 9 distinct amino acid positions were subjected to site-directed mutagenesis. In total 31

rationally designed mini-BP4 constructs and the wild type construct were engineered as fusion proteins, *in vitro* expressed and biotinylated, purified and functionally tested by SPR-analyses. The aim was the elucidation of the structure-functional implications of the mutations on the IGF-I binding behavior of mini-BP4.

Moreover, ribosome display permitted the selection of mini-BP4 mutants revealing IGF-I binding activity from a library otherwise too large to be processed. It further enabled the characterization of distinct amino acid positions in the mini-BP4 binding domain according to their relevance for IGF-I binding.

2.7 Using HTPP as a platform for the engineering of *de novo* binding proteins

A final goal was to evaluate whether the HTPP platform technology could be used for the selection, production and analysis of proteins to which *de novo* binding features versus predefined molecular targets were assigned.

Besides the supremacy of the antibody as a natural binding protein, new approaches were made to engineer proteins as affinity reagents to use them as antibody-analogues in biochemical, diagnostic or therapeutic applications (Nygren *et al.* 2004). In the development of biochemical and diagnostic tools these protein scaffolds of non-immunoglobulin origin take advantage of their accelerated and cost-effective production and some even provide a higher conformational stability or solubility when compared to the antibody protein fold. In the pharmaceutical application antibody-like molecules can take advantage of their prolonged half-life and offer the potential to be dosed less frequently than antibodies. These proteins might also be applied, where the antibody protein scaffold is limited due to its size in biodistribution and tissue penetration. As these molecules usually lack the effector function of the antibodies constant FC region they are pursuing alternatives for medical applications, which do not require the antibody dependent cell cytotoxicity (ADCC) or the complement dependent cytotoxicity (CDC).

A considerable amount of engineered binding-molecules like e.g. the γ crystallin based "Affilin" molecules (Fiedler *et al.* 2001), the Lipocalins "Anticalins" (Skerra 2001), protein A "Affibodies" (Nord *et al.* 1997) ankyrin repeat proteins (Binz *et al.* 2003) and even glutathione transferase "Glubodies" (Napolitano *et al.* 1996) were reported to be used as affinity reagents in diverse approaches.

Site directed random mutagenesis of 8 surface exposed amino acids located in the rigid first greek key motive of the N-terminal γ crystallin domain was performed to generate a theoretical library size of 2.6×10^{10} different γ crystallin mutants (SPC-library, Scil Proteins, Halle a. d. Saale). In collaboration with Scil Proteins GmbH (Germany) two γ crystallin mutants were selected from this protein library.

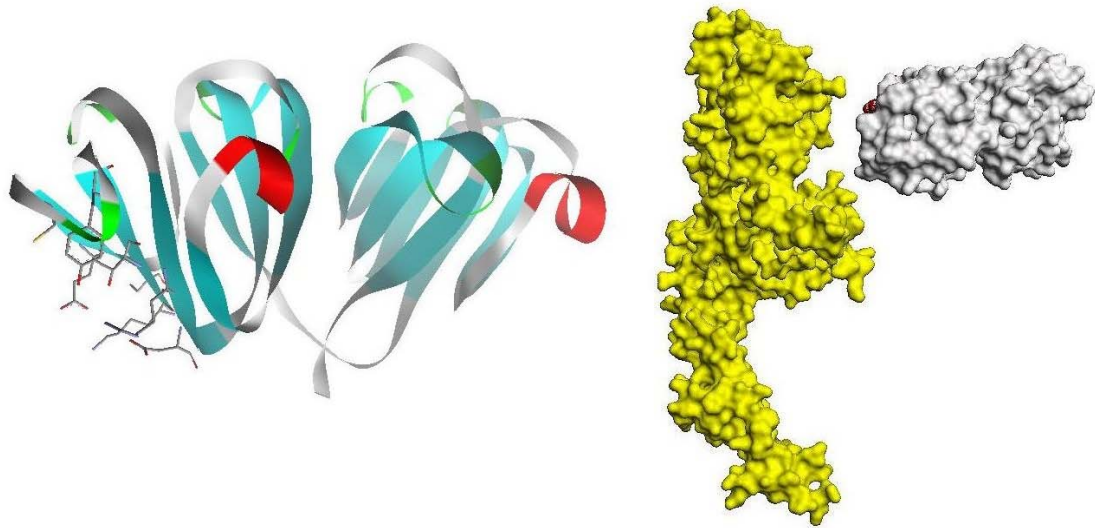


Fig. 5: The human eye lens protein γ crystallin was subjected to an engineering approach (Fiedler *et al.* 2001). 8 amino acids located in the rigid beta-sheets of the solvent exposed first N-terminal greek-key motive were genetically randomized to assign a *de novo* binding site into the scaffold. It should be elucidated whether this scaffold performs in a ribosome display approach. Here the bovine γ crystallin is shown as a ribbon diagram and as an electron surface density map (Najmudin *et al.* 1993). The relevant amino acids are symbolized as sticks. The *de novo* binding site should enable γ crystallin derivatives to recognize the erbB2 receptor-ectodomain as a molecular target (right). The ectodomain of the human erbB2 receptor is shown in yellow (Cho H. *et al.* 2003)

The mutants were able to recognize the ectodomains of the human receptor-tyrosine kinases erbB2 and erbB3 with moderate affinity.

The γ crystallin mutants were selected from the library using the phage display technology (Smith *et al.* 1997). On the basis of these pre-selected “first generation” binders it was our aim to evaluate the suitability of the crystallin scaffold to perform in ribosome display and in the automated cell-free protein production and analysis process. The aim was to develop a γ crystallin based diagnostic tool, which should recognize and differentiate between the erbB2 and erbB3 ectodomains in clinical tissue samples. This is currently reflected by the need to develop reliable and

significant assays to classify cancer patient-populations for the treatment with anti-cancer drugs like Herceptin (Cho H. *et al.* 2003).

A final goal of this study was to investigate the hemopexin-like protein family for its suitability to perform as a general source of protein affinity reagents. Here a proposal is made, to engineer PEX2, the C-terminal protein domain of the human MMP2, as a multi purpose binding-protein for the recognition of predefined target molecules (Bode 1995).

3 Material and Methods

3.1 Devices

Äkta Explorer		Amersham Pharmacia Biotech, Freiburg
BIAcore 3000 and BIAcore Software 4.0.1		Amersham Pharmacia Biotech, Freiburg
BIAcore Evaluation Software 4.0.1		Amersham Pharmacia Biotech, Freiburg
Biorobot 8000 and Qiasoft 4.1 Software		Qiagen, Hilden
BioRad Biodot Apparatur		BioRad, München
Cary 50-Bio		Varian, Australien
Curix HT-330U X-ray developer		AGFA, Köln
Columbus Microplate Strip Washer		Tecan, Crailsheim
Ice-machine		Ziegler, Isernhagen
Electronic balance		Sartorius, Göttingen, Mettler Toledo, Gießen
Elektrophoresis chamber for agarose gels		Biorad, München
Power supply EPS3500		Amersham Pharmacia Biotech, Freiburg
FluoroMax-2 Spex Fluorimeter + Software		Jobin Yvon, Horiba, Edison, USA
Fireboy		Integra Biosciences, Fernwald
Frac 950		Amersham Pharmacia Biotech, Freiburg
GeneAmp PCR System 2400 Thermocycler		Perkin Elmer, Weiterstadt
Gynkotec HPLC System		Dionex, Idstein
Heat Sealer		Eppendorf, Hamburg
HiTrap chelating HP column		Amersham, Freiburg
Imageplate Detektor		Marresearch, Hamburg
Combi shaker KL2		E. Bühler, Hechingen
KS 250 basic		IKA Staufen
Incubator		Rubarth Apparate, Hannover
Illuminator		Neolab, Heidelberg
Lumi-Imager F1 Workstation + Lumianalyst Software		Roche Applied Sciences, Mannheim
Magnetic stirrerREO		IKA, Staufen
Mastercycler gradient		Eppendorf, Hamburg
Microtiter-plate shaker		MTS4 IKA, Staufen
Microwave		AEG, Nürnberg
Milli-Q Water Purification System		Millipore, Eschborn
MS2- Minishaker		IKA Staufen
Nano N-DSC II Differential Scanning Kalorimeter CSC		American Fork, USA
Neslab RTE 111 Kryostat		Newington, NH
pH Meter inoLab		WTW, Weilheim
Pipettes Eppendorf Research		Eppendorf, Hamburg
Pipet Easypet		Eppendorf, Hamburg
Power Ease 500		Invitrogen, Carlsbad, CA
Precision kuvettes Suprasil Quarz	1-10 mm	Hellma, Müllheim
Precitherm waterbath		Roche Applied Sciences, Mannheim
Provario Ultrafiltrationssystem		Pall Filtron, Dreieich
RM5 Assistent 348 Roller		Karl Hecht GmbH & Co KG, Sondheim
Rotors SS34, GSA, GS-3 Sorvall RC-5B		Kendro Laboratory Products, Hanau
Sonifier Cell Disruptor B15		Branson, Heusenstamm
Sorvall RC-5B centrifuge		Kendro Laboratory Products Hanau

Sunrise ELISA Reader
Thermomixer 5436
Table top centrifuge 5417R
Tabletop centrifuge Galaxy Mini
Western Blot Elektrophoresis chamber
BioMax Filmcassette
X Cell SureLock Elektrophoresis cell

Tecan, Crailsheim
Eppendorf, Hamburg
Eppendorf, Hamburg
VWR, International, München
Amersham Pharmacia Biotech, Freiburg
Kodak, Rochester, NC USA
Invitrogen, Carlsbad, Karlsruhe

3.2 Chemicals and reagents

Agarose MP
Ampicillin
Antifoam SE-35
Bacto Agar
Bacto Tryptone
Bacto Yeast Extract
BIAcore HBS-EP Puffer
BIAcore HBS-P Puffer
Blocker 10% BSA in PBS
Blocking Reagent
Bromphenolblue S
Chloramphenicol
Complete Protease Inhibitor Cocktail, EDTA-free
Coomassie Brilliant Blue R250
D-(+)-Biotin
D-desthiobiotin solution
Dimethylsulfoxide (DMSO)
Dithiothreitol (DTT)
Acetic Acid
Ethanol
Ethidiumbromide
Glutathione
Glycerol (99%)
Guanidiniumhydrochloride (GdnCl)
HPLC-Water
Hydroxyethylpiperazinethansulfonic acid (HEPES)
Imidazole
Indian Ink
pefabloc
Potassium chloride
Kanamycine
Copper sulfate
L-Arginine
Lumi-Light Western Blotting Substrate
Skim milk powder
Magnesiumacetate-Tetrahydrate
Mark12 unstained Wide Range Protein Standard
Methanol
2-Mercapthoethanol
Mineral oil, DNase RNase free
Sodiumchloride
Sodiumdihydrogenphosphate Monohydrate
NuPage Antioxidant
NuPage LDS Sample Buffer (4x)
NuPage MOPS SDS Buffer 20x
PCR dNTP Nucleotide-Mix
Phosphate-buffered Saline (PBS), Buffer, 10x
Phosphate-buffered Saline (PBS), Tablets Gibco
Polyoxyethylensorbitanmonolaurate (Tween 20)
Propanol
RNA 16S-23S ribosomal from *E.coli* MRE 600
RNaseZap
RNasin

Roche Applied Sciences, Mannheim
Roche Applied Sciences, Mannheim
Sigma Aldrich, Irvine, UK
Difco, Detroit, USA
Difco, Detroit, USA
Difco, Detroit, USA
Amersham Pharmacia Biotech, Freiburg
Amersham Pharmacia Biotech, Freiburg
Pierce, Rockford, IL, USA
Roche Applied Sciences, Mannheim
Serva, Sigma Aldrich, Irvine, UK
Merck Eurolab, Darmstadt
Roche Applied Sciences, Mannheim
Serva, Sigma Aldrich, Irvine, UK
Sigma Aldrich, Irvine, UK
IBA GmbH, Göttingen
Sigma Aldrich, Irvine, UK
Roche Applied Sciences, Mannheim
Sigma Aldrich, Irvine, UK
Merck Eurolab, Darmstadt
BIOrad, München
Roche Applied Sciences, Mannheim
Sigma Aldrich, Irvine, UK
Sigma Aldrich, Irvine, UK
J.T. Baker, Deventer, Holland
Roche Applied Sciences, Mannheim
Merck Eurolab, Darmstadt
Pelikan, München
Serva, Sigma Aldrich, Irvine, UK
Merck Eurolab, Darmstadt
Roche Applied Sciences, Mannheim
Merck Eurolab, Darmstadt
Sigma Aldrich, Irvine, UK
Sigma Aldrich, Irvine, UK
Merck Eurolab, Darmstadt
Merck Eurolab, Darmstadt
Invitrogen, Karlsruhe
Merck Eurolab, Darmstadt
Serva, Sigma Aldrich, Irvine, UK
Sigma Aldrich, Irvine, UK
Merck Eurolab, Darmstadt
Merck Eurolab, Darmstadt
Invitrogen, Karlsruhe
Invitrogen, Karlsruhe
Invitrogen, Karlsruhe
Roche Applied Sciences, Mannheim
Roche Applied Sciences, Mannheim
Invitrogen, Karlsruhe
Merck Eurolab, Darmstadt
Merck Eurolab, Darmstadt
Roche Applied Sciences, Mannheim
Ambion Inc. USA
Promega, Madison, WI USA

Sample Reducing Agent 10x	Invitrogen, Karlsruhe
SuRE/Cut Buffer A, B, H, L, M	Roche Applied Sciences, Mannheim
TE Puffer 1x	Promega, Madison, WI USA
TMBplus substrate	Kem-En-Tec, Copenhagen, DK
Titriplex	Merck Eurolab, Darmstadt
TRIS-(hydroxymethyl)-aminomethane (TRIS)	Sigma Aldrich, Irvine, UK
Tris-Glycine SDS Running buffer 10x	Invitrogen, Karlsruhe
Tris-Glycine Transferpuffer 25x	Invitrogen, Karlsruhe
Tris-Glycine SDS Sample Buffer (2x)	Invitrogen, Karlsruhe
TRIZMA BASE DNase, RNase Protease free	Sigma Aldrich, Irvine, UK
tRNA from <i>E.coli</i> MRE 600 RNase free	Roche Applied Sciences, Mannheim
Water, PCR grade	Roche Applied Sciences, Mannheim

3.3 Kits

Biotinylation kit EZ-Link Sulfo-NHS-Biotin	Pierce, Rockford, IL, USA
C.therm RT-Polymerase ONE Step PCR System	Roche Applied Sciences, Mannheim
DNA-free Kit	Ambion Inc. USA
DNA-Molecular weight standard XIII und VIII	Roche Applied Sciences, Mannheim
Expand High Fidelity PCR System	Roche Applied Sciences, Mannheim
GeneMorph II Random Mutagenesis Kit	Stratagene, La Jolla, CA USA
High Pure PCR Product Purification Kit	Roche Applied Sciences, Mannheim
High Pure RNA Isolation Kit	Roche Applied Sciences, Mannheim
Mark 12 Unstained Standard	Invitrogen, Karlsruhe
<i>Pwo</i> Master	Roche Applied Sciences, Mannheim
QIAGEN Plasmid Maxi Kit	Qiagen, Hilden
QIAprep Spin Miniprep Kit	Qiagen, Hilden
QIAquick Gel Extraction Kit	Qiagen, Hilden
Rapid DNA Ligation Kit	Roche Applied Sciences, Mannheim
Rapid Translation System RTS 100 HY <i>E.coli</i>	Roche Applied Sciences, Mannheim
RTS GroE Supplement	Roche Applied Sciences, Mannheim
SA-HRP Westernblotting Kit	Roche Applied Sciences, Mannheim
Zero Blunt TOPO Cloning Kit	Invitrogen, Karlsruhe

3.4 Materials

0.5ml tubes, DNase-, RNase-, protease free	Eppendorf, Hamburg
1.5ml tubes, DNase-, RNase-, protease free	Eppendorf, Hamburg
10 µl Pipette tips with filter, sterile	Roche Applied Sciences, Mannheim
100µl Pipette tips with filter, sterile	Molecular BioProductsInc.SanDiego,CA USA
1000µl Pipette tips with filter, sterile	Eppendorf, Hamburg
15ml polypropylene centrifugal tubes, sterile	labcon, San Rafael, CA USA
2.0ml vials, DNase-, RNase-, free	Eppendorf, Hamburg
20ml Pipette tips, sterile	Becton Dickinson Labw., Franklin Lakes, NJ
BIAcore CM5-Chip research grade	Amersham Pharmacia Biotech, Freiburg
BIAcore SA-Chip research grade	Amersham Pharmacia Biotech, Freiburg
Filter paper	Whatman, Fairfield, USA
Heat-Sealing Foil	Eppendorf, Hamburg
Syringe	B. Braun, Melsungen
Lumi-Film Chemiluminescent Detection Film	Roche Applied Sciences, Mannheim
Ni-NTA Magnetic Agarose Beads	Qiagen, Hilden
Ni-NTA Agarose	Qiagen, Hilden
Novex 18% Tris-Glycine Gel 1.0 mm x 12 well	Invitrogen, Karlsruhe
Novex 16% Tris-Glycine Gel 1.0 mm x 12 well	Invitrogen, Karlsruhe
NuPage 12% Bis-Tris Gel 1.0 mm x 12 well	Invitrogen, Karlsruhe
Parafilm	American National Can, Neenah, USA
PCR tubes 0.5ml	Eppendorf, Hamburg
Polycarbonate centrifugal tubes	Beckmann, München
Protein G Magnetic Beads	New England Biolabs,
Reacti-Bind Protein A Coated Plates	Pierce, Rockford, USA
Reacti-Bind Protein G Coated Plates	Pierce, Rockford, USA
Reacti-Bind NeutrAvidin	Pierce, Rockford, USA
Slide-a-Lyzer dialysis frames	Pierce, Rockford, USA
Filter Durapore	Millipore, Bedford, USA

Filter (0.2 µM) Durapore, sterile
 Bottle-based filter top
 Streptavidin Magnetic Particles
 StreptaWell 12x8-well stripes
 Trans-Blot Nitrocellulose Membran
 twin.tec PCR plate 96, skirted
 Ultrafree-0.5, -4, -15 Centrifugal Concentrators 5K

Millipore, Bedford, USA
 Nalgene, Rochester, USA
 Roche Applied Sciences, Mannheim
 Roche Applied Sciences, Mannheim
 BIO Rad, München
 Eppendorf, Hamburg
 Millipore, Bedford, USA

3.5 Proteins

Alkaline Phosphatase (shrimp)
 Anti-FLAG M2-Peroxidase conjugate
 Biotin Ligase BirA [E.C.6.3.4.15]
 Biotinylated TIMP2
C. therm. RT Polymerase
 Penta-His Peroxidase conjugate
 recombinant human PEX2
Pwo DNA-Polymerase
 Recombinant human ErbB2/FC Chimera
 Recombinant human ErbB3/FC Chimera
 Recombinant human IgG1/FC
 Recombinant human IGF1
 Restriction enzymes
 SPC-12 A 5/2 γ crystallin
 SPC-13 B 11/2 γ crystallin
 Anti γ crystallin IgG-HRP
 Streptavidin-HRP conjugate
 Taq-DNA Polymerase
 Tgo-DNA-Polymerase
 Recombinant human TIMP2

Roche Applied Sciences, Mannheim
 Sigma Aldrich, Irvine, UK
 Avidity, Denver USA
 Labor Dr. Lanzendörfer, Roche, Penzberg
 Roche Applied Sciences, Mannheim
 Qiagen, Hilden
 Labor Dr. Lanzendörfer, Roche, Penzberg
 Roche Applied Sciences, Mannheim
 R&D Systems GmbH, Wisbaden
 R&D Systems GmbH, Wisbaden
 R&D Systems GmbH, Wisbaden
 R&D Systems GmbH, Wisbaden
 Roche Applied Sciences, Mannheim
 Scil Proteins GmbH, Halle a.d.Saale
 Scil Proteins GmbH, Halle a.d.Saale
 Scil Proteins GmbH, Halle a.d.Saale
 Roche Applied Sciences, Mannheim
 Roche Applied Sciences, Mannheim
 Roche Applied Sciences, Mannheim
 Labor Dr. Lanzendörfer, Roche, Penzberg

3.6 Vectors

name	kb	insert	tag	cloning site	origin	comment
pACYCY184 birA	4.2	<i>E.coli</i> birA	--		Avidity	Template for birA
pET20bplus	3.7	γ crystallin	(his) ₆ Ct	Nde; XhoI	Scil Proteins	γ crystallin
pIVEX2.1MCS AvBirA	4.7	<i>E.coli</i> BirA	AviTag Ct	NdeI; XmaI	Roche	AviTag
pIVEX2.1MCS AvPEX2	4.3	hu. PEX2	AviTag Nt.	NdeI; XmaI	Roche	Template for N-terminal AviTag-Module
pIVEX2.1MCS BirA	4.6	<i>E.coli</i> BirA	--	NdeI; XmaI	Roche	Template for T7P-Module
pIVEX2.1MCS HDAC1Av	5.1	hu.HDAC1	AviTag Ct.	NotI; SacI	Syngen	Template for C-terminal AviTag-Module
pIVEX2.1MCS PEX2Av	4.3	hu. PEX2	AviTag Ct.	NdeI; XhoI	Syngen	Template for T7T-Module
pIVEX2.3MCS γ2(his) ₆	4.1	γ crystallin	(his) ₆ Ct.	Nde; XhoI	Roche	Universal-Vector for γ-crystallins
pIVEX2.3 RDno	3.9	"No Stalling"	Spacer	EcoRI; XhoI	Roche	ribosome display spacer no attenuating sequences
pIVEX2.4a	3.5	--	(his) ₆ Nt.		Roche	Template for N terminal (his) ₆
pIVEX2.4d RD	3.9	"Stalling"	Spacer	NdeI; XhoI	Roche	ribosome display spacer with attenuating sequences
pUC18	2.7	Universal		PstI; EcoRI; NdeI	Roche	Cloning of mini-BP4 Cloning of PEX2
pDSPEX	4.1	PEX2	--	SacI; NotI	Roche	Expression vector PEX2

3.7 DNA-Modules

Module	PCR- template
T7Pg10ε	pIVEX2.1MCS BirA
T7P (his) ₆ FXa	pIVEX2.4a
T7P AviTag FXa	pIVEX2.1MCS AvPEX2
T7T	pIVEX2.1MCS HDAC1Av
FXa AviTag T7T	pIVEX2.1MCS HDAC1Av
Ribosome Display Spacer "NoStalling"	pIVEX2.4d RD NO
Ribosome Display Spacer "Stalling"	pIVEX2.3 RD
FXa (his) ₆ T7T	pIVEX2.3MCS

3.8 Buffers and solutions

10x DNA sample buffer	4% (w/v) Xylencyanol 50 % (v/v) Glycerol
10xTAE-running buffer	400 mM TRIS/Acetate (pH 8.0) 10 mM EDTA
10x PBS-buffer	0.1 M NaH ₂ PO ₄ ; 0.01 M KH ₂ PO ₄ (10x pH 7.0; 1x pH 7.4); 1.37 M NaCl; 27 mM KCl
10x Washing buffer	0.5 M Tris; pH 7.5 (4°C) adjusted with AcOH
WP Ribosome Display	1.5 M NaCl; 0.5 M Magnesiumacetate
10x Elution buffer EP	0.5 M Tris pH 7.5 (4°C) adjusted with AcOH
Ribosome Display	1.5 M NaCl; 200 mM EDTA
Lysis buffer	50 mM NaH ₂ PO ₄ (pH 8.0) adjusted with NaOH 300 mM NaCl; 20 mM Imidazol; 1 mM 2-Mercapthoethanol; 1 mg/ml lysozyme, 5 mM Pefabloc; 0.5% TWEEN 20 (v/v);
RedOx A: Refolding buffer mini-BP4	50 mM Tris (pH 8.0) adjusted with HCl 200 mM Arginin; 1 mM GSH; 1 mM GSSG
Oxidation B: Oxidation buffer mini-BP4	50 mM Na ₂ HPO ₄ (pH 8.0) adjusted with NaOH 300 mM NaCl; 20 mM Imidazol; 0.05% TWEEN 20; 20µM CuSO ₂
Reduktion C: Reducing buffer mini-BP4	10 mM HEPES (pH 8.0) adjusted with NaOH 10 mM DTT; 3 mM EDTA; 150 mM NaCl; 0.005% Polysorbat 20 (v/v)
IMAC-10: washing buffer	50 mM NaH ₂ PO ₄ (pH 8.0) adjusted with NaOH 300 mM NaCl; 10 mM Imidazol; 0.5% TWEEN 20 (v/v);
IMAC-20Me: washing buffer	50 mM NaH ₂ PO ₄ (pH 8.0) adjusted with NaOH 300 mM NaCl; 20 mM Imidazol; 1 mM 2-Mercapthoethanol; 0.5% TWEEN 20 (v/v);
IMAC-20: washing buffer	50 mM NaH ₂ PO ₄ (pH 8.0) adjusted with NaOH 300 mM NaCl; 20 mM Imidazol; 0.5% TWEEN 20 (v/v);
IMAC-250Me: elution buffer	50 mM NaH ₂ PO ₄ (pH 8.0) adjusted with NaOH 300 mM NaCl; 250 mM Imidazol; 1 mM 2-Mercapthoethanol; 0.5% TWEEN 20 (v/v);
IMAC-500: elution buffer	50 mM Tris (pH 8.0) adjusted with HCl 300 mM NaCl; 500 mM Imidazol; 0.5% TWEEN 20 (v/v); 200 mM Arginin; 1 mM GSH; 1 mM GSSG
TE	buffer 10 mM Tris (pH 8.0) 1 mM EDTA
Denaturing buffer	100 mM TRIS/HCl (pH 7.5) 6 M GdnCl/HCl; 10 mM DTT
Complete EDTA Free Inhibitor Cocktail	1 Tablette resolved in 1.5 ml PCR Wasser
Blocker® 10% BSA in PBS	10 mM NaH ₂ PO ₄ (pH 7.4) 10% BSA 150 mM NaCl, Kathon® storage at 4 °C
tRNA Stock	1mg/ml (<i>E. coli</i> MRE 600 tRNA) in PCR water storage at -20 °C
Camp Stock 1000x	25 mg / ml CAMP in EtOH storage at -20 °C
TBS buffer	200 mM TRIS-HCl (pH 7.5) 500 mM NaCl
TBS-T buffer	200 mM TRIS-HCl (pH 7.5) 500 mM NaCl, 0.05 % TWEEN 20
TBS-CaCl ₂ buffer	100 mM Tris (pH 7.2) 150 mM NaCl, 1 mM CaCl ₂
PBST-buffer	10 mM NaH ₂ PO ₄ ; 1 mM KH ₂ PO ₄ pH 7.4 137 mM NaCl; 2.7 mM KCl 0.1 % TWEEN 20

PBST-ME-buffer 10 mM NaH₂PO₄; 1 mM KH₂PO₄ pH 7.4 137 mM NaCl; 2.7 mM KCl 0.1 %
TWEEN 20, 1 mM 2-Mercapthoethanol

3.9 *E.coli* strains

For the cloning and propagation of plasmid DNA the *E.coli* strain XL-2 blue was used (Stratagene). For the expression of γ crystallin derivatives the *E.coli* strain BL21 codon plus was used.

<i>E.coli</i> strain	Genotype
XL-2Blue	recA1 endA1 gyrA96 thi-1 hsdR17 supE44 relA1 lac [F'proAB lacqZ β M15 Tn10 (Tet') amy Camr]a
BL21Codon plus.	<i>E.coli</i> B F- ompT hsdS(rB- mB-) dcm+ Tetr gal β (DE3) endA Hte [argU ileY leuW Camr]*

3.10 Cell culture media

Culture media were produced as described (Sambrook and Russell 2001). LB-Agar was produced by addition of 15 g/l Bactoagar (Difco) before sterilisation. For the antibiotic selection after sterilisation 100 μ g/ml ampicillin or 50 μ g/ml kanamycin was added to the medium at 50 °C. The medium consisted of 17 g/l bactotrypton; 10 g/l bacto yeast extract; 5 g/l NaCl

3.11 Transformation of chemical competent *E.coli* cells

Plasmid-DNA transformation of chemical competent *E.coli* cells was performed on ice (Hanahan 1983) and (Cohen *et al.* 1972). 20 μ l cell suspension was supplemented with 200 ng Plasmid-DNA. 30 min incubation on ice. The cells were heat-shocked for 90 sec at 42 °C and were incubated for 10 min on ice. After addition of 450 μ l LB-Medium the transformants were incubated at 37 °C for 45 min under shaking at 250 rpm. 200 μ l suspension was plated on antibiotic-selective LB-agarplates. The plates were incubated at 37 °C until bacterial colonies were visible.

3.12 Cultivation and conservation of *E.coli* strains

E.coli strains were cultivated in LB-medium at 37 °C under supplementation of the respective antibiotics. Cell-growth was performed in culture-tubes and in Erlenmeyer shaker flasks (shaker, 250 rpm). The cultures were inoculated from a single colony or from a glycerol cell-storage. The optical density (OD) of the cell suspension was measured at 600 nm. 1 OD equals to 10x⁹ cells per ml. For the long-term storage 0.5 ml of cell suspension was mixed with 0.5 ml 96 % glycerol. The mixture was shock-frozen in l.N₂ and stored at – 80 °C.

3.13 Isolation of Plasmid-DNA from *E.coli* cells

1 µg to 5 µg Plasmid-DNA was isolated with the Qiagen QIAprep Spin Miniprep Kit according to the manufacturer's instructions and to the method of (Birnboim *et al.* 1979) If more plasmid-DNA was needed the Qiagen Plasmid Maxi Kit was used.

3.14 Determination of the DNA-concentration and -purity

Double stranded DNA was spectrometrically quantified. The absorption was measured at 260 nm (OD₂₆₀) and 280 nm (OD₂₈₀) and the DNA-amount of the sample was calculated according to the method of Warburg and Christian (Warburg *et al.* 1941). The purity of the DNA was determined by the ratio (OD₂₆₀) / (OD₂₈₀). The ratio of the DNA-samples used in this study was always beyond 1.8. The measurements were performed in TE-buffer according to Sambrook (Sambrook *et al.* 2001). The DNA-concentration and -purity was determined by comparison to pre-quantified DNA-molecular weight standards using the Lumi-Imager F1 Workstation and the Lumianalyst Software.

3.15 Agarose-gel electrophoresis

Analytical and preparative separation of DNA fragments according to their molecular weight was performed after electrophoresis in agarose-gels (1 % w/v). 1.5 g of multi purpose agarose (Roche) were boiled for 6 min in 1 x TAE buffer (10 x TAE-buffer: 400 mM TRIS/Acetate (pH 8.0) 10 mM EDTA) in a microwave. After chilling to 60 °C 100 µg ethidiumbromide were applied to the solution and the slurry was casted into a horizontal gel-chamber. After the gel was polymerized, 6 µl DNA-containing samples were spiked with 4 µl 10x DNA sample buffer (4 % (w/v) Xylenecyanol, 50 % (v/v) Glycerin). The electrophoresis was performed with constant voltage at 110 V. The electrophoresis buffer was 1 x TAE. DNA was identified by the fluorescence of the intercalating ethidiumbromide-cation. (Excitation 254 nm - 366 nm, Emission 590 nm). The molecular weight was determined by comparison with DNA molecular weight markers.

3.16 Isolation and purification of DNA-fragments from agarose-gels

The extraction of DNA-fragments from agarose-gels was using the Qiagen QIAquick Gel Extraction Kit. The protocol was performed according to the manufacturer, based on the method of Vogelstein and Gillespie (Vogelstein *et al.* 1979).

3.17 Dephosphorylation of vector DNA

To suppress the religation of vector-DNA, enzymatically restricted vector-DNA was dephosphorylated by alkaline phosphatase according to the manufacturer's instructions.

3.18 Enzymatic DNA-Ligation

Enzymatic ligation of isolated DNA-fragments was performed using T4-DNA ligase according to the manufacturer's instructions (Roche). 150 ng restriction-digested and dephosphorylated vector-DNA was supplied with a five-fold molar excess of digested DNA-insert. Ligation reaction was performed at RT for 10 min. The ligation product was transformed into chemical competent *E.coli* cells.

3.19 Enzymatic restriction of DNA

0.5 µg to 1 µg double-stranded DNA fragments or plasmid DNA were incubated with restriction endonucleases according to the manufacturer's instructions. A simultaneous digestion with two compatible restriction enzymes performed the sequence-specific digestion of DNA-fragments.

3.20 DNA sequence analysis

DNA-fragments and vector-DNA were sequenced by Fa. Sequiserve (Vaterstetten) according to the method of Sanger (Sanger *et al.* 1977)

3.21 Polymerase Chain Reaction (PCR)

PCR was performed to amplify template DNA (Mullis *et al.* 1987), to determine the cloning-efficacy (Gussow *et al.* 1989), to synthesize transcriptionally active DNA-transcripts (Horton *et al.* 1989),(Kain *et al.* 1991) and to generate randomized gene-libraries and *de novo* genes. With the exception of the single colony PCR and the error-prone PCR the *Pwo* DNA-Polymerase was used according to the manufacturer's instructions (Roche). All standard *Pwo*-PCRs were assembled as 100 µl assays supplied with 10 µl 10x MgSO₄ *Pwo*-PCR buffer (as supplied from the manufacturer), 200 µM dNTPs and 2.5 units *Pwo* DNA-polymerase. The forward and reverse primers were typically supplied at 1 µM each. The temperature- and time-profiles were calculated according to the physical parameters of the template-DNA and the oligonucleotide primers. For the calculation of these data the software Vector

NTI suite, Vers. 8, (Informax) was used. The identity and accuracy of the PCR-products were confirmed by DNA-sequencing.

3.21.1 Introduction of restriction sites

DNA-fragments, which were to be cloned into vector DNA were amplified with sequence-specific terminal primers, which introduced flanking DNA-sequences, encoding endonuclease restriction sites. 30 PCR cycles were performed to amplify the DNA-fragments using the hot-start method (D'Aquila *et al.* 1991).

3.21.2 Colony PCR

The single colony PCR (Gussow *et al.* 1989) was performed to analyze a bacterial clone for the uptake of a plasmid after a plasmid-transformation. The plasmid was analyzed for the content of an insert with correct length. A 50 µl Expand High Fidelity PCR (Roche) was assembled: An insert-specific primer and a plasmid-specific primer at 0.2 µM each; 200 µM dNTPs PCR Nucleotide Mix; 2.5 U Polymerase-Mix (*Taq*, *Tgo*); in 1 x Expand High Fidelity PCR buffer containing 1 mM MgCl₂. A portion of a single bacterial colony was transferred into the mixture. The plasmids within the bacteria served as a template during the PCR amplification.

3.21.3 Production of DNA-modules

Double stranded, blunt-end DNA-fragments (Promotor- and Terminator-modules) were amplified from vector-templates in 30 cycles by standard *Pwo*-PCRs. The PCR-products were subjected to an agarose gel-electrophoresis and were purified from a preparative 1 % agarose-gel. The DNA was spectrometrically quantified and was aliquoted in 10 µl TE-buffer at 70 ng/µl. The aliquots were stored at – 20 °C until use. The DNA sequences of the modules and the terminal primer-oligonucleotides (red) used for their amplification are referred in the appendix.

3.21.4 Overlapping Extension Ligation PCR (OEL)

Linear Expression Elements (Sykes *et al.* 1999) were modularly assembled by a two step-PCR protocol, using the overlapping DNA ligation principle (Shuldiner *et al.* 1991) (Ho *et al.* 1989) In a standard *Pwo*-PCR an intron-less open reading frame was amplified by sequence-specific terminal bridging primers, which generated overlapping homologous sequences to flanking DNA sequences. 2 µl of the first PCR

mixture containing approximately 50 ng of the elongated gene-fragment were transferred into a second *Pwo*-PCR mixture. The mixture was supplied with 50 ng to 100 ng of preproduced (see paragraph 3.7) DNA-fragments and respective sequence specific, terminal primers at 1 μ M each. Typically, this second PCR-step comprized 30 cycles. The physical parameters of the PCR profiles were adjusted according to the requirements of the DNA-fragments to be ligated.

3.21.5 Production of the LEE T7Pg10 ϵ -HDACI- FXaAviTagT7T

The human HDACI-gene was amplified in a standard *Pwo*-PCR from 10 ng plasmid template pDSHDACI (Roche) using the bridging primer 5'-GTTTAACTTTAAGAAGGAGATATACATATGAGCGGCCGCGCTCAAACCTCAAGG-3' and 5'-GCTTCGAAGATGTCGTTTCAGACCG TCGACGGCTAGCTTGACCTCC-3'. The PCR-product was purified from an agarose-gel and quantified. 70 ng of the PCR-product were fused by OEL-PCR to the DNA-modules T7Pg10 ϵ and FXaAviTagT7T using the primers T7Pforw. and XAvT7Trev. (see paragraph 9).

3.21.6 Production of the LEE T7PAviTagFXa-PEX2-T7T

The human PEX2-gene was amplified in a standard *Pwo*-PCR from 10 ng plasmid template pDSPEX2 (Roche) using the bridging primer 5'-GTTTAACTTTAAGAAGGAGATATACATATGCCTGAAATCTGCAAACAGGATATCG-3' and 5'-GTCGTTTCAGACCACGACCCTCGATGCAGCCTAGCCAGTCGGATTTGATGC-3'. The overlapping gene was fused by an OEL-PCR to the DNA-modules T7PAviTagFXa and T7T using the primers T7P forw and T7Trev (see paragraph 9).

3.21.7 Production of the LEE T7PbirAT7T

The *E.coli* gene *birA* was amplified in a standard *Pwo*-PCR from 50 ng plasmid template pACYCY184 *birA* using the bridging primer 5'-GCTCCAAGCGCTCCCGGGAGCTCATTATTTTTCTGCACTACGCAGGG-3' and 5'-GTTTAACTTTAAGAAGGAGATATACATATGAAGGATAACACCGTGCC-3'. The overlapping gene was fused by an OEL-PCR to the DNA-modules T7Pg10 ϵ and T7T using the primers T7P forw. and T7Trev. (see paragraph 9).

3.21.8 Synthesis of the ribosome display spacers „Stalling“ and „NoStalling“

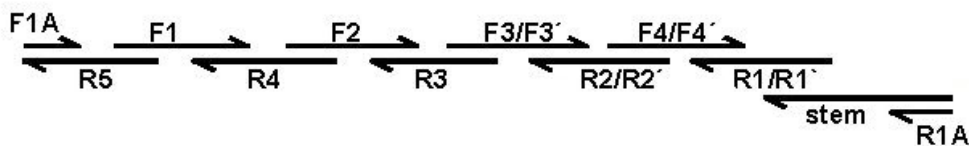


Fig. 6: The ribosome display spacers “Stalling” and “No Stalling” were synthesized by template-free PCR. For the synthesis of the spacer “Stalling” the oligonucleotides F3, F4, R1 and R2 were replaced by F3', F4', R1' and R2'. The oligonucleotides are referred in the appendix.

For the template-free PCR synthesis of the ribosome display spacer “Stalling” the terminal primers F1A and R1A were used at 1 μ M each and the primers F1, F2, F3, F4, stem, R1, R2, R3, R4 and R5 were used at 0.2 μ M each. For the synthesis of the ribosome display spacer “NoStalling” the primers F3, F4, R1 and R2 were replaced by the primers F3', F4', R1' and R2' at 0.2 μ M each. The syntheses of the 345 bp sequences were performed in standard 100 μ l *Pwo*-PCRs. The PCR profile was: TIM: 1 min 94 $^{\circ}$ C, TM: 20 sec 94 $^{\circ}$ C, TA: 40 sec 60 $^{\circ}$ C, TE: 30 sec 72 $^{\circ}$ C, 25 cycles, TFE: 2 min 72 $^{\circ}$ C. The PCR-product was gel-purified and reamplified with the cloning-primers EcoRI-forw and XhoI-rev in a standard *Pwo*-PCR and the above-described PCR-profile. The PCR-product was subcloned via the EcoRI and XhoI restriction sites into the vector pIVEX 2.3 MCS and the insert was confirmed by sequencing. The spacer modules were amplified in standard *Pwo*-PCRs from the vector template with the primers F1A and R1A at 1 μ M each. The PCR products were gel-purified and spectrophotometrically quantified. The DNA was aliquoted at 70 ng/ μ l in TE buffer and stored at -20 $^{\circ}$ C.

3.21.9 Synthesis of 32 specifically mutated mini-BP4 gene-constructs

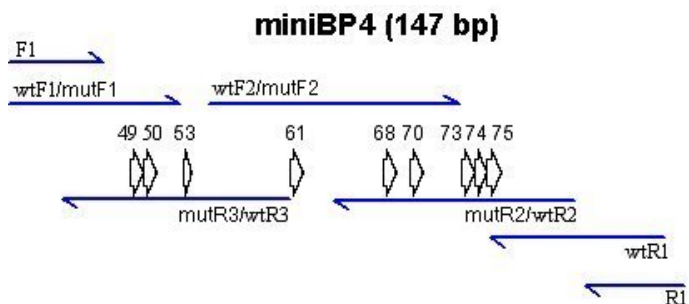


Fig. 7: The 147 bp mini-BP4 gene-constructs were synthesized by template-free PCR. One construct was assembled by 7 oligonucleotides (blue arrows). Single mutations were introduced by the exchange of one or two wild type primers versus site directed mutated primers (e.g. wtF2 by mutF2 to generate a mutation at position 61). Black arrows: amino acid mutation coordinates based on the mini-BP5 nomenclature.

For the template-free PCR synthesis of 32 mini-BP4 constructs 55 different oligonucleotides were used (see appendix). Each construct was assembled by a combination of 7 primers. All PCR assays contained the terminal primers F1 and R1 at 1 μ M each. For the synthesis of a specific gene-construct the PCR contained 5 specific oligonucleotides at 0.25 μ M each. The PCR-profile was: TIM: 1 min at 94 $^{\circ}$ C, TM: 20 sec 94 $^{\circ}$ C, TA: 40 sec 50 $^{\circ}$ C, TE: 30 sec 72 $^{\circ}$ C, 25 cycles, TFE: 3 min 72 $^{\circ}$ C.

3.21.10 Generation of 32 T7P(his)₆FXa-miniBP4-FXaAviTagT7T LEEs

To generate 32 T7P(his)₆FXa-miniBP4-FXaAviTagT7T Linear Expression Elements, an OEL-PCR was performed as described under the paragraph "Overlapping Extension Ligation PCR". In the first PCR-step the bridging primers T7Ph6Xa_BP4 5'-CATCATAGCAGCGGCATCGAAGGTCGTGCGTTAGGCTTAGGTATGCC-3' and BP4_XaAvT7T 5'-CGAAGATGTCGTTTCAGACCACGACCCTCGATCGCTTCAATTTCCGCTAATTCC-3' introduced sequence-overlaps and in the second PCR-step the DNA-modules T7P(his)₆Xa and FXaAviTagT7T were fused to the overlapping genes using the terminal primers T7Pfor. and FXAvT7Trev. (see paragraph 9). The identity and sequence accuracy of the Linear Expression Elements were confirmed by sequencing.

3.21.13 Synthesis of the PEX2 DNA library

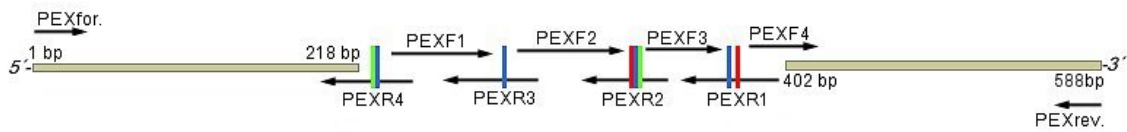


Fig. 9: Synthesis of the PEX2 gene-library. 8 randomized positions are colored. The reverse primers PEXR1, PEXR2, PEXR3 and PEXR4 introduced the NNK triplets. Together with the forward primers PEXF1, PEXF2, PEXF3, PEXF4 the fragment 196 bp - 432 bp was synthesized by template-free PCR. The flanking fragments were preproduced by PCR and were ligated via OEL-PCR to the library PCR-fragment

The PEX2 triplet codons coding for the amino acid coordinates Q64, E65, R86, K112, N113, K114, V130 and K132 were randomized by NNK-motives. The human wild type PEX2 DNA sequence was divided up into three sequence sections. A standard *Pwo*-PCR, which was supplied with 10 ng Vector-template pIVEX2.1MCS PEX2 and the primers PEXfor and PEXR4 at 1 μ M each amplified the 1 bp - 218 bp fragment. The 402 bp – 605 bp fragment was amplified in a standard *Pwo*-PCR with 10 ng Vector-template pIVEX2.1MCS PEX2 and the primers PEXF4 and PEXrev at 1 μ M each. The sequence 196 bp – 432 bp formed overlaps with the DNA fragments 1 bp - 218 bp and 402 bp – 605 bp and was synthesized by template-free PCR with the primers PEXF1 and PEXR1 at 1 μ M each and PEXR3, PEXR2 and PEXF2 at 0.25 μ M each. The PCR-profile was the same for all three PCRs: TIM: 1 min 94 $^{\circ}$ C, TM: 20 sec 94 $^{\circ}$ C, TA: 30 sec 60 $^{\circ}$ C, TE: 15 sec 72 $^{\circ}$ C, 25 cycles, TFE: 2 min 72 $^{\circ}$ C. The full length randomized PEX2 sequence (588 bp) was obtained when 70 ng of each DNA sequence-fragment was applied to a standard *Pwo*-PCR with the bridging primers T7P_PEX2 5'-GTTTAACTTTAAGAAGGAGATATACATATGCCTGAAATCTGCAAACAGG ATATCG-3 and PEX2_RD 5'-CCTGCACCAGCTCCAGAGCCAGCGCAGCCTAGCCAGTCGGATT TGATGC-3 at 1 μ M each. The PCR-profile was: TIM: 1 min 94 $^{\circ}$ C, TM: 20 sec 94 $^{\circ}$ C, TA: 30 sec 60 $^{\circ}$ C, TE: 60 sec 72 $^{\circ}$ C, 25 cycles, TFE: 5 min 72 $^{\circ}$ C. The bridging primers introduced homologous DNA overlaps for an assembly of the PEX2 gene-library into a ribosome display template by OEL-PCR (see paragraph 3.23.3).

3.21.14 PCR-mutagenesis of γ crystallin constructs

The γ crystallin gene-construct 12/A5-2 was amplified in a *Pwo*-PCR from 10 ng template vector pET20bplusSPC12/A5-2 with the primers T7P_12/A52 5'-GTTTAACTTTAAGAAGGAGATATACATATGGGTTTTATCTTTTTCTGTGAAGACC-3' and Univ_RD 5'-GCCTGCACCAGCTCCAGAGCCAGCGTACAAATCCATGACTCGTCTAAGAGAGC-3' at 1 μ M each. The γ crystallin construct 13/B11-2 was amplified in a standard *Pwo*-PCR from 10 ng template vector pET20bplus SPC13/B11-2 with the primers T7P_13/B11-2 5'-GTTTAACTTTAAGAAGGAGATATACATATGGGTGATATCCAGTCCGTGAAGACCGTGC-3' and Univ_RD at 1 μ M each. The PCR-products were fused by OEL-PCR to the DNA-modules T7Pg10 ϵ and the "NoStalling" ribosome display spacer as described in the paragraph 3.23.3. The PCR profile for this assembly was TIM: 1 min 94 °C, TM: 20 sec 94 °C, TA: 30 sec 60 °C, TE: 70 sec 72 °C, 30 cycles, TF: 7 min 72 °C. The ribosome display templates T7Pg10_12/A5-2_"NoStalling" and T7Pg10_12/A5-2_"NoStalling" were purified from a preparative 1 % agarose gel. Random PCR-mutagenesis (Cadwell *et al.* 1994) was performed with both templates. The GeneMorph II Random Mutagenesis Kit was used according to the instructions of the manufacturer. A 50 μ l PCR mixture was assembled as follows: 200 μ M dNTP's from the kit, 250 ng/ μ l of the oligonucleotide-primer T7Pforw and R1A, 5 U Mutazyme II DNA Polymerase, 50 ng ribosome display template-DNA in 1x Mutazyme II reaction buffer. The PCR profile was as described above. The PCR-products were quantified using the LUMI Imager System.

3.22 Cell-free *in vitro* transcription and translation

According to the instructions of the manufacturer, Linear Expression Elements were transcribed and translated in the RTS 100 HY *E.coli* System. 100 ng – 500 ng linear DNA template were incubated at 30 °C. Optionally 6 μ l GroE-supplement (Roche) was added.

3.22.1 Site-specific biotinylation of fusion proteins

The RTS 100 *E.coli* HY System was modified for the sequence specific, enzymatic biotinylation. 60 μ l RTS mixture were assembled according to the manufacturer's instructions. The mixture was supplemented with 2 μ l stock-solution Complete EDTA-Free Protease Inhibitor, 2 μ M d-(+)-biotin, 50 ng T7P_BirA_T7T Linear Expression Element (1405 bp), coding for the *E.coli* Biotin Ligase (BirA, EC 6.3.4.15) and 100 ng to 500 ng linear template coding for the substrate fusion-protein. The substrate fusion

protein was N- or C-terminally fused to a Biotin Accepting Peptide sequence (BAP). In all experiments a 15-mer variant of sequence #85 as identified by Schatz (Schatz 1993; Beckett *et al.* 1999) was used (Avitag, Avidity Inc., Denver, Colo. USA). Biotin Ligase was coexpressed from the linear template T7Pg10ε_birA_T7T (see paragraph 3.21.7).

3.23 Ribosome Display Protocol

All buffers were kept on ice. All devices were sterile, DNase- and RNase-free. The workbench was cleaned with RNase-ZAP.

10x Washing buffer WB Ribosome Display	0.5 M Tris; pH 7.5 (4 °C) adjusted by AcOH, 1.5 M NaCl; 0.5 M magnesiumacetate, store at -20°C
10x Elution buffer EB Ribosome Display	0.5 M Tris pH 7.5 (4 °C) adjusted by AcOH, 1.5 M NaCl; 200 mM EDTA, store at -20 °C
10 ml Ribosome Display Washing buffer (WB)	1200 µl 10x Stock WB pH 7.5, 0.05 % TWEEN 20 (50 µL 10 % TWEEN 20), 5 % BSA (5 ml Blocker BSA 10 %), 5 µg/ml t-RNA, 670 mM KCl (0.5 g KCl) ad. 10 ml with PCR-grade water
10ml Ribosome Display Stopbuffer (SB)	1200 µL 10x Stock WB pH 7.5, 0.05 % TWEEN 20 (50 µL 10 % TWEEN 20), 5 % BSA (5 ml Blocker BSA 10 %), 5 µg/ml t-RNA, 670 mM KCl (0.5 g KCl), 4 mM GSSG , 25 µM Camp (10µl Stock), ad. 10mL with PCR-grade water
2 ml Ribosome Display Elutionbuffer (EB)	200 µL 10x Stock EB, 0.25 % BSA (50 µl Blocker BSA 10 %), 5000 units r-RNA 16S-23S ribosomal, 5 µg/ml t-RNA, ad. 2 ml with PCR-grade water
Blocking Reagent	5 % BSA Puffer (2.5 ml Blocker BSA 10 %), 50 % Conjugate Buffer Universal

3.23.1 Preparation of the ectodomains erbB2 and erbB3

The human receptor ectodomains erbB2 and erbB3 were obtained from R&D Systems as receptor chimeras. The receptor ectodomains were genetically fused to the human protein IgG₁FC. Both molecules revealed a molecular mass of 96 kDa and contained a hexahistidine-peptide at their C-terminus. As a result of glycosation the apparent molecular weight of the proteins was increased to 130 to 140 kDa. The chimeric proteins were obtained as lyophilized proteins and were resolubilized in PBS buffer containing 0.1 % BSA. The proteins were stored at – 80 °C until use.

3.23.2 Coating of micro titre plates

One Reaction Volume (RV) of an MT-plate was washed three times with Conjugate Buffer Universal. 2.5 µg ligand was resolved in 100 µl Blocking Reagent. Biotinylated ligands were alternately immobilized in the wells of Streptavidin- and Avidin-coated MT-plates. The erbB2/FC- and erbB3/FC-chimeras were immobilized alternately in the wells of protein A and protein G coated MT-plates. The ligand-solution was incubated for 1 h at room temperature in the MT-plate under 500 rpm shaking on the

Biorobot 8000 robotic shaker platform. To determine the background-signal a well was coated with 100 µl Blocking Reagent without ligand. The wells were washed with 3 RV Blocking Reagent. 300 µl Blocking Reagent were incubated in each well for 1 h at 4 °C and 200 rpm. Before the stopped translation-mixture was applied, the wells were washed with 3 RV ice-cold buffer WB.

3.23.3 Generation of ribosome display templates

For the standard ribosome display procedure a single gene or a gene-library was elongated with specific bridging primers (see paragraphs 3.21.5 to 3.21.12). The elongated DNA-fragments were fused by OEL-PCR to the DNA-modules T7Pg10ε and to one of the ribosome display spacers “Nostalling” or “Stalling” using the terminal primers T7Pfor 5'-GGTGATGTCGGCGATATAGGCGCCAGC-3' and R1A 5'-AAATCGAAAGGCCAGTTTTTCG-3'. The PCR profile for the PCR assembly was: TIM: 1 min 94 °C, TM: 20 sec 94 °C, TA: 30 sec 60 °C, TE: 60 sec for 1000 bp at 72 °C, 30 cycles, TFE: 5 min 72 °C.

3.23.4 Preparation of the ribosome display translation mixture

The RTS *E.coli* 100 HY System was prepared according to the manufacturer's instructions. 100 µl of the mixture were supplemented with 40 units (1 µl) Rnasin, 2 µM (2 µl) anti ssrA-oligonucleotide 5'-TTAAGCTGCTAAAGCGTAGTTTTCGTCGT TTGCGACTA-3', 1 µL stock solution of Complete Mini Protease Inhibitor EDTA-free and 500 ng linear ribosome display DNA-template in 20 µl *Pwo*-PCR mixture. The ribosome display DNA-template was transcribed and translated in 1.5 ml reaction tubes at 30 °C for 40 min under shaking at 550 rpm. Complexes consisting of mRNA, ribosome and displayed polypeptide were stabilized when the reaction was immediately stopped with 500 µl ice-cold buffer SB. The mixture was centrifuged at 15.000 g at 2 °C for 10 min. The supernatant was transferred into a fresh, ice-cooled 1.5 ml reaction tube. 250 µl of the mixture were transferred into a ligand-coated MT-plate well (signal) and another 250 µl into a non-ligand coated well (background). The mixture was incubated for 1 h at 4 °C and 300 rpm on the shaker. To remove background protein and weak binding ternary complexes the wells were washed with ice-cold buffer WB. Messenger RNA from the bound ternary complexes was eluted by 100 µl ice-cold buffer EB for 10 min at 4 °C and 750 rpm.

3.23.5 Preparation of Protein G coated magnetic beads

Protein G coated magnetic beads were used to deplete the stopped ribosome display translation mixtures from protein derivatives, which unspecifically recognized IgG₁-FC binders. 100 µl of the magnetic bead suspension was equilibrated in stopping buffer SB by washing the beads five times in 500 µl buffer SB. The beads were incubated for 1 h at 4 °C in 500 µl buffer SB containing 50 µg IgG₁-FC protein. The beads were washed three times with buffer SB and were stored on ice in 100 µl buffer SB. Prior to their use the beads were magnetically separated and stored on ice. The stopped ribosome display translation mixture displaying crystallin derivatives was added to the beads. The mixture was incubated for 30 min at 4 °C at 750 rpm. Prior to use the beads were magnetically separated from the mixture.

3.23.6 Purification of mRNA and removal of remaining DNA

Messenger RNA was purified using the High Pure RNA Isolation Kit (Roche). Remaining DNA-template in the eluate was removed with a modified protocol of the Ambion DNA-free kit. 50 µl eluate were supplemented with 5.7 µl DNase I buffer and 1.3 µl DNase I containing solution. After incubation of the mixture at 37 °C for 30 min 6.5 µl DNase I inactivating reagent was added. The slurry was incubated in the digestion-assay for 3 min at room temperature followed by 1 min centrifugation at 11.000 g. The supernatant was used in the reverse transcription.

3.23.7 Reverse Transcription and cDNA amplification

For the reverse transcription of the mRNA the *C.therm* RT Polymerase Kit (Roche) was used. 20 µl reactions were assembled: 4 µl 5x RT buffer, 1 µl DTT solution, 1.6 µl dNTP's, 1 µl DMSO solution, 0.1 µM (1 µl) RT 5'-CAGAGCCTGCACCAGCTCCAGAGCCAGC-3', 40 units (1 µl) RNAsin, 1.5 µl *C.therm* RNA-Polymerase, 9 µl mRNA containing eluate. Transcription was performed for 35 min at 70°C. Further amplification of the cDNA was performed in 100 µl *Pwo*-PCRs containing 10 µl 10x *Pwo*-PCR buffer with MgSO₄, 200 µM dNTPs, 12 µl transcription mixture, 2.5 units *Pwo* DNA-Polymerase and the primers RT 5'-CAGAGCCTGCACCAGCTCCAGAGCCAGC-3' and F1 5'-GTTTAACTTTAAGAAGGAGATATACATATG-3' at 1 µM each. The PCR profile was TIM: 1 min 94 °C, TM: 20 sec 94 °C, TA: 30 sec 60 °C, TE: 60 sec 72 °C, 20 cycles, TFE: 5 min 72 °C. A reamplification by a standard *Pwo*-PCR was performed. 2 µl of the PCR mixture were transferred into a second standard *Pwo*-PCR. Gene-specific bridging

primers were used wherever possible (see paragraphs 3.21.13; 3.21.9 and 3.21.12). For the reamplification of γ crystallin derivatives the primers F1 and Univ_RD were used (see paragraph 3.21.14). The PCR-profiles were according to the physical parameters of the gene-templates and oligonucleotide-primers. 25 PCR cycles were performed. The gene-sequences were elongated with DNA overlaps to hybridize with the DNA-modules T7Pg10 ϵ and the ribosome display spacer „NoStalling“ in a further OEL-PCR like described in paragraph 3.23.3. The ribosome display DNA-templates were then reused in further ribosome display cycles.

3.23.8 Subcloning of genes after ribosome display

The PCR-products were subcloned into vector-systems as described under the paragraph 3.21.1 and 3.19. Mini-BP4 constructs were amplified with the primers PstI-Mini-BP4for 5'-CTTGCATGCCTGCAGATGGCGTTAGGCTTAGGTATGCC-3' and EcoRI-MiniBP4rev 5'-GATTACGAATTCGCTTCAATTCGCTAATTCC-3' and cloned by the PstI/EcoRI restriction sites into the pUC18-vector. The gamma crystallin derivatives were subcloned via the NdeI/XhoI restriction sites into the vectors pIVEX 2.3MCS and pET20bplus using the primers NdeI-crystfor 5'-GTTTAACTTTAAGAAGGAGATATACATATGGGTGATATCCAGTTCGGTG AAGACCGTGC-3' and XhoI-crystrev 5'-GCTCGCTCGAGGTACAAATCCATGACTCGTCTAAGAGAGC-3'. Library members of PEX2 were subcloned via the NdeI/EcoRI sites into the vector pUC18 using the primers NdeI-PEX2for 5'-CTGAGAGTGCACCATATGCCTGAAAT CTGCAAACAGG-3' and EcoRI-PEX2rev. 5'-CCATGATTACGAATTCGCAGCCTAGCCAGTCCGG-3'

3.24 Electrophoretic separation of proteins

Protein bands were resolved by continuous, denaturing electrophoresis under reduced conditions. Electrophoresis was performed in the vertical X Cell Sure Lock System (Invitrogen) connected to the power supply Power Ease 500 (Pharmacia) according to the manufactures instruction. The sample buffer for 12 % Bis-Tris gels was NuPage LDS Sample Buffer, for the 18 % Tris-Glycine gels Tris-Glycine SDS Sample Buffer was used (Invitrogen). Typically 3 μ l of the sample was centrifuged and diluted in 15 μ l Sample Buffer, 7 μ l water and 5 μ l 10x sample reducing agent (Invitrogen). After boiling at 95 °C for 7 min, 10 μ l were resolved on precasted gels (Invitrogen). Using 12 % Bis-Tris gels the anode- and cathode-buffer was the 1x MOPS SDS buffer. Using the 18 % Tris-Glycine gels the buffer was the 1x TrisGly SDS Running Buffer. The protein molecular weight standard was mark 12

(Invitrogen). 500 µl antioxidant was supplied to the anode-buffer to keep the samples reduced during electrophoresis.

3.25 Semi-Dry Western blotting

The transfer of proteins in a 0.22 µm nitrocellulose-membrane was performed electrophoretically with the semidry Multiphor II Apparat (Pharmacia) for 2 h and 100 mA according to Gravel (Gravel *et al.* 1987). The blot sandwich was wetted in 1 x transfer buffer containing 20 % methanol (Invitrogen). After the transfer the membrane was blocked for 2 h with 5 % Blocking Reagent (Roche) in TBS buffer containing 0.1 % TWEEN 20 (TBS-T).

3.26 Slot Blotting

Another method to transfer proteins from a gel into a 0.22 µM nitrocellulose-membrane was slot blotting under native conditions according to the method of Thomas (Thomas 1980) The Bio-Dot SF Microfiltration Apparatus from BioRad was used according to the instructions of the manufacturer. The membrane was prewetted in TBS-buffer. The Bio-Dot assembly was washed three times with TBS buffer. Typically 5 µl sample was diluted in 250 µl TBS-buffer and was soaked through the membrane, followed by extensive washing with TBS buffer. Subsequently the membrane was blocked in 5 % Blocking Reagent in TBST-buffer.

3.27 Detection of biotinylated polypeptides

Biotinylated proteins were detected with SA-HRP conjugate (Roche). The preblocked nitrocellulose-membrane was incubated for 45 min in TBS buffer containing 0.1 % TWEEN 20, 2.5 % Blocking Reagent (Roche) and SA-HRP conjugate at a dilution of 1: 15.000. The membrane was washed three times with 100 ml of TBS-T buffer. Chemiluminescent detection of biotinylated proteins was performed using the Western Blotting Substrate (Roche) and the Lumi Imager System (Roche) according to the manufacturers instructions.

3.28 Detection of the Flag-Epitope peptide

Polypeptides containing the flag-epitope peptide DYKDDDDK were detected after Western blotting by a monoclonal anti-flag IgG1-HRP conjugate (Sigma). The preblocked nitrocellulose-membrane was incubated for 45 min in TBS buffer

containing 0.1 % TWEEN 20, 2.5 % Blocking Reagent (Roche) and anti-flag IgG-HRP conjugate at a dilution of 1:100. The subsequent procedure was the same as described under paragraph 3.27.

3.29 Configuration of the robotic pipettor

The worktable of the BIORobot 8000 was configured as follows: XYZV-robotic arm; robotic handling system; dilutor system equipped with 8 pipetting channels configured as combination of four 300 µl tip-adapters supplied from 1000 µl dilutors and four 0.9 mm steel probes supplied from 2500 µl dilutors; technical tower with reagent carousel and computer controlled membrane pump; 8-channel dispenser head; wash station; cooling and heating system (VariTherm); high speed shaker system (Shaker); vacuum manifold (RoboVac); sensor arrays to detect the liquid levels in all liquid containers and the QIASoft 4.0 Software Operating System.

The 96-well small-scale affinity purification of cell-free expressed, hexahistidine-tagged fusion proteins was performed with the BIORobot-8000 workstation. A program-script was established to process RTS lysates with the devices of the Biorobot 8000 workstation.

3.30 Small-scale robotic affinity purification

The user had to define the parameters: sample number (8-96), incubation temperature (4 °C – 37 °C), incubation time (1 s – 86400 s), number of washing steps (1 - 100) of the Ni-NTA coated magnetic beads (Qiagen), the lysate-volume to be processed per well (5 µl – 70 µl) and the elution of the bead-immobilized fusion-proteins (yes/no).

A pre-calculated volume of the cell-free translation system was provided to the system in a 14 ml test-tube. The predetermined lysate volume was aliquoted into an MT-plate, which was temperature-equilibrated on the heating-cooling device on the workstation. 15 µl PCR-mixture containing a specific Linear Expression Element were transferred from a MT-plate source into the lysates. The lysates were incubated for the predetermined time and temperature. 20 µl of the 4 % Ni-NTA magnetic-bead suspension was distributed into the wells of a clean MT-plate destination on the shaker-platform. The beads were buffer-equilibrated by two times of washing with 200 µl IMAC-10 buffer under shaking at 750 rpm for 2 min. Finally the beads were resolubilized in 20 µl buffer IMAC-10 under shaking at 750 rpm for 2 min. The

incubated lysates were diluted 1:4 with IMAC-10 buffer and was incubated for 5 min under shaking at 750 rpm. The diluted lysates were transferred into the equilibrated bead suspensions and were incubated under shaking at 750 rpm for 30 min to bind the hexahistidine-tagged fusion proteins to the Ni-NTA bead surface. The mixtures were magnetically separated during the predefined number of 200 µl washing steps with IMAC-20 buffer under shaking at 750 rpm for 2 min. Optionally, bound (his)₆ fusion proteins were eluted from the beads with 60 µl IMAC500 buffer under shaking at 750 rpm for 10 min. The eluate was finally transferred into a clean MT-plate.

3.31 Spectrometrical determination of the protein concentration

The protein concentration was spectrometrically determined according to Beer Lamberts law: $E = \epsilon * c * d$ (ϵ : absorbance coefficient [$M^{-1} cm^{-1}$]; c : concentration [M]; d : pathlength [cm]). The extinction coefficient at 280 nm of the respective polypeptides was calculated using the software Vector NTI suite 8 according to the method of Edelhoch (Edelhoch 1967). For a reduced protein with the concentration 1 mg/ml in a cuvette with the layer thickness 1 cm the absorbance coefficient was calculated for hPEX2: 51590; hTIMP2: 33160, hIGF1: 4560.

3.32 Dialysis

Protein samples and cell-lysates were dialysed for 24 h at 4 °C and 120 rpm using Slide-A-Lyzer dialysis cassettes (PIERCE) or dialysis membranes (Spectrapor). The respective molecular weight cut-off was according to the molecular weight of the proteins to be dialysed. Dialysis cassettes were used with a MWCO from 3000 to 10000 kDa.

3.33 Ultrafiltration

Ultrafiltration was used to concentrate protein samples or to exchange buffers. For the ultrafiltration of small sample volumes the ultrafree-0.5 Centrifugal Filter Device (Millipore) was used according to the instructions of the manufacturer.

3.34 Fluorescence Spectroscopy

Fluorescence-measurements with PEX2 were performed as follows: Native PEX2 protein in 100 mM Tris/HCl pH 7.2, 150 mM NaCl, 1mM CaCl₂ was diluted to 4 µM PEX2 under stirring in denaturing buffer 100 mM Tris/HCl pH 7.5 with GdnCl/HCl

concentrations varying from 0 M to 6 M in concentration-steps of 0.5 M. The mixture was incubated for 30 min. The measurements were performed in temperature-equilibrated quartz-cuvettes with 1 ml volume and 10 mm pathlength at 15 °C. The excitation wavelength was 295 nm and the emission wavelength was determined by a scan from 300 nm to 450 nm. The device was the FluoroMax-2 Fluorimeter (Spex, Jobin Yvon).

3.35 Differential Scanning Calorimetry (DSC)

DSC-experiments were performed with the N-DSC II Nano Differential Scanning Calorimeter (Applied Thermodynamics) with a cell-volume of 299 µl to determine the transition temperature of native PEX2 under different chemical conditions. A reversible, isobar temperature-scan from 10 °C to 90 °C was performed with a heating rate of 2 °C/min and a constant pressure of 3.0 atmospheres. The measurements were performed according to the manufacture's instructions. PEX2 was measured in degassed PBS-buffer, in PBS buffer with 1 mM DDT and in PBS buffer with 1 mM EDTA. Native PEX2 protein was first reduced in PBS buffer containing 10 mM DDT for 10 min and subsequently alkylated by 15 mg/ml iodoacetic acid for 2 h at room temperature. To remove DDT and iodoacetic acid the alkylated PEX2 was dialysed (MWCO: 10.0000, Pierce slide-a-lyzer, Pierce) for 24 h at 4 °C versus PBS buffer. The respective dialysis buffer of each protein-sample was used for the calibration of the instrument's baseline and for the filling of the reference-cell. The thermograms were evaluated with the software CpCalc version 2.5.029s. The data were normalized by the subtraction of the respective buffer-baseline. The apparent transition-temperature was determined from the maximum peak of the thermogram.

3.36 ELISA for the detection of gamma crystallin derivatives

50 µl PBS-buffer with the proteins IgG1FC (2 µg/well), erbB2/Fcchimera (20 µg/well), erbB3/FC chimera (5 µg/well) and BSA (10 µg/well) were coated over night on a NUNC-MT-plate by hydrophobic-hydrophilic interactions. The wells were washed 3 times with PBST followed by blocking with 300 µl/well 3 % BSA/0.5 % TWEEN 20 in PBS for 2 h at 37 °C. The wells were again washed three times with with 300 µl PBST. Purified and quantified γ crystallin derivatives were applied at 50 µl/well and were incubated for 1 h at room temperature. The wells were washed three times with 300 µl PBST. A monoclonal, HRP-labeled antibody was used to detect immobilized γ

crystallin. The immune-conjugate was applied 1:1000 at 50 µl/well and was incubated for 1 h at room temperature. The wells were washed three times with PBST and three times with PBS to remove the TWEEN 20 detergent. 50 µl/well TMBplus substrate was applied and incubated at RT for 20 min. The HRP-substrate reaction was stopped with 50 µl/well 0.2 M H₂SO₄. The signal intensity was quantified with the ELISA reader at 450 nm with background-subtraction at 620 nm.

3.37 Expression and IMAC purification of γ crystallin derivatives

Competent *E.coli* BL21 *codon plus* cells were transformed with the pET20bplus plasmid encoding γ crystallin derivatives. The transformed cells were plated on LB-agar plates containing ampicillin at 100 µg/ml and chloramphenicol at 25 µg/ml. A single bacterial colony was transferred from the agar plate to inoculate a sterile 50 ml LB-medium/Amp/Camp overnight culture. 50 ml overnight culture was used to inoculate 1 L of sterile LB/Amp/Camp medium. Bacterial growth was performed at 37 °C under shaking at 130 rpm in 3500 ml Erlenmeyer flasks (with baffles). Protein expression was IPTG-induced at OD₆₀₀ = 0.8 at 30 °C for 12 h. Cells were harvested by centrifugation at 5000 g for 40 min. The cell pellet was resuspended in 50 ml lysis buffer. After 20 min incubation at RT the cells were sonified on ice until the suspension was no more viscous. The cell-lysate was centrifuged at 10.000 g for 30 min at 4 °C. The supernatant was charged at 2.5 ml/min on a Hi Trap Chelating column using the Äkta explorer sample pump. The column contained 5 ml Ni-NTA sepharose (CV = 5). The running buffer was IMAC-20Me buffer. The column was washed with 7 CV 10 % IMAC-500Me buffer. A linear elution gradient was applied in 15 CV from 10 % to 60 % IMAC-500 Me, followed by an isocratic 5 CV elution step of 100 % IMAC-250Me. The absorbance was measured at 280 nm and the elution was fractionated at 2.5 ml. Samples containing eluted protein were pooled and dialyzed over night at 4 °C versus PBS-buffer containing 1 mM 2-mercaptoethanol.

3.38 Biomolecular Interaction Analysis (BIA)

Real-time BIA (BIAcore 3000) uses surface plasmon resonance (SPR) to investigate interactions between biomolecules on the surface of a sensor-chip. (Granzow *et al.* 1992). One of the components is immobilized on a chip surface (ligand) and the second one is injected in free solution (analyte) to flow over the chip surface. Surface-adsorption of the analyte provokes an SPR response, which can be followed in real

time. The change of the SPR-angle is monitored in a sensorgram as Response Units (RU). 1 RU corresponds to 1 pg/mm² in surface mass protein concentration. The RU-signals are plotted as a time-dependent function, which enables the determination of kinetic data.

For the immobilization of biotinylated proteins on a streptavidin-coated sensor surface the BIAcore SA sensor chip was used. The BIAcore CM5 chip was used to immobilize proteins via an amine-coupling chemistry on the sensor chip. The equilibrium constant K_D (M⁻¹) was determined from sensorgrams using numeric models provided by the BIAcore 3000 Evaluation Software (Version 3.1). All methods were performed according to the instructions of the manufacturer (Amersham Pharmacia, BIAapplication Handbook, version AB).

4 Results

4.1 Generation of Linear Expression Elements (LEEs)

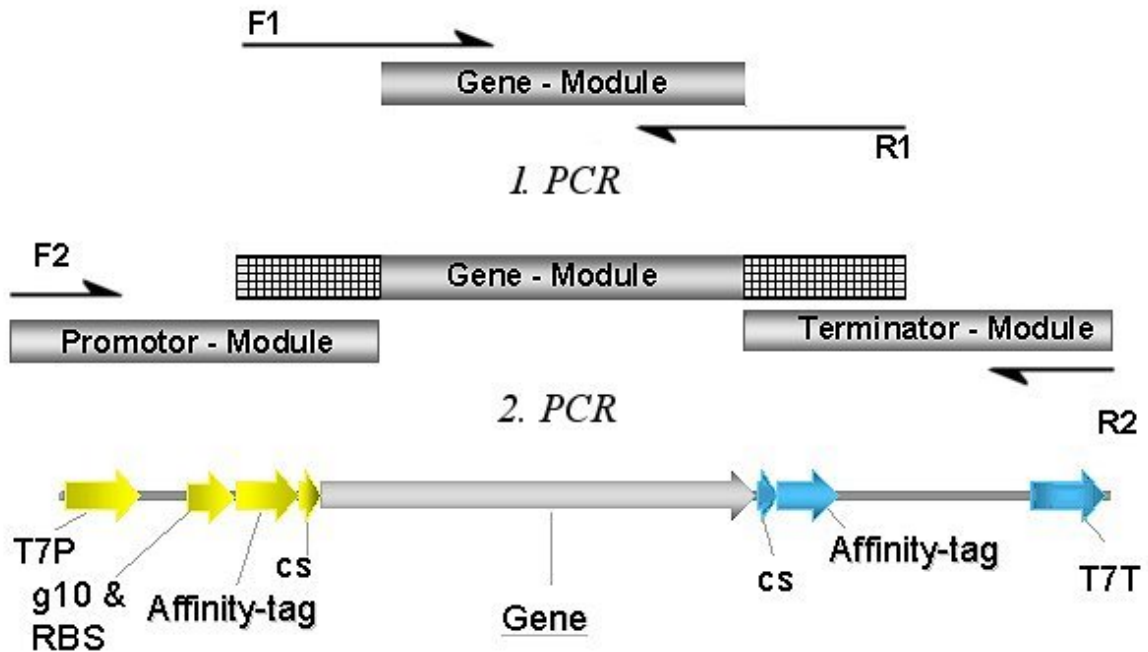


Fig.10: Generation of Linear Expression Elements (LEE). An intron-less gene (gene-module) is amplified by the primers F1 and R1. The gene-module is elongated by flanking sequences (1. PCR). In a second PCR the gene-module is fused to a promotor- and a terminator-module. The LEE is amplified by the terminal primers F2 and R2 (2. PCR). T7P: T7 RNA polymerase promoter; g10: gene 10 enhancer; RBS: ribosome binding site; cs: protease cleavage site; T7T: T7 RNA polymerase termination motive; Affinity-tag: peptide used for the affinity chromatography or the detection of expressed recombinant fusion protein.

The development of a rapid DNA-transcript generating method using the principle of the Overlapping Extension Ligation PCR was the basis to rapidly support *in vitro* coupled transcription and translation reactions with engineered gene constructs.

Conventional overlapping extension PCR protocols are mostly performed to ligate two DNA fragments (Ho *et al.* 1989; Kain *et al.* 1991; Shuldiner *et al.* 1991). This technique was extended adding a third DNA fragment to the reaction. A gene-transcript was segmented into the modules “promotor-module”, “gene-module” and “terminator-module” (see fig.10).

The engineered promotor-module encoded the T7 phage transcription promotor sequence, a translation control sequence RBS and the T7 phage *g10ε* enhancer sequence (Sang Soo Lee *et al.* 1991). These regulatory sequences enabled the coupled transcription and translation in the RTS 100 *E.coli* HY System. The terminator-modules encoded a translation stop-codon and a palindromic T7 phage termination motive. The use of the T7T motive instead of run-off transcripts was also reported to increase the yield of cell-free expressed proteins (Nakano *et al.* 1999). Optionally, the modules comprised DNA sequences encoding polypeptides, which were used in subsequent affinity purification or labeling procedures. Linear Expression Elements (LEEs) (Sykes *et al.* 1999) were assembled in a modular manner using three DNA modules (see fig. 10). In a first standard *Pwo*-PCR an intron-less open reading frame was amplified by sequence-specific flanking primer oligonucleotides, which introduced overlapping complementary sequences to the promotor- and terminator modules. The PCR-mediated ligation required a free hybridization energy of these complementary sequences, which had to be lower than $\Delta G = -25$ kcal/mol. This was achieved by sequence extensions, which were in average 25 bp in length. The primer oligonucleotides were designed to hybridize with the gene template at a temperature between 48 °C to 55 °C. This enforced the use of primer oligonucleotides with an average length of 45 bp to 55 bp. After 30 PCR cycles 2 µl of the first PCR mixture containing approximately 50 ng of the elongated gene-module DNA were transferred into a second PCR mixture. This PCR was supplied with 50 ng to 100 ng of the respective promotor- and terminator DNA-modules and sequence specific terminal primers. In the presence of a DNA polymerase the 3'-ends of the hybridized complementary DNA-fragments were enzymatically elongated to a full length DNA transcript (Barik 2002).

4.2 Preproduction of a DNA-module library

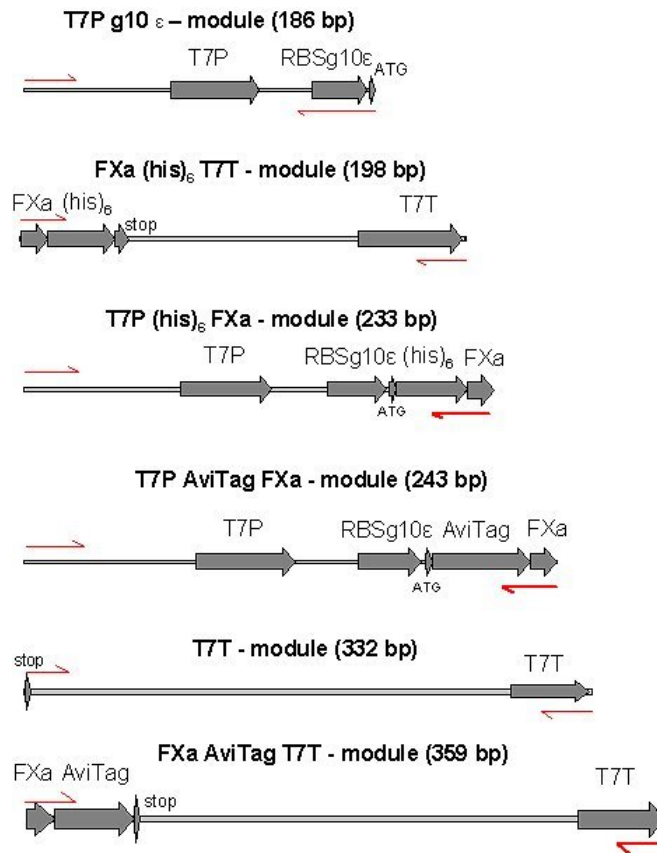


Fig. 11: Library of double stranded DNA modules for the use in the OEL-PCR. T7P: T7P-promotor, AviTag: 15 aa Biotin Accepting Peptide; (his)₆: hexahistidine-tag; FXa: factor Xa protease cleavage site; RBSg10 ϵ : Ribosome Binding Site implemented into the gene 10 sequence; T7T termination motive; primers for the amplification are red. The modules are referred in the appendix.

To rapidly support the OEL-PCR with desired DNA-fragments, a library of DNA-modules was pre-produced (see fig. 11). In order to obtain a sufficient yield of PCR-product it was a prerequisite to use HPLC purified primer oligonucleotides and a DNA polymerase with a 3'-5' exonucleolytic activity, producing blunt-end DNA fragments (Garrity *et al.* 1992).

4.3 Generation and Quantification of Linear Expression Elements (LEEs)

The quality and yield of the Linear Expression Elements produced by this method were determined. Exemplarily, the genes encoding the proteins PEX2, TIMP2, HDAC-I, BirA and GFP were fused to different combinations of DNA-modules. Two differently concentrated portions of each PCR-mixture containing the respective PCR-products

were electrophoretically resolved in an agarose-gel (see fig. 12). The concentration of the PCR-products was determined by a comparative densitometric quantification using the LUMI Imager System. The average PCR-product yield of the obtained Linear Expression Elements was 60 ng/μl ± 20ng/μl (ng DNA per μl of PCR-mixture). Using the *Pwo* DNA polymerase it was possible to generate LEEs up to 2 kb in length, like the T7P-HDAC1-FXaAviTagT7T DNA transcript (fig. 12, lane 9 and 10).

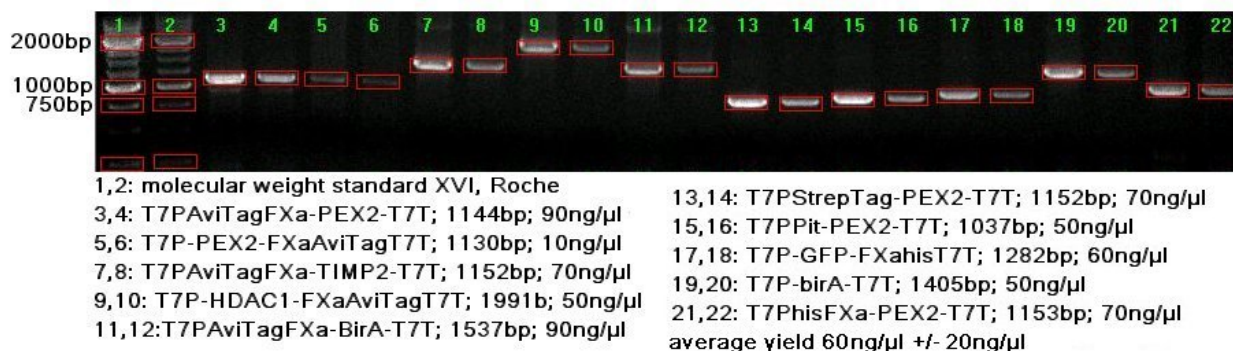


Fig. 12: 1 % EtBr-stained agarose gel with 10 different Linear Expression Elements produced by the Overlapping Extension Ligation PCR. From each PCR mixture two samples were applied 1:1 and diluted 1:2. The average PCR-product yield was determined by a comparative densitometric analysis versus the molecular weight standard. The average PCR-product yield was 60 ng/μl ± 20ng/μl. The longest fragment produced was the 1991 bp HDAC-1 transcript (lane 9 and 10).

4.4 Development of the cell-free enzymatic *in situ* mono biotinylation

The labeling of proteins to support structural and functional protein analyses is a striking advantage of a cell-free protein synthesis system (Budisa *et al.* 2004). To exploit the high affinity interaction (10^{-14} M) of biotin with streptavidin for the immobilization of biotinylated proteins on SA-coated SPR sensor surfaces, an enzymatic *in situ* monobiotinylation of cell-free expressed BAP-fused proteins was developed.

For this purpose the short BAP (15 aa) AviTag was found superior to the 1.3S transcarboxylase unit of *P. shermanii* or to BCCP (Schräml *et al.* 2002). The *E.coli* biotin ligase (BirA) accepts the Avitag peptide as a substrate and catalyzes the enzymatic monobiotinylation of a specific lysin in the peptide (see fig. 13). In order to obtain sufficient amounts of biotinylated fusion proteins the *in situ* monobiotinylation was optimized. BirA was coexpressed from a second LEE.

In order to preserve the translational resources of the cell-free system and to obtain a maximum yield of monobiotinylated protein, the optimal ratio of the supplied template DNAs was determined in an experiment.

The linear DNA-templates T7PAviTagFXa-PEX2-T7T and T7P-HDAC1-FXaAviTagT7T

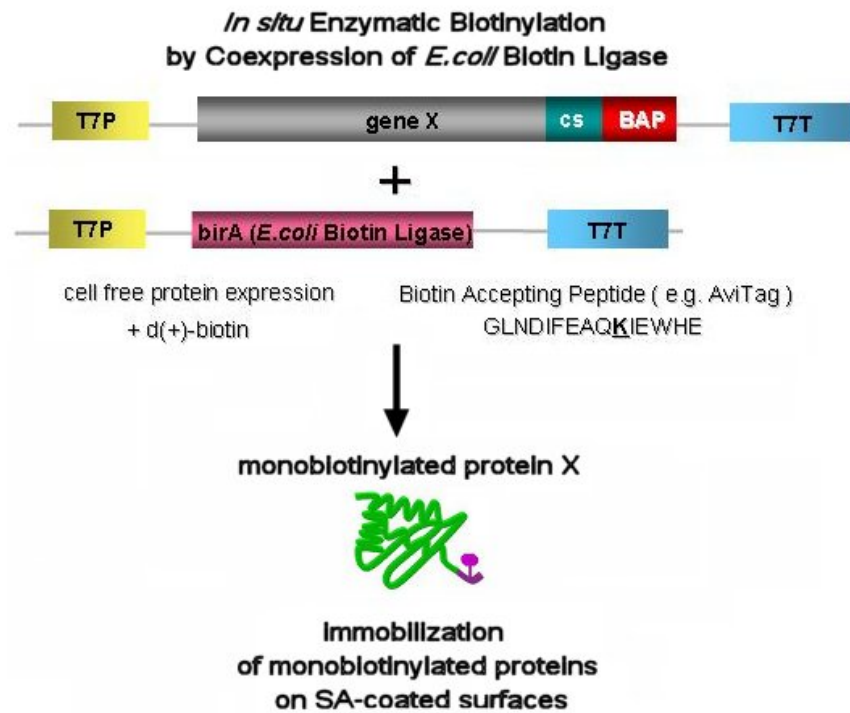


Fig. 13: Scheme of the cell-free enzymatic *in situ* biotinylation of biotin accepting peptide-fused proteins by coexpressed *E. coli* biotin ligase (BirA). Two Linear Expression Elements are simultaneously transcribed and translated into functional protein. In an ATP-dependent two step reaction (Fall 1979) the coexpressed BirA covalently attaches a single biotin moiety to the ϵ -amino group of a specific lysine within the AviTag peptide.

(see fig. 12) were transcribed and translated from constant amounts of DNA-template (see fig. 14). Since the addition of d-(+)-biotin was found to be necessary to obtain biotinylated fusion proteins the reactions were supplied with 2 μ M free d-(+)-biotin. After an incubation for 4 h at 30 °C soluble biotinylated protein was detected after Western blotting by SA-HRP conjugate. When either d-(+)-biotin or the BirA encoding DNA template was omitted no biotinylated Avitag-PEX2 protein was detectable.

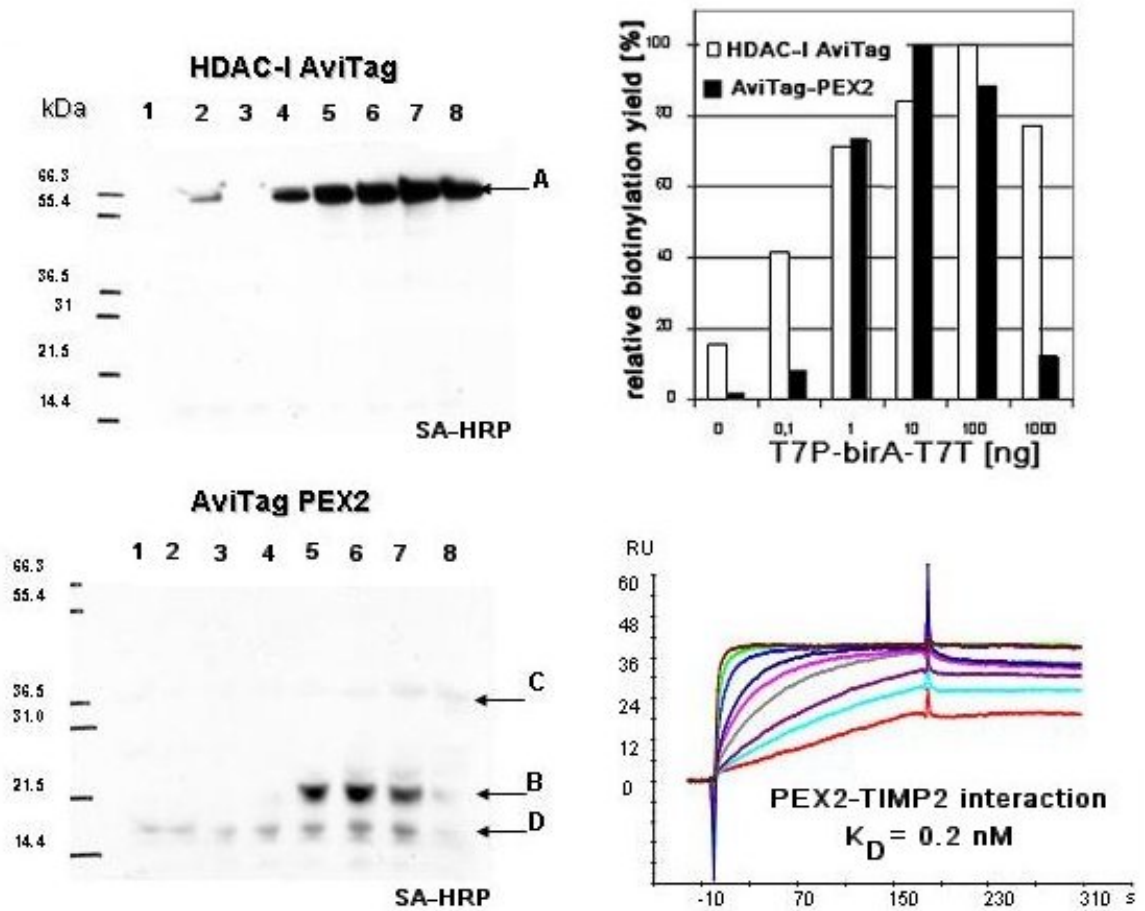


Fig.14: Optimization of the enzymatic *in situ* monobiotinylation. Biotinylated protein was detected by HRP-conjugate after Western-blotting. Lanes 1: incubated RTS lysate; lanes 2: samples with d-(+)-biotin but no BirA template. In the HDAC-I AviTag blot a background biotinylation activity was detectable despite the BirA DNA-template was omitted; lanes 3: samples containing no d-(+)-biotin but 10 ng BirA template; lanes 4-8: constant amounts of the LEEs AviTag PEX2 (1 μ g) and HDAC-I AviTag (0.6 μ g) were incubated with 0.1 ng (4), 1 ng (5), 10 ng (6), 100 ng (7) and 1 μ g (8) BirA template and 2 μ M d-(+)-biotin. Due to a longer exposure time a background signal from BCCP and BirA was detectable in the AviTag PEX2 blot (arrows at BirA (C) and BCCP (D)). Densitometric evaluation of both blots revealed the highest biotinylation yield at a supplementation of BirA-template between 10 ng to 100 ng. The activity of expressed and biotinylated AviTag-PEX2 was confirmed by SPR analysis. After dialysis, 600 RU AviTag PEX2 were immobilized on a BIAcore SA chip. The analyte TIMP2 was injected into the system in 1:2 diluted concentration series from 100 nM to 0.3 nM in HBS-P running buffer at 20 μ l/min. Regeneration was performed by three injections of 10 mM HCl. A binary Langmuir model was fitted to the data. The affinity of the PEX2-TIMP2 interaction was determined at $K_D = 0.2$ nM.

Despite of a weak biotinylation-activity of the RTS extract, which yielded a low amount of biotinylated HDAC-I-AviTag protein, the coexpression of BirA was necessary to obtain an increased yield of biotinylated fusion protein. The maximum biotinylation yield of the substrate proteins was found at a supplementation between 10 ng to 100 ng BirA encoding DNA template. The addition of the BirA encoding DNA template at 1 μ g decreased the yield of the biotinylated fusion proteins. The optimal ratio of substrate protein encoding DNA template to BirA encoding template was approximately 20:1. The RTS mixture provided ATP and Mg^{2+} -ions, the required cofactors for the BirA catalyzed biotinylation.

A further experiment should reveal, whether a monobiotinylated fusion protein could be stably presented in an oriented and active manner on the surface of a streptavidin coated sensor chip in order to enable SPR measurements.

Mono-biotinylated AviTag-PEX2 was subjected to a SPR interaction analysis with its natural protein-binding partner TIMP2. Excess d-(+)-biotin was removed from the sample mixture (*lane 6, B*) by ultrafiltration of the incubated crude lysate versus Biacore HBS-P buffer. Finally, the mixture was diluted 1:5 in HBS-P buffer. 30 μ l were injected into the system. 600 RU (1 RU = 1 pg of protein / mm^2) AviTag PEX2 were captured from the crude mixture on the surface of the SA coated sensor chip. The baseline drift was below the instruments resolution. 20 RU were captured during the injection of incubated template-free RTS lysate on the reference flow cell FC1 and served as a background control. The analyte TIMP2 was injected into the system in 1:2 diluted concentration series from 100 nM to 0.3 nM in HBS-P running buffer at 20 μ l/min. Differential signals FC2-FC1 were measured. Full ligand regeneration of the chip surface was achieved by three consecutive injections of 10 mM HCl. Due to the high affinity interaction of biotin with streptavidin the instrument baseline was stable also after several regeneration cycles. A binary Langmuir model was fitted to the obtained SPR data and the equilibrium constant of the interaction was determined at $K_D = 0.2 \pm 0.1$ nM. This corresponded to published data (Schräml *et al.* 2002).

4.5 Cell-free production of mini-BP4 constructs

The established methods should enable the rapid cell-free production and analysis of rationally planned protein constructs. A mutagenesis study with the 7.5 kDa IGF-binding domain of human IGFBP-4 should demonstrate the capability of the system to process and handle protein sequence constructs in parallel.

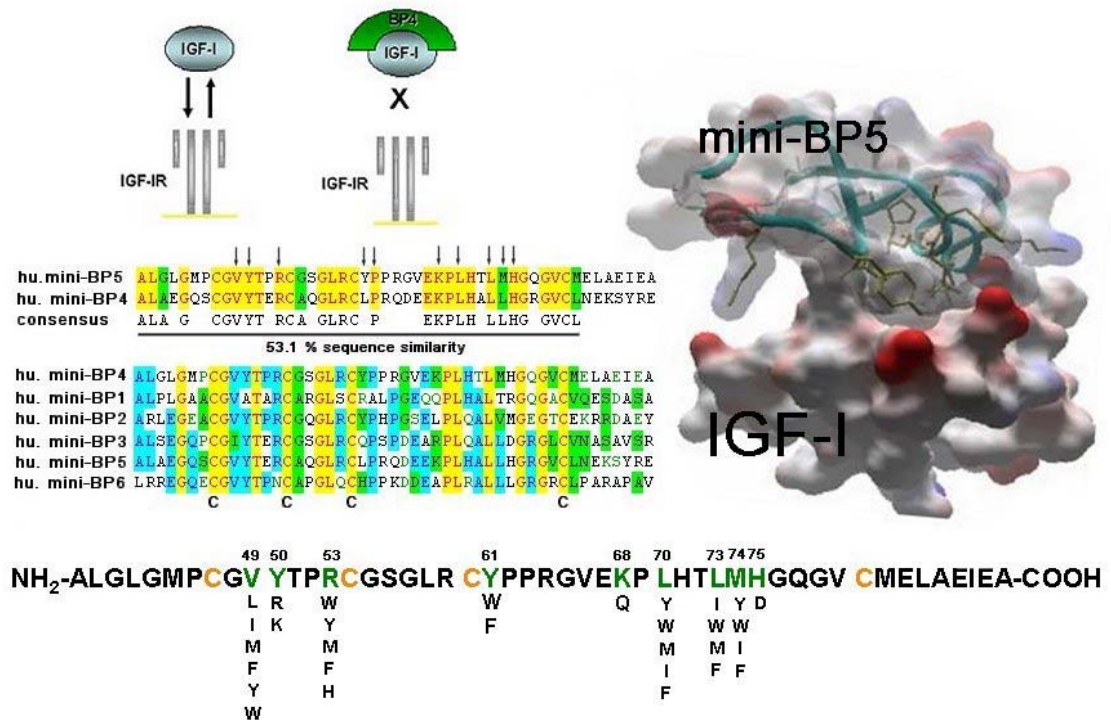


Fig.15: Human IGFBP-4 binds to IGF-I and inhibits the IGF-interaction with its receptor IGF-IR. The family of six human Insulin-like Growth Factor Binding Proteins (IGFBPs) reveals high amino acid sequence similarity. The homologous IGF-binding domains of IGFBP-5 and -4 share 53.1 % sequence similarity. All human IGF-binding domains (mini-BPs) contain 4 highly conserved cysteines. Mini-BP4 was elucidated for its binding affinity towards IGF-I. In order to modulate its IGF-I interaction 9 amino acids of mini-BP4 (arrows) were substituted (below). In the homologous mini-BP5 these positions are supposed to mediate the interaction to IGF-I (cartoon at the right with amino acids presented as sticks) (Zeslawski *et al.* 2001).

In mini-BP5 Val49, Tyr50, Pro62, Lys68 to His75 and particularly Val49, Leu70 and Leu74 are reported as the key determinants, which constitute the predominantly hydrophobic interaction towards IGF-I I-II (Kalus *et al.* 1998; Zeslawski *et al.* 2001). In the amino acid sequence of mini-BP4 9 amino acid positions were substituted (see fig. 15), which are presumably homologous to the mini-BP5 positions.

With the exception of Tyr50, Lys68 and His75 mostly replacements by more bulky and space filling amino acids were made. These substitutions were supposed to enlarge the binding surface of mini-BP4 thus contributing to the interface-interaction of mini-BP4 with IGF-I. The aim was to study the impact of these amino acid replacements on the IGF-I binding behavior of the mini-BP4 mutants.

The production began with the robot-assisted synthesis of the mini-BP4 gene constructs (see fig. 16). 55 site-directed mutated primer oligonucleotides were designed to generate 32 different mini-BP4 constructs by template-free PCR. Each of the 147 bp mini-BP4 gene sequences was synthesized by 5 complementary oligonucleotides. The amino acid substitutions were introduced by the replacement of one or two synthesis oligonucleotides by site-directed mutated ones.

Wherever it was possible, rare codons were eliminated and the optimal *E.coli* codon usage was applied. The PCR mixtures of the gene-synthesis reactions were robotically assembled, as 224 pipetting steps were to be performed in a highly reliable and reproducible manner.

The primers F1 and R1 amplified the *de novo* synthesized genes (see fig. 16). In a second PCR-step flanking primers elongated the gene-constructs by complementary sequences. In a third PCR-step the DNA-modules were PCR-mediated ligated to the mini-BP4 genes. Linear Expression Elements were generated, which encoded tandem tagged (his)₆-miniBP4-AviTag constructs (723 bp).

The LEEs were resolved in a 2 % EtBr-stained agarose-gel (see fig. 17). The parallel synthesis of the 32 LEE-templates was finished in 1 working day.

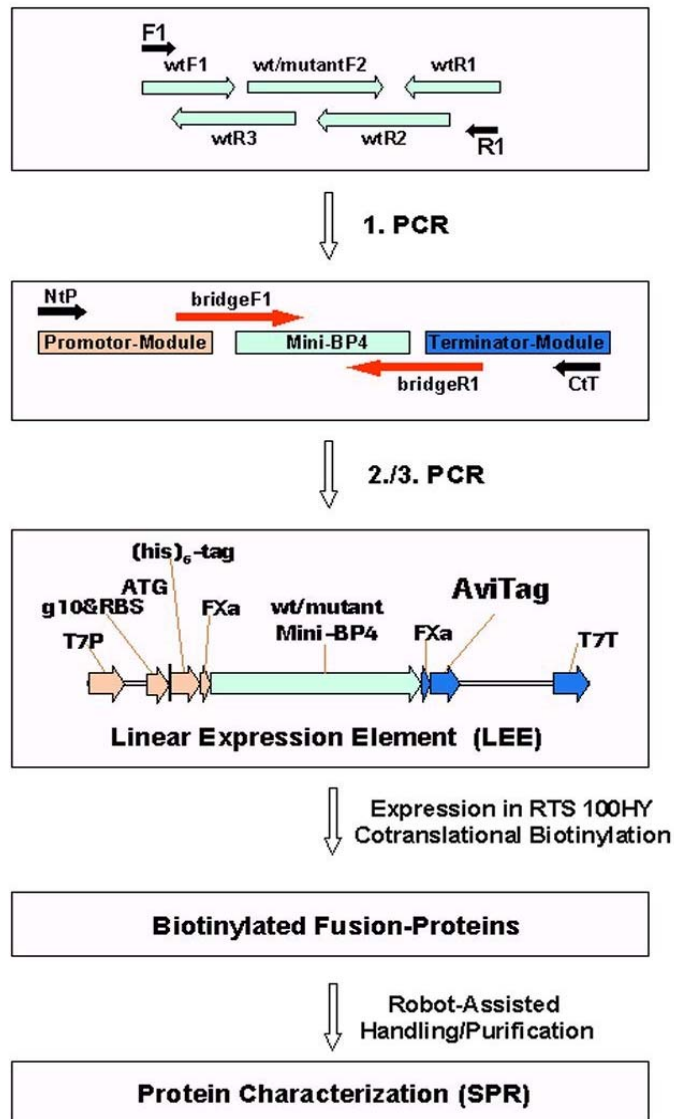


Fig. 16: Process overview of the synthesis, expression, purification and analysis of 32 different mini-BP4 constructs. The template-free PCR-mixtures were robotically constituted from 55 different oligonucleotides. Subsequently the constructs were assembled into LEEs. Mini-BP4 fusion proteins were *in vitro* expressed and monobiotinylated. After a robot-assisted refolding and purification procedure, the constructs were immobilized on SA-Biacore sensors for subsequent SPR analyses.

Approximately 500 ng to 700 ng of each LEE, contained in 15 μ l of its respective PCR mixture, was robotically transferred into the *in vitro* protein synthesis system. The system was supplemented with the respective additives to facilitate the enzymatic *in situ* monobiotinylation as described.

The transcription and translation reaction was performed on the heating-platform of the BIORobot 8000 for 2 h at 30 °C. The gene products were 9.5 kDa mini-BP4 fusion proteins, fused to an N-terminal hexahistidine-tag and a C-terminal, mono-biotinylated AviTag peptide. A soluble portion of each fusion-protein was PAGE-resolved for subsequent Western blotting (see fig. 17).

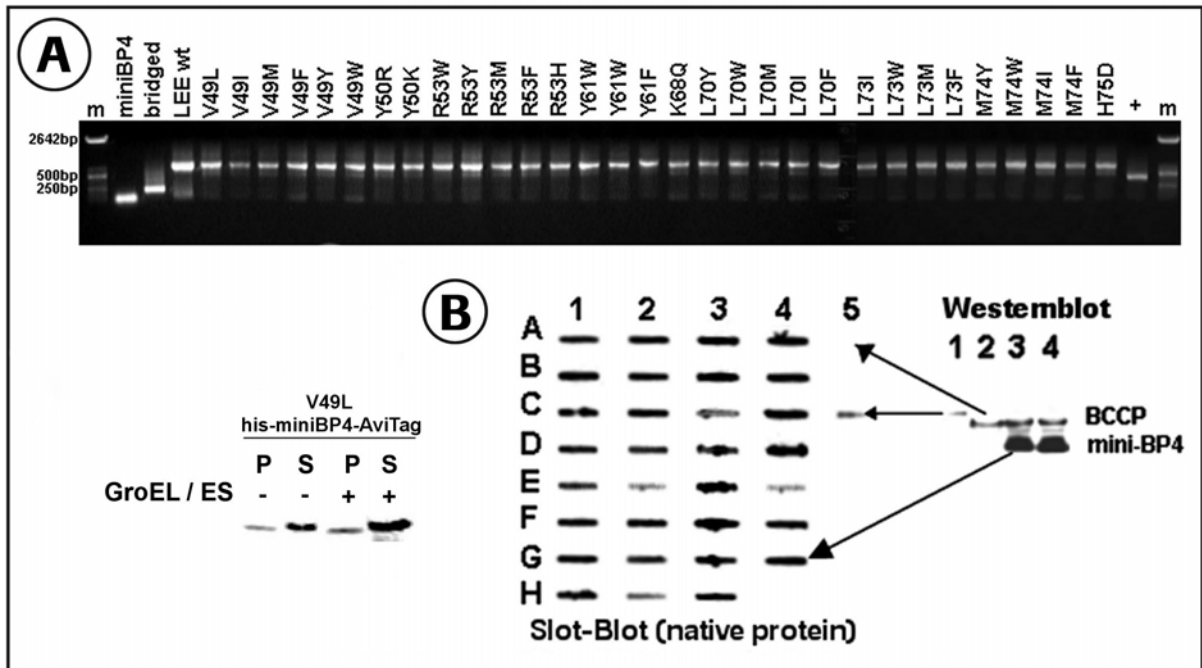


Fig. 17: A: EtBr-stained 2 % agarose-gel with Linear Expression Elements coding for 31 mini-BP4 mutants. *miniBP4*: wild-type after the template-free PCR synthesis. *bridged*: wild type mini-BP4 elongated by the bridging primers. *LEE wt*: Linear Expression Element of wild type mini-BP4. *V49L-H75D*: Different mini-BP4 LEES, LEE Y61W was produced twice, +: reaction without gene-module; *m*: marker. B: Expression monitoring with native Slot blotting and denatured Western blotting to detect biotinylated protein by SA-HRP conjugate. C5 and *lane 1* show biotinylated PEX2 protein. *H4* and *A5* correspond to *lane 2* and show incubated template-free lysate. BCCP produces no background signal in native slot blotting, whereas it was detected after non-native Western blotting (*lanes 2-4*). The arrows indicate the same samples subjected to both procedures. *A1-G4* are solubly expressed and mono-biotinylated mini-BP4 mutants. GroE-supplementation increased the yield of soluble expressed protein, exemplarily shown with the V49L-mutain.

A second fraction was subjected to native slot blotting. BCCP, the only naturally occurring biotinylated protein in *E.coli* was not detectable by native slot blotting. BCCP was only detected after Western blotting under denaturing conditions.

It was found that supplementation with the *E.coli* chaperonine system GroES/GroEL (Hartl *et al.* 2002) increased the soluble and biotinylated protein portion of the fusion-proteins up to six-fold. Fig. 17B exemplary shows the effect of this supplementation on the expression of monobiotinylated V49L mini-BP4. For this reason a GroES/GroEL supplementation was standardly performed during the mini-BP4 production. In average 80 % of the total protein yield of each mini-BP4 mutant was expressed as a soluble fraction. All 32 biotinylated mini-BP4 constructs were detected as soluble proteins after the *in vitro* expression.

4.6 Activation of the IGF-I binding activity of mini-BP4

Since all six human IGF-BPs contain highly conserved cystein residues and reduced IGF-BPs exhibit little or no IGF-binding activity (Landale *et al.* 1995) (Qin *et al.* 1998; Neumann *et al.* 1999), (Hashimoto *et al.* 1997) it was expected that the mini-BP4 constructs would require oxidation in order to obtain full structural IGF-binding activity. The ligand-binding activity of immobilized mini-BP4 fusion proteins was used as a parameter to examine the effect of different buffer pre-treatments on the IGF-binding-activity of the mini-BP4 mutants. Exemplary, the V49I mini-BP4 mutant is shown (see fig. 18). The mutant was *in vitro* expressed and enzymatically monobiotinylated as described. Three fractions of the crude mixture were dialyzed versus different buffers. A soluble portion (Load) of each dialyzed and 1:5 diluted fraction was captured on a Biacore SA-chip and the ligand-binding activity versus IGF-I was determined. A reducing buffer system revealed no binding-activity (fig. 18 C). Direct capturing from the lysate, which contains reducing agents (personal communication E. Fernholz, Roche), revealed no binding-active mutein, too (no data shown). Oxidation was necessary to obtain mini-BP4 protein revealing IGF-binding activity. The treatment with a buffer system (fig. 18 B), which should catalyze the disulfide bond formation by oxygen oxidation from air revealed a moderate IGF-I ligand-binding activity of 3 %. This was already enough for a successful SPR analysis. Best IGF-binding activity was obtained with a redox-shuffling, arginine-containing buffer system (fig. 18 A). Here a mini-BP4 ligand-binding activity of 20 % was achieved.

An on-chip activation of mini-BP4 immobilized under reducing conditions was possible by a 10 min injection at 20 μ l/min with this redox/arginine buffer system. The reduced ligand was oxidized and a ligand-binding activity of 3 % was observed (data not shown). The mini-BP4 IGF-binding domain requires the oxidation of its four cysteins to obtain IGF-I binding activity.

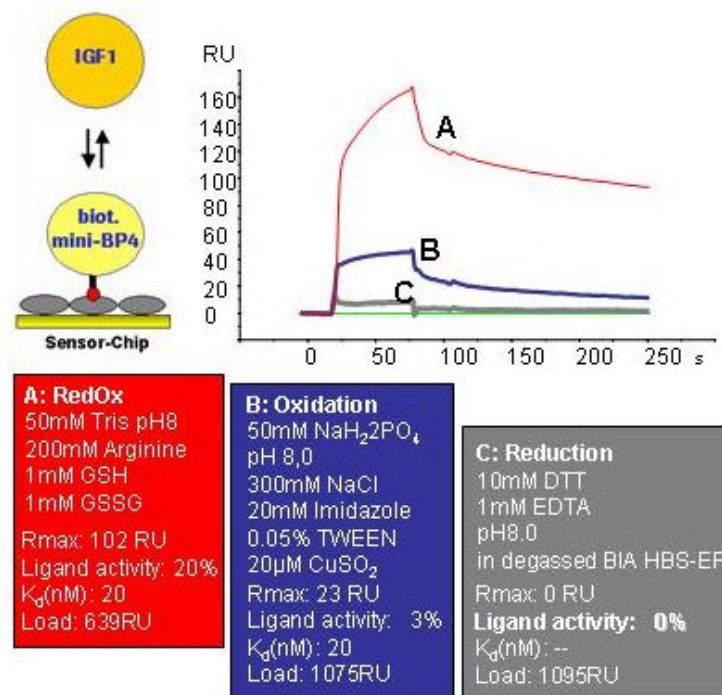


Fig. 18: The surface ligand-binding activity of the mini-BP4 constructs was determined and optimized. V49I mini-BP4 was *in vitro* expressed and monobiotinylated, followed by dialysis versus different buffers. A soluble portion of the mini-BP4 mutant was captured on the flow cells of a Biacore SA-chip (RU_{Load}). Saturation (R_{MAX}) of the chip surface was achieved by an 800 nM IGF-I injection. The ligand-binding activity was calculated by the ratio R_{MAX}/RU_{Load} . Highest mini-BP4 ligand binding activity (20 %) was achieved with buffer A (*RedOx*), moderate activity (3 %) was observed in buffer B (*Oxidation*). No activity was detectable in buffer C (*Reduction*).

4.7 Robot-assisted cell-free synthesis and purification of recombinant proteins

According to our requirements the technical devices of a Biorobot 8000 workstation were combined and accommodated to assemble PCR-mixtures, to handle and to incubate the *in vitro* protein synthesis system and subsequently to purify the expressed proteins using the magnetic bead technology in one process-line (fig.19).

An optimized program script for the automated separation of hexahistidine-tagged proteins by Ni-NTA functionalized magnetic agarose beads was established.

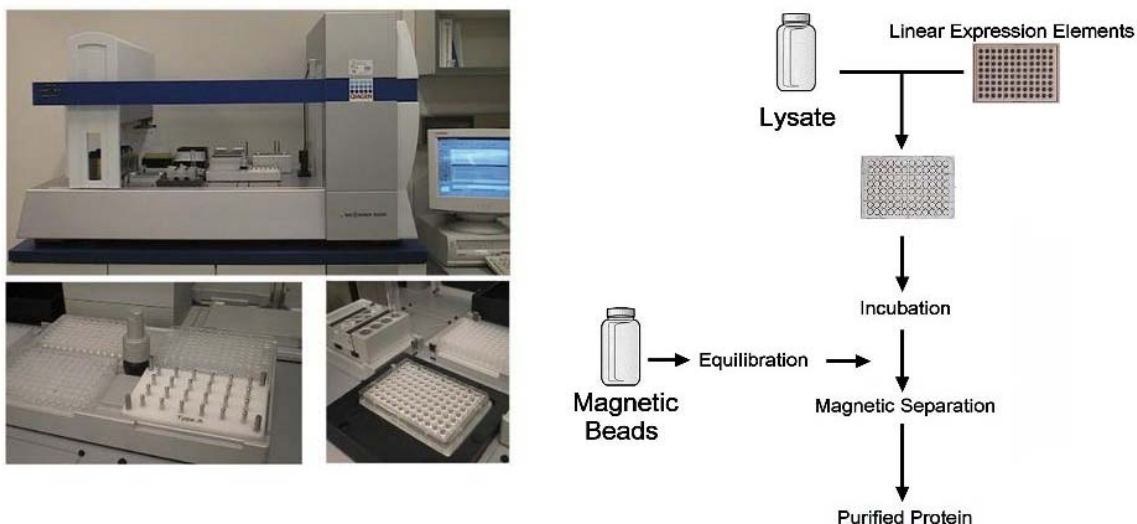


Fig. 19: *left*: the BIOrobot 8000 workstation carries a robotic shaker platform, a magnetic stiff plate and 96-well MT-plates with magnetic beads, the cell-free system and the LEEs. *picture, below right*: the peltier element incubating RTS lysate. *right*: schematic cartoon showing a process-overview of the expression and purification of the cell-free expressed proteins.

temperature equilibrated 96-well MT-plate on the heating-platform of the BIOrobot 8000. 15 μ l PCR-mixture containing up to 500 ng of the respective Linear Expression Element were transferred into the lysates. The lysates were incubated for 2 h. Since the aim was to obtain up to 1 μ g of purified recombinant protein, 20 μ l aliquots of the Ni-NTA magnetic bead suspension were used. The beads were equilibrated in IMAC-10 buffer. Prior to the purification procedure it was found to be necessary to dilute the incubated lysates four-fold with IMAC-10 buffer to dilute reducing agents from the RTS System below an uncritical concentration. The Ni-NTA coated magnetic beads were thus preserved from reduction and inactivation. The viscosity of the lysates was reduced and the wettability of the magnetic beads was improved. Foaming was not observed. The samples were transferred to buffer equilibrated bead suspension and were incubated for 30 min under shaking. The hexahistidine-tagged proteins bound to the Ni-NTA bead surface. Two 200 μ l washing steps with IMAC-20 buffer were sufficient to remove free biotin and unspecific bound proteins from the beads. The immobilized fusion proteins were eluted from the bead-surface using 60 μ l elution buffer. In order to completely wetten the beads and to successfully elute the fusion

proteins from the beads this was the lowest possible volume of elution buffer. Therefore the proteins were separated, but not concentrated, since there was only a 1.2-fold concentration of the purified proteins. For the separation of the mini-BP4 mutants the optimized redox-buffer conditions were implemented into the elution buffer IMAC 500: 50 mM NaH₂PO₄ (pH 8.0), 200 mM arginine; 1 mM GSH; 1 mM GSSG, 300 mM NaCl; 500 mM Imidazole; 0.5 % TWEEN 20 (v/v). The eluates were transferred into a clean 96-well MT-plate. The purified mini-BP4 fusion proteins were centrifuged at 10.000 g for 10 min.

4.8 SPR protein-protein interaction analysis of 32 mini-BP4 constructs

Between 800 RU to 1300 RU (1 RU = 1 pg of protein / mm²) of each monobiotinylated mini-BP4 fusion protein was immobilized on SA coated sensors. Concentration steps (6.1 nM; 12.5 nM; 25 nM, 50 nM, 100 nM and 200 nM) of IGF-I in HBS-P running buffer were injected at 20 µl/min for 3 min association and 10 min dissociation. Full regeneration of the mini-BP4/IGF-I complexes was achieved by three consecutive 1 min injections with 10 mM HCl. To subtract a concentration dependent aggregation effect caused by the IGF-I analyte, biotinylated IGF-I was spiked in five-fold diluted RTS *E.coli* 100HY lysate in HBS-P buffer. In average 300 RU of this mixture were immobilized on the reference cell FC1. Kinetic data were determined using a binary Langmuir binding model. 26 mini-BP4 constructs were determined as functional active IGF-I binders (see fig. 20 and 21). 6 constructs were either inactive IGF-binders or were not determinable. 11 constructs revealed a complex, non-binary IGF-I binding behavior. No Langmuir model could be fitted to these SPR data. The equilibrium constant K_D of 15 mini-BP4 constructs could be determined. The wild type revealed the highest IGF-binding affinity of $K_D = 32$ nM (see fig. 21). The IGF-I binding affinities of the remaining mini-BP4 derivatives were found reduced between 2- to 12-fold. In order to compare the impact of an amino acid replacement on the mini-BP4/IGF-I complex stability a k_{off} -rate ranking was performed. Using these strategy mini-BP4 constructs, which revealed a non-Langmuir complex-binding behavior were also accessible for analysis.

From each mutant, the dissociation data of the interval [450 s to 550 s] of 5 IGF-I injections (100 nM to 6.1 nM) were taken to calculate the average k_{off} rate (kd [1/s]). The ratio k_{off} wild type to k_{off} mutant was calculated to compare the wild types IGF-I complex stability with the IGF-I complex-stabilities of the mutated mini-BP4 derivatives.

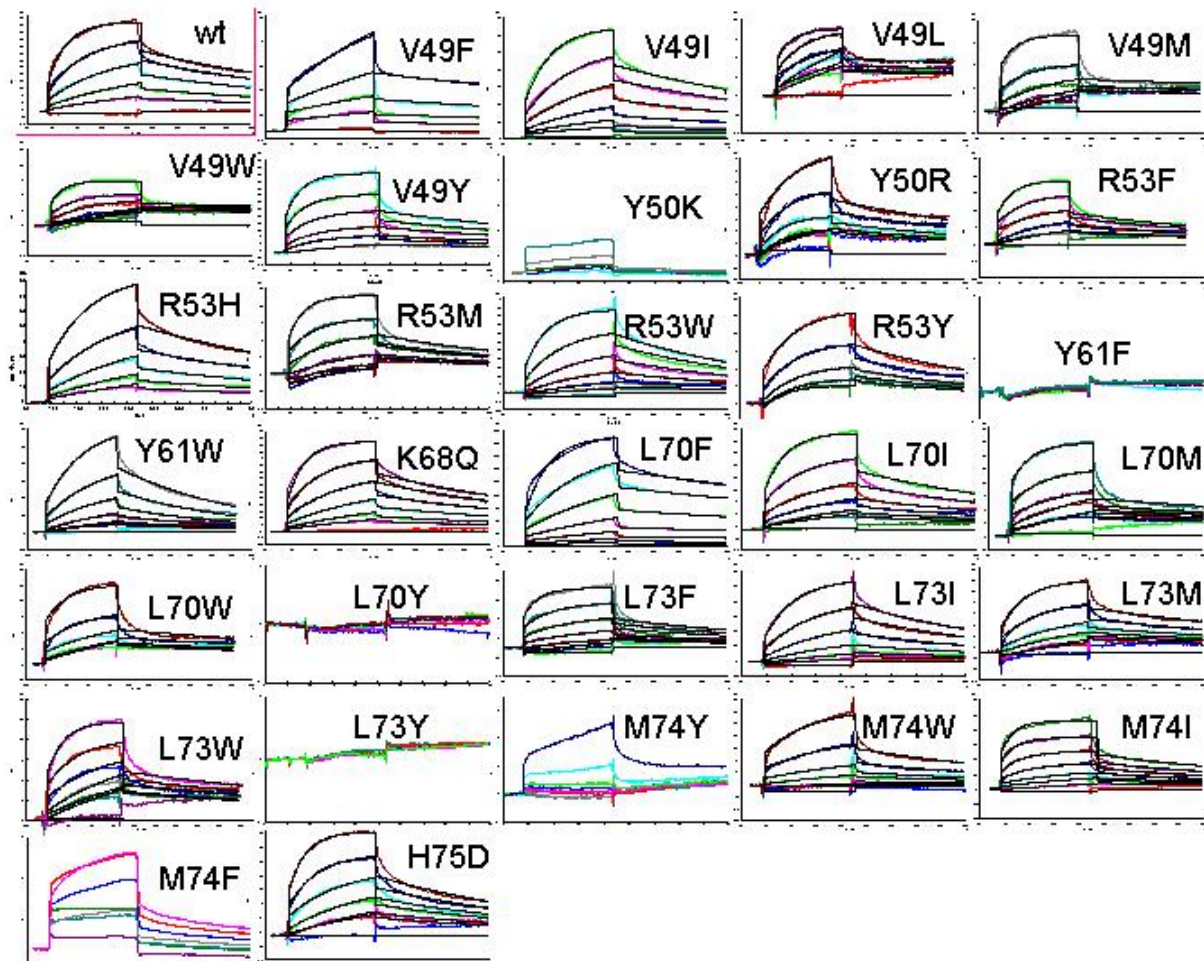


Fig. 20: 32 BIAcore 3000 sensorgrams showing protein-protein interaction measurements of different mini-BP4 (ligand) constructs with IGF-I (analyte).

10 constructs revealed a superior IGF-I complex stability, 2 constructs revealed an equal complex stability and 13 constructs showed an inferior complex stability when compared to the wild type construct. The mutant V49F mini-BP4 exhibited the highest complex stability (see fig. 21) showing a 2.8-fold improved k_{off} -rate, when compared to the wild type mini-BP4.

Construct	k_d [1/s]	k_a [1/Ms]	K_D [nM]	k_d wt / k_d mutant
wt	1.57E-03	5.06E+04	32 ± 2	1.0 ± 0.1
V49Y	1.98E-03	complex binding		0.8 ± 0.3
V49W	n.d.	n.d.	n.d.	n.d.
V49M	1.77E-03	complex binding		0.9 ± 0.1
V49L	n.d.	n.d.	n.d.	n.d.
V49I	1.23E-03	1.05E+04	117 ± 15	1.3 ± 0.1
V49F	5.59E-04	5.59E+03	100 ± 18	2.8 ± 0.4
Y50K	n.d.	n.d.	n.d.	n.d.
Y50R	1.67E-03	complex binding		0.9 ± 0.4
R53Y	1.00E-03	complex binding		1.6 ± 0.5
R53W	1.89E-03	3.26E+04	58 ± 11	0.8 ± 0.1
R53M	1.52E-03	2.45E+04	62 ± 34	1.0 ± 0.4
R53H	1.19E-03	1.61E+04	74 ± 21	1.3 ± 0.3
R53F	2.62E-03	4.37E+04	60 ± 15	0.6 ± 0.1
Y61F	n.d.	n.d.	n.d.	n.d.
Y61W	2.66E-03	7.11E+03	374 ± 37	0.6 ± 0.1
K68Q	1.46E-03	2.35E+04	62 ± 12	1.1 ± 0.2
L70Y	n.d.	n.d.	n.d.	n.d.
L70W	1.75E-03	complex binding		0.9 ± 0.2
L70M	4.32E-03	complex binding		0.4 ± 0.1
L70I	7.67E-04	9.70E+03	80 ± 21	2.0 ± 0.5
L70F	9.00E-04	1.50E+04	60 ± 13	1.7 ± 0.3
L73Y	n.d.	n.d.	n.d.	n.d.
L73W	4.90E-03	complex binding		0.3 ± 0.1
L73M	5.65E-04	8.43E+03	67 ± 22	2.8 ± 0.7
L73I	1.53E-03	2.12E+04	72 ± 6	1.0 ± 0.1
L73F	1.68E-03	complex binding		0.9 ± 0.3
M74Y	4.84E-03	complex binding		0.3 ± 0.1
M74W	6.35E-03	complex binding		2.5 ± 0.7
M74I	2.70E-03	complex binding		0.6 ± 0.1
M74F	6.73E-04	1.10E+04	61 ± 25	2.3 ± 0.7
H75D	3.54E-03	5.21E+04	68 ± 17	0.4 ± 0.1

Fig. 21: The influence of single point mutations on the binding behavior of mini-BP4 to IGF-I was determined by SPR protein-protein interaction analyses. 26 constructs were functional active, 6 constructs were inactive and 12 mutants revealed a complex binding behavior. Since no Langmuir-model could be fitted to these sensorgrams no equilibrium constant K_D was determined from this data. The ratio k_d wild type / k_d mutant reflects the influence of the mutations on the IGF-I complex stability of the mini-BP4 mutants. *wt*: wild type mini-BP4.

4.9 Ribosome display complements the HTPP concept

The next aim was to analyze multiple mutated mini-BP4 mutants for their binding-behavior towards IGF-I. A systematic impact analysis of amino acid substitutions at various positions in the mini-BP4 sequence would have overextended the throughput of the protein production and analysis process. To overcome this bottleneck the aim was to generate a library of multiple mutated mini-BP4 constructs, from which screening should select a pool of functional active binding proteins. Subsequently, a tractable amount of samples should be processed by the protein production and analysis assembly line. The idea was to complement the process by a selection driven technique. Ribosome display was ideal to meet these requirements. According to the protocols of Mattheakis, Hanes and He, (Mattheakis *et al.* 1994; Hanes *et al.* 1997; He *et al.* 1997) a ribosome display protocol was established on the basis of the coupled transcription and translation system RTS 100 *E.coli* HY.

4.10 Background information: tmRNA and ribosome display

In general, ribosome display requires the stalling of the ribosome while reaching the 3'-end of the mRNA without the dissociation of the ribosomal subunits. This has been achieved by removing translation stop codons (Mattheakis *et al.* 1994; Hanes *et al.* 1997) from the DNA spacer sequence of the ribosome display construct. As a consequence a high molecular weight complex consisting from mRNA, the ribosome and the translationally stalled polypeptide is generated. The ribosomes t-RNA entry site (A-site) is unoccupied after the ribosome has encountered the 3'- end of the mRNA. In prokaryotes, this state results in the activation of a ribosome rescue mechanism (see fig. 22), induced by tmRNA (Abo *et al.* 2000; Hayes *et al.* 2003), (Keiler *et al.* 1996). The tmRNA recognizes the free ribosome A-site and mediates the addition of an 11-residue peptide tag to the C-terminus of the nascent polypeptide by a process called trans-translation. Since the peptide tag encodes a stop codon, the polypeptide emerges from the ribosome and is immediately degraded by ATP dependent proteases, which recognize the C-terminal sequence extension as signal for the proteolytic degradation (Keiler *et al.* 1996; Karzai *et al.* 1999; Karzai *et al.* 2000). With regard to a ribosome display selection, this mechanism reduces the amount of functional ternary complexes and the PCR-product yield is significantly reduced (Hanes *et al.* 1997). Furthermore, Hanes found that the tmRNA activity was

suppressed by an tmRNA antisense oligonucleotide supplemented to the cell-free system (Hanes *et al.* 1997).

4.11 Regulatory nascent peptides reduce the PCR-product yield of ribosome display

During the establishment of the mini-BP4 ribosome display protocol, the aim was to examine, whether this tmRNA induced ribosome rescue mechanism could be bypassed, when the ribosome translation machinery had been forced to stall before the 3'-end of the mRNA was encountered by the ribosome.

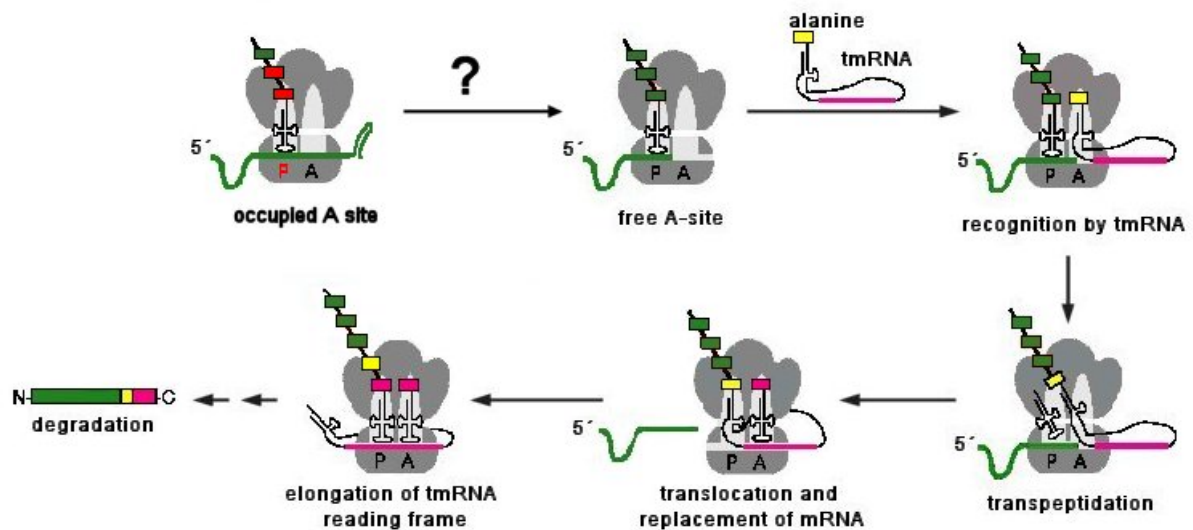


Fig. 22: According to the model of Keiler a free ribosome entry site (A) is recognized by tmRNA. tmRNA mediates the addition of a 11-residue peptide tag to the C-terminus of the nascent polypeptide and induces the degradation of the tagged polypeptides by ATP dependent proteases. The question was whether a complex, in which the ribosome A-site is occupied by sense-mRNA is also subjected to the tm-RNA mediated protein degradation (?). Regulatory active nascent peptides should pause or arrest the translation by inhibiting the peptidyltransferase center (P, in red) or by interacting with components of the ribosome exit tunnel (red boxes). The influence on the performance of ribosome display was examined.

Here it was expected that an induced translation arrest would still occupy the ribosome A-site by sense mRNA.

This premature translation arrest should be induced by regulatory nascent peptides, which were implemented in the display spacer sequence of the ribosome display construct. The focus was on the regulatory nascent peptides *cmla*, *catA112/221* and *SecM* (see fig. 23).

Subinhibitory levels of the co-effector chloramphenicol (Camp) together with the nascent peptides *cmlA* and *catA112/221* from the upstream region of the chloramphenicol transferase gene (*cat*) pause the translation by the reversible inhibition of the peptidyltransferase activity (Lovett *et al.* 1996). The *SecM* arrest peptide-sequence causes an elongation arrest by the interaction with components in the ribosome exit tunnel (Nakatogawa *et al.* 2002).

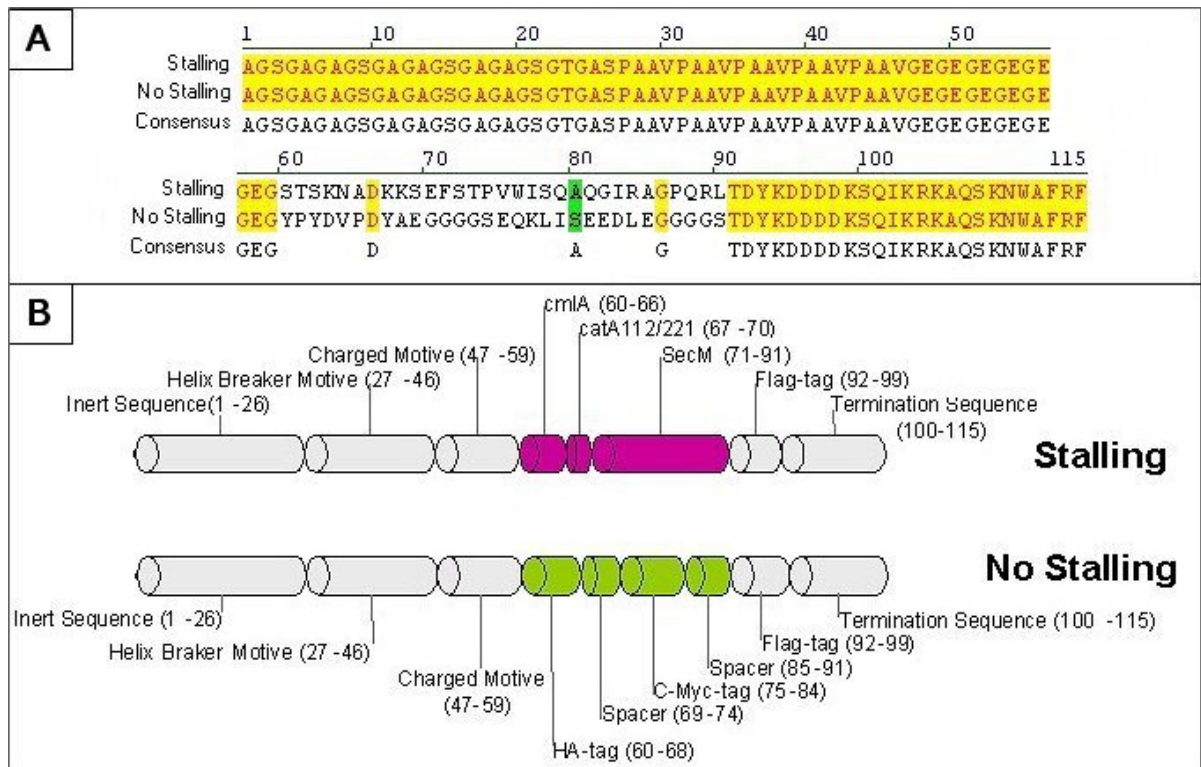


Fig. 23: A: Alignment of the ribosome display spacers "Stalling" and "No Stalling". The sequences are identical with the exception of the intersection 60 aa – 91 aa. B: Sequence description of the spacers. The attenuator sequences of "Stalling" *cmlA*, *catA112/221* and *SecM* are replaced in the "No Stalling" spacer by the epitope tags HA, C-myc, Flag and two G₄S-linker sequences.

The aim was to examine, whether these regulatory peptides could circumvent the tmRNA mediated protein degradation mechanism. In order to analyse the effect of the regulatory peptides two ribosome display spacers (fig. 23 A) were synthesized. Both spacers (see fig. 23B) encoded an inert amino acid sequence, a helix-breaker motive, a negatively charged motive, the Flag epitope tag and a palindromic stem-loop mRNA structure. The sequences only differed at the bases 158 bp to 300 bp. Here the translation attenuating sequences from *cmlA* (STSKNAD), *catA112/221* (KKSE) and *SecM* (FSTPVWISQAQGIRAGP) were implemented in the Spacer "Stalling".

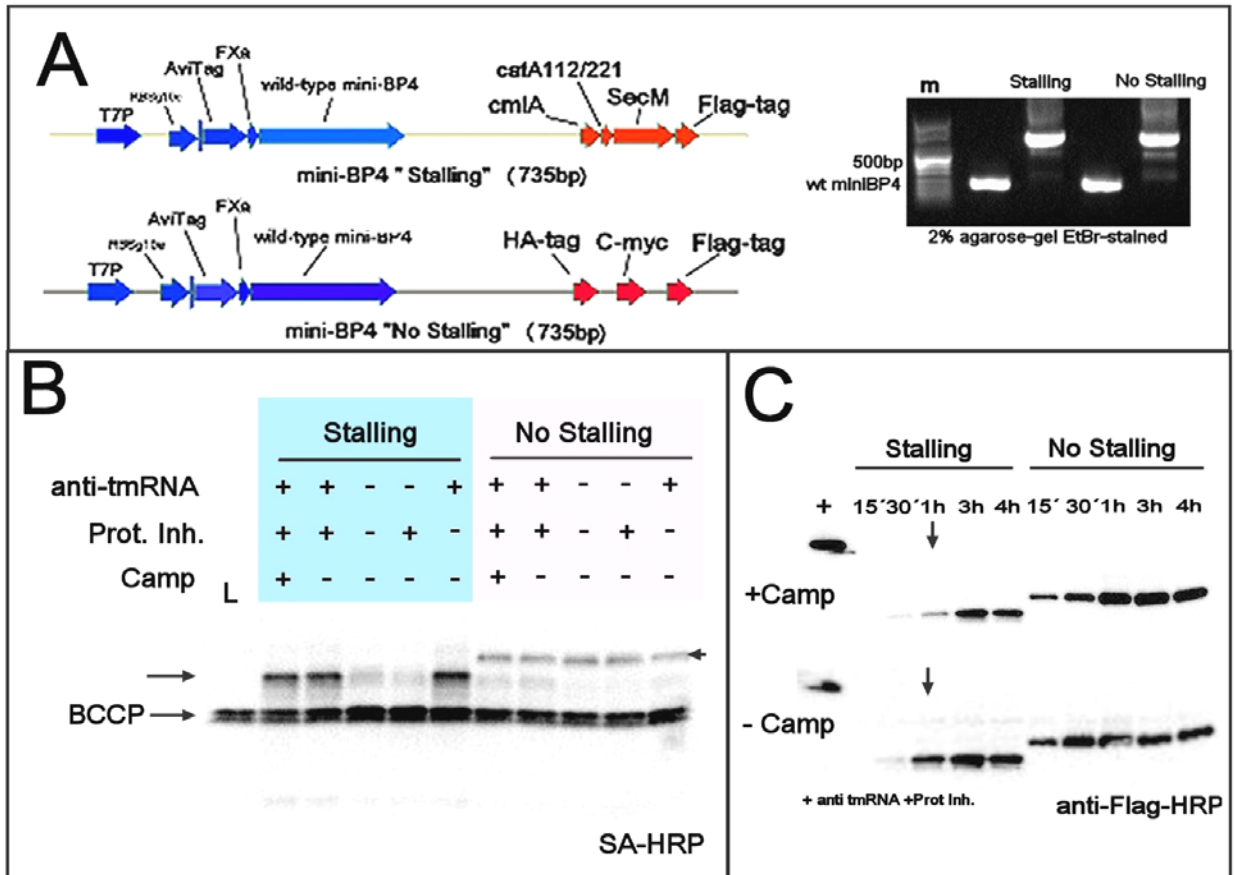


Fig. 24: **A**: The spacers “NoStalling” and “Stalling” were fused to T7P_{g10e}AviTagFXa-mini-BP4 constructs. The constructs are identical with the only exception of the attenuating sequence-motives (in red). **B**: To examine the tmRNA dependency of the constructs, expressed and enzymatically biotinylated constructs were detected via SA-HRP conjugate after Western blotting (B, black arrows). Plus and minus indicate supplementation of the additives protease inhibitor (Complete EDTA-free), 2 μ M antisense tmRNA oligonucleotide and 0.1 μ g/ml Camp. L: incubated lysate with solely the BCCP protein-band (at 12 kDa). The construct “Stalling” is highly sensitive to the tmRNA induced protein degradation. **C**: Expression kinetic to examine the translation attenuating effect of the “Stalling”-sequence by supplementation with 0.1 μ g/ml Camp. The Flag-tag was detected after Western blotting by anti-Flag-HRP IgG. +: Incubated lysate spiked with 50 ng of HDAC-I-Flag (55 kDa). + Camp / - Camp: Reactions with and without Camp at 0.1 μ g/ml. Camp supplementation induces a translation attenuating effect at the “Stalling” construct.

In the spacer “No Stalling” the effector peptides were replaced by the epitopes HA and C-Myc, connected by two (Gly)₄Ser linker motives (fig. 23B).

There were no stop-codons in all three DNA reading-frames. At the 3'-end of the spacers the DNA sequence was designed to generate a palindromic hairpin structure on the mRNA-level in order to protect the mRNA from the exonucleolytic digestion by RNAses (Hanes *et al.* 1997).

The stem-loop structure at the 3'-end of the DNA derived from the *E.coli rrnB* terminator (Hartvig *et al.* 1996). A 2-D mRNA secondary structure prediction (Brodsky *et al.* 1991) calculated identical secondary structure formation energy of -26.6 kcal/mol in both spacers (no data shown). An amino acid secondary structure prediction (Psi-Pred) proposed a flexible structural conformation between the positions 1 aa to 75 aa (no data shown) in both spacers.

Two ribosome display DNA templates were generated, which encoded the fusion proteins AviTagFXa-miniBP4-"Stalling" and AviTagFXa-miniBP4-"No Stalling" (fig. 24 A). The aim was to examine the susceptibility of the constructs for the tmRNA induced degradation mechanism. Both constructs were *in vitro* expressed and monobiotinylated for 4 h at 30 °C. The expression reactions were supplemented with combinations of the additives anti-tmRNA antisense oligonucleotide (anti tmRNA) (Hanes *et al.* 1997), protease inhibitor and Camp (fig.24 B).

A portion of each supernatant was resolved in an 18 % Tris-Tricine gel. Biotinylated protein was detected by SA-HRP conjugate after transfer of the protein bands into a 0.2 µM nitrocellulose-membrane. Although both ribosome display derivatives encoded wild type mini-BP4 fusion proteins with a predicted molecular weight of 18 kDa, the detectable protein-bands from the "Stalling" construct showed an apparently reduced molecular weight when compared to the "No Stalling" signals. The regulatory peptides induced a translation arrest in the "Stalling" construct. C-terminally truncated protein constructs were expressed. Protease inhibitor and/or a subinhibitory level of Camp at 0.1 µg/ml did not significantly influence the protein band-heights or the protein-band intensities of both constructs.

The most dominant effect was observed, when the tmRNA activity inhibiting antisense oligonucleotide (anti tmRNA) was omitted. This strongly reduced the protein-band intensities of the "Stalling" construct, whereas the "NoStalling" intensities remained at a lower, but constant level (fig. 24B). The antisense oligonucleotide was the major influence factor on the expression-level of the "Stalling" construct. Surprisingly, the translation arrest in the "Stalling" construct induced the tmRNA mediated protein degradation mechanism, whereas the "No Stalling" constructs remained unaffected from the tmRNA activity.

In a second experiment, the DNA templates were *in vitro* expressed at 30 °C for 15 min, 30 min, 1 h, 3 h and 4 h (fig. 24C). Protease inhibitor and the antisense tmRNA oligonucleotide were present. The attenuating effect of Camp supplementation on the expression yield of the constructs was examined (fig. 24 C). After Western blotting the Flag-tag was detectable in both constructs. Like in the SA-HRP Western blot, the signals of the “Stalling” construct revealed a reduced molecular weight of approximately 2 kDa, when compared to the “NoStalling” construct. The signal-increment of the Camp-supplied “Stalling” expression reactions was retarded. Especially the 60 min signal revealed a significant difference in the blot intensities of the Camp-supplied “Stalling” reactions versus the non-supplied ones (arrow, fig. 24C). The “NoStalling” construct did not show a significant difference in the blot-intensities, when Camp was omitted or supplied. These results indicated, that one or both of the regulatory peptides cmlA and catA112/221 caused a Camp-inducible pausing, but no translation arrest. These peptides were not responsible for the apparent molecular weight shift of the “Stalling” constructs. The SecM arrest peptide must have been the major determinant for the expression of truncated “Stalling” constructs.

In a further experiment, the influence of the regulatory peptides on the efficacy of a ribosome display process was determined. The ribosome display constructs T7Pg10ε-miniBP4-“Stalling” and T7Pg10ε-miniBP4-“No Stalling” were used as templates in a ribosome display cycle (see fig. 25 and fig. 26). 500 ng +/- 20 ng of each construct was transcribed and translated for 40 min at 30 °C in the RTS 100 *E.coli* HY System. The *in vitro* protein synthesis system was supplemented with anti tmRNA oligonucleotide, protease- and RNase inhibitor. Camp was omitted. The reactions were stopped by addition of ice-cold stopping buffer (SB).

As shown before (see 4.6), oxidation was necessary to obtain a mini-BP4 protein revealing IGF-I binding-activity. Oxidation of a ribosome displayed mini-BP4 was also a prerequisite to perform ribosome display. 4 mM oxidized glutathione (GSSG) was added to the ribosome stopping buffer. It was presumed, that the ribosome displayed mini-BP4 construct was oxidized. Furthermore this procedure prevented the disulfide bonds of the plate-presented IGF-I ligand from reduction. Omitting GSSG revealed no PCR products (no data shown). A redox buffer system, similar to the mini-BP4 activation procedure, revealed no visible PCR-products, too (no data shown). Since the supplementation of up to 100 mM arginine in the buffers still revealed PCR-products (no data shown), it seemed likely that the redox shuffling system negatively influenced the ribosome display PCR product yield.

A panning procedure with the stopped translation mixtures was performed (see fig. 25). To determine the background signal of the process, an aliquot of each mixture was incubated in the wells of a SA-coated MT-plate. Further aliquots were incubated in wells, in which biotinylated IGF-I was presented as a ligand. The wells were washed five times with ice cold washing buffer WB. Ternary complexes, which remained on the plate surface, were dissociated by chelating Mg^{2+} ions with EDTA. The mini-BP4 encoding mRNA from these complexes was purified and a DNase I

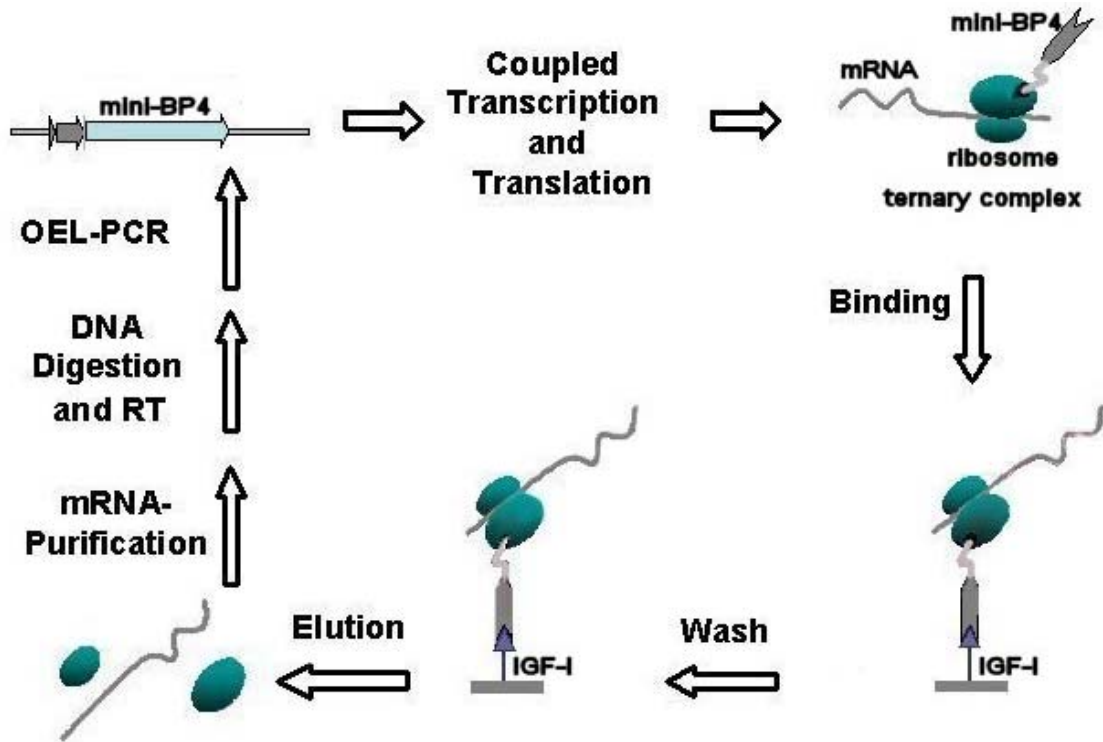


Fig. 25: A: Schematically one ribosome display cycle with mini-BP4 is shown. A mini-BP4 ribosome display construct was transcribed and translated in the RTS 100 *E.coli* HY System. Ternary complexes were generated, in which the mRNA was fused to the displayed mini-BP4 construct by the ribosome. These complexes were used in an affinity selection (Binding, Wash). Biotinylated IGF-I was presented as a ligand on a SA-coated surface. Weak binding constructs were washed away. The mRNA from bound complexes was isolated (Elution, mRNA Purification) and reversely transcribed (DNA digestion and RT). An OEL-PCR regenerated the DNA-template for further display cycles. Subcloning of the PCR-products revealed information about the bound phenotypes.

digestion removed remaining DNA. The mRNA was reversibly transcribed and amplified by 20 PCR cycles. The resulting PCR products were resolved in a 2 % EtBr-stained agarose gel (see fig. 26).

The miniBP4-“NoStalling” construct yielded approximately five-fold more PCR-product than the miniBP4-“Stalling” DNA template (see fig. 26). Both constructs retained background signals, which were significantly below the signal intensity of the sample signals.

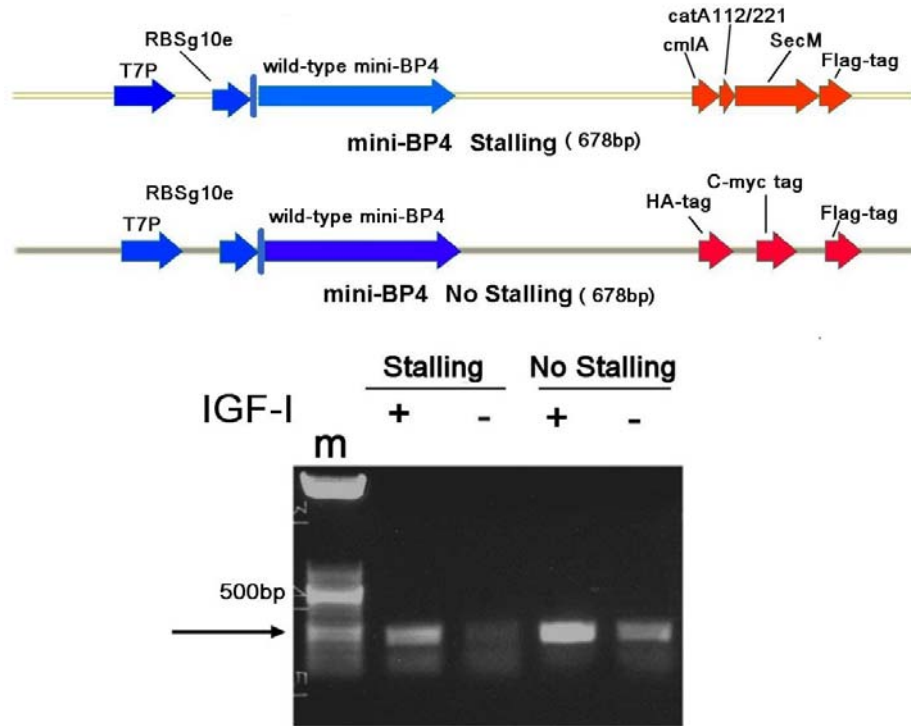


Fig. 26: 2 % EtBr-stained agarose-gel with PCR-product yields obtained after one ribosome display cycle with the mini-BP4-“Stalling” and mini-BP4-“No Stalling” constructs. IGF-I plate presence is indicated by (+): sample and (-): background. Exemplary, two signals are shown with their respective background signals. The mini-BP4-“Stalling” construct revealed less PCR-product yield despite of the presence of the tmRNA inhibiting antisense oligonucleotide. The regulatory peptides seemed to reduce the ribosome display PCR-product yield by a further tmRNA independent way, too.

Despite the presence of the antisense oligonucleotide, the regulatory peptides in the “Stalling” template reduced the displays PCR-product yield. From these results the “NoStalling” spacer was used for all further ribosome display experiments.

4.12 Selection of mini-BP4 mutants with IGF-binding activity

The development of the ribosome display protocol offered the possibility to analyse multiple mutated mini-BP4 constructs for their binding-behavior versus IGF-I. The amino acid positions in the mini-BP4 sequence Arg53, Pro62 and Met74 were analyzed for their relevance in the interaction of mini-BP4 towards IGF-I.

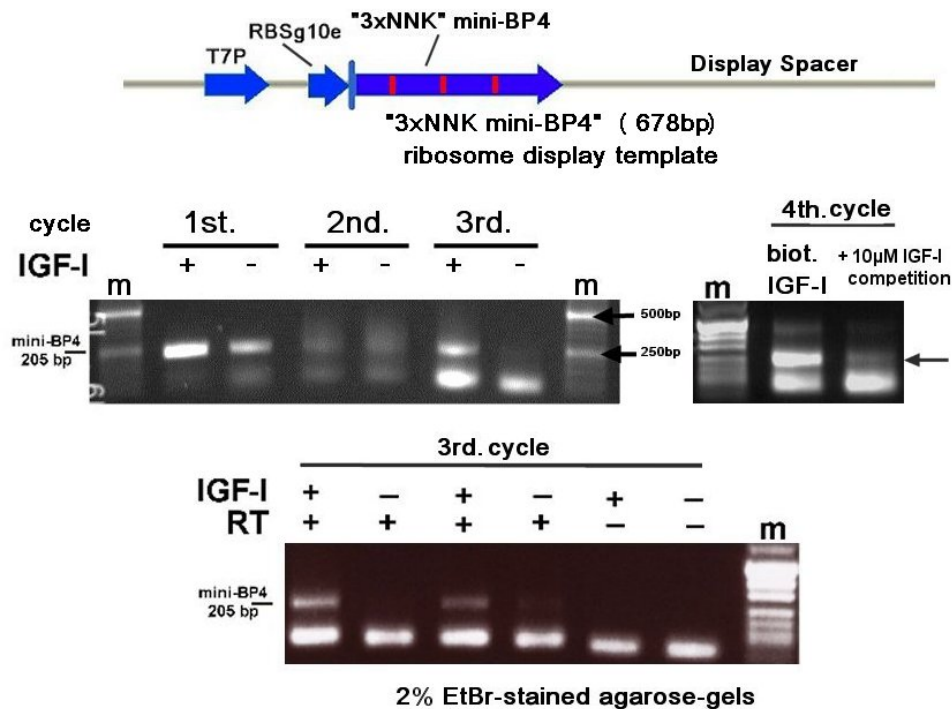


Fig. 27: Above: Ribosome display template figuring the mini-BP4 library. 3 NNK codons replaced the encoding Arg53, Pro62 and Met74 triplets (in red). Below: EtBr-stained 2 % agarose gels with left: Three exemplary ribosome display cycles with PCR-product signals from the sample and background. IGF-I plate presence is indicated by (+) and (-). right: In the fourth ribosome display cycle the selection was competed with 10 μM IGF-I (+10 μM IGF-I competition). Below: The reproducible signals clearly derived from mRNA. Performance of reverse transcription (RT) is indicated by (+) or (-).

6 % of the mini-BP4 polypeptide was site directed randomized. A mini-BP4 DNA-library was synthesized, in which the amino acid position Arg53, Pro62 and Met74 were randomized (see fig. 27).

The library comprised a theoretical size of 8000 triple mutated mini-BP4 constructs. DNA sequencing of 10 subcloned PCR-products revealed no further mutations besides these positions. Each mutant was unique (no data shown). The ribosome display procedure was performed as it was optimized before (see fig. 25). After each display cycle, the selected mini-BP4 DNA-fragments were reassembled into a new ribosome display template by OEL-PCR. In this way, a new promoter-module and a new “NoStalling” spacer was fused to the selected pool of mini-BP4 constructs and the accumulation of unfavorable mutations in these DNA sequences was bypassed.

During the ribosome display cycles the background mini-BP4 PCR-signals continuously decreased, indicating the specific selection of IGF-I binding proteins (see fig. 27). Surprisingly, after the second display cycle the PCR-product signal was reduced to the level of its background signal. After the third cycle the mini-BP4 specific PCR signal retained with a significantly reduced background signal. The pool of IGF-I binding constructs was first reduced and subsequently enriched.

The mini-BP4 PCR-product signal could be suppressed by competition with 10 μ M free IGF-I protein in the stopping buffer (see fig. 27). This verified the ligand specificity of the selected constructs. To confirm that the PCR-products derived from mRNA and not from remaining template-DNA the reverse transcription (RT) was omitted (-). No PCR-products were obtained (see fig. 27). After the third and fifth ribosome display cycle the PCR products were subcloned into the vector pUC18 and 10 DNA constructs from each cycle were sequenced. No wild type amino acid sequence was among these constructs. 8 sequences from the third display cycle and two sequences from the fifth display cycle were selected. The derivatives contained 2 to 4 amino acid replacements per construct. Additional diversity was obviously introduced by the various polymerase-dependent PCR- and RT-steps during the ribosome display cycling (see fig. 28). The constructs were processed by the established mini-BP4 protocol. The SPR analyses revealed 7 IGF-I binding-active mutants. 3 mutants did not recognize the IGF-I analyte. The amino acid sequences of the IGF-I binding-active and binding-inactive mutants were separately aligned and a consensus was calculated (see fig. 28).

The alignment algorithm of the IGF-I binding-active constructs revealed no consensus at the amino acid positions 53 and 62. Although both amino acids are highly conserved in 83 % of the human IGFBPs, they were of less importance for the IGF-I binding of mini-BP4.

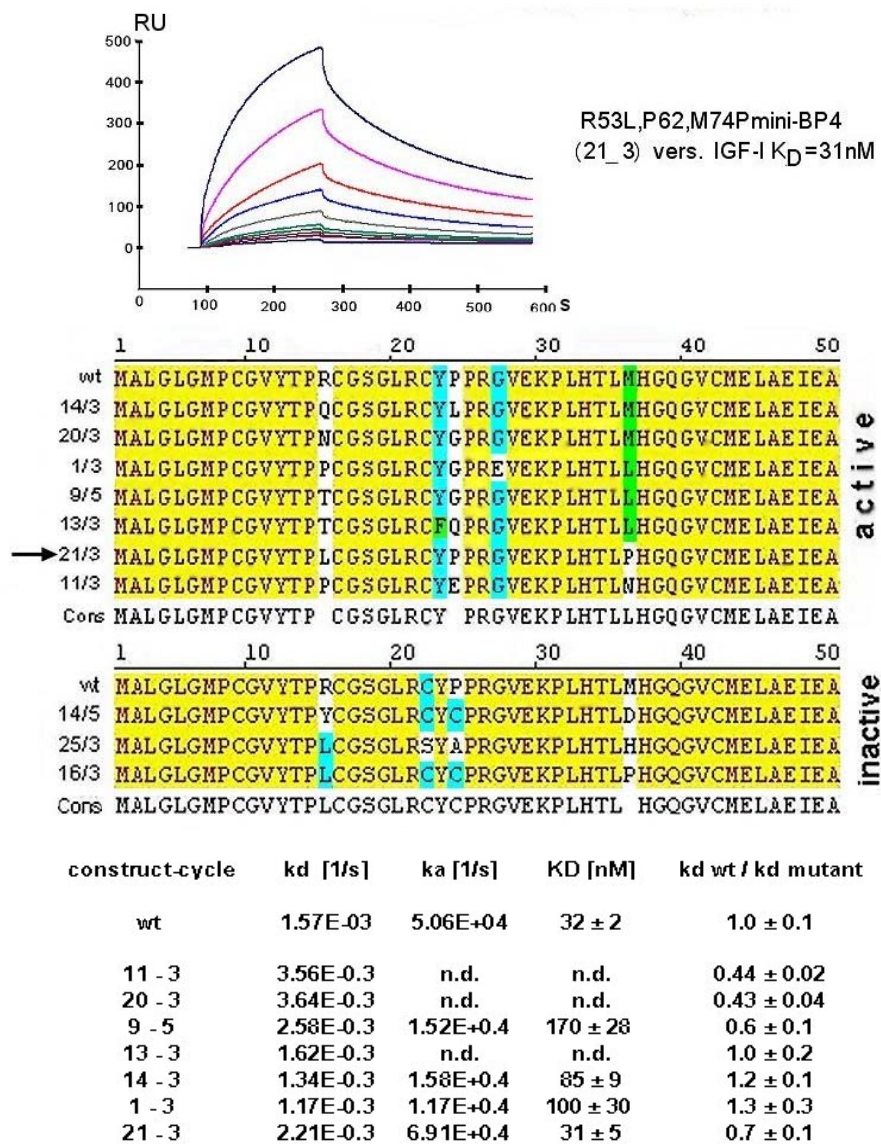


Fig. 28: 10 mini-BP4 constructs were processed in the automated assembly line. 7 of 10 constructs were determined as active binders. Alignment of active and inactive mini-BP4 sequences revealed no consensus at the amino acid positions 53 and 62 and a consensus Leu at the amino acid position 74. The double mutated construct 21_3 (above) revealed wild-type IGF-I affinity in SPR analysis. Inactive constructs revealed additional or lacking cysteins.

At the amino acid position 74 three leucines and two methionines were retained. A consensus Leu was calculated (see fig. 28). The amino acid position 74 was the most important residue to keep up the structure-functional demands of the mini-BP4 IGF-I interaction. Like before a k_{off} rate ranking was performed and the equilibrium constant was determined from those constructs, where a binary Langmuir binding model could be fitted to the SPR data.

The doubly mutated construct 21/3 R53L; M74P featured the highest IGF-I binding affinity ($K_D = 31\text{nM}$), similar to the wild type ($K_D = 32\text{nM}$). This mutant showed a 30 % reduced IGF-I complex stability and a 1.4-fold increased association-rate when compared to the wild type.

Despite the constructs 11/3, 20/3 and 13/3 were functional active IGF-I binding proteins the determination of K_D was impossible because the complex with the analyte IGF-I was not fully reversible. In these cases, the IGF-I/mini-BP4 complex could not be completely dissolved even under harsh chemical conditions (e.g. 100 mM HCl, 3 M GUACl, no data shown).

The mini-BP4 constructs 14/5, 25/3 and 16/3 were inactive. They all contained mutations afflicting cystein residues in the mini-BP4 sequence. These constructs probably derived from the unspecific background of the selection procedure or were not able to cope with the altered conditions of the *in vitro* selection versus the *in vitro* expression and analysis.

Mini-BP4 libraries, which were randomized at 5 or all 9 positions of the formerly generated mutants were not successful. The background signals kept constant throughout the cycles and could not be reduced. No ligand-specificity could be generated (no data shown).

The ribosome display protocol was successfully established with the threefold randomized mini-BP4 library. As a proof of principle functional IGF-binding mini-BP4 constructs with structure-function parameters similar to the wild type were evolved. The amino acid position 74 was subjected to the most selective pressure and retained the structure-functional demands of the hydrophobic mini-BP4/IGF-I interaction, whereas the positions 53 and 62 played a minor role in the interaction. The importance of the cystein residues for the structure-functional activity of the IGF-binding domain could be shown.

4.13 Engineering human γ crystallin for its use in HTPP

4.13.1 Ribosome display of engineered γ crystallin versus erbB2 and erbB3

The γ crystallins belong to a protein family, which are well known for their high thermodynamic stability (Jaenicke 1994; Jaenicke 1996). The exploitation of the human γ crystallin as an engineered *de novo* binding protein is the intellectual property of the Scil Proteins GmbH. In collaboration with Scil Proteins the human γ crystallin scaffold was examined for its capability to perform in a ribosome display selection procedure and furthermore in the established automated protein production and analysis system.

Two γ crystallin derivatives were examined, exhibiting a moderate affinity versus the ectodomains of the human receptor tyrosine kinases erbB2 and erbB3. These “first generation” constructs 12/A5-2 (versus erbB2) and 13/B11-2 (versus erbB3) contained 7 surface exposed amino acids in the first greek-key motive of the N-terminal γ crystallin domain, which constituted a *de novo* binding site (see fig. 36 and appendix). The amino acid patches of the construct 12/A5-2 (K2F, T4F, Y6C, S15V, E17K, T19A, R36F) and 13/B11-2 (K2D, T4Q, Y6R, S15G, E17A, R36C, E38R) enabled these derivatives to recognize their respective receptor target. The constructs were preselected by three cycles of phage display (Smith *et al.* 1997) from Scils human γ crystallin *SPC* library. The affinities of both derivatives were determined by a concentration dependent ELISA. A Langmuir binding model was fitted to the obtained data and revealed binding affinities in the micromolar range (see fig. 29). Astonishingly, and in contrast to the ELISA data, Biacore kinetic measurements of both derivatives revealed no binding activity versus the respective ErbB receptor targets, which were aminocoupled on the surface of a Biacore CM-5 sensor (no data shown).

The constructs 12/A5-2 and 13/B11-2 were used for the establishment of a ribosome display protocol.

"first generation" binders

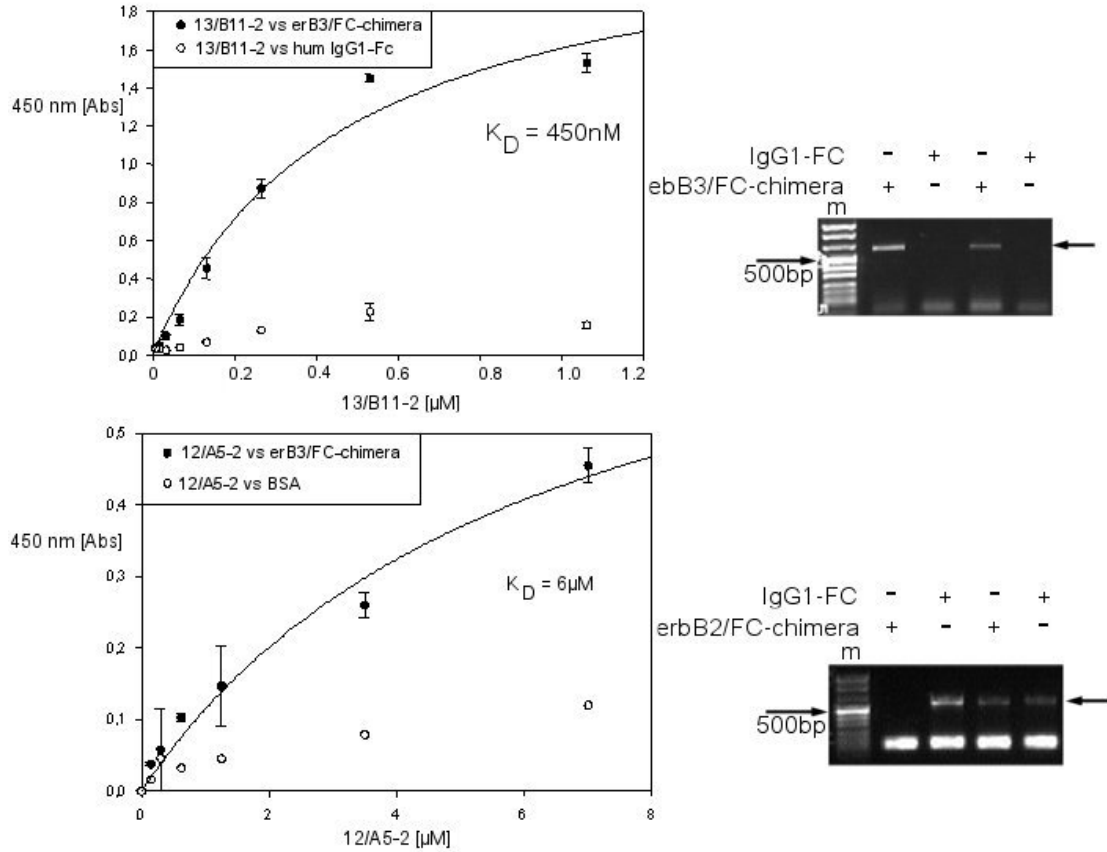


Fig. 29: *Left*: Concentration dependent ELISA to determine the affinity of the pre-selected constructs 13/B11-2 (versus erbB3) and 12/A5-2 (vers. erbB2). Scil Proteins friendly provided the data. *Right*: 1 % EtBr-stained agarose gels. Both constructs were tested for their ability to recognize their respective receptor targets in a ribosome display approach. Above: The construct 13/B11-2 revealed reproducible PCR-products and no background signals. Below: The construct 12/A5-2 revealed non-reproducible PCR-product signalling. The construct 12/A5-2 revealed more PCR by-products in the low-molecular weight range than the 13/B11-2 construct.

The respective receptor targets were presented in an oriented manner as erbB2/IgG₁FC- and erbB3/IgG₁FC-chimeras on protein A coated MT-plates. A ribosome display experiment was performed. Both γ crystallin ribosome display constructs were C-terminally fused to the 345 bp "NoStalling" display spacer. After one display cycle specific PCR-products were obtained from the erbB3-binding construct 13/B11-2 (see fig. 29).

No background signals versus the IgG₁FC control protein were detectable. The erbB2-binding γ crystallin construct 12/A5-2 revealed non-reproducible PCR-product signals and the PCR background-signal showed similar signal intensity to the sample signal (see fig. 29).

Principally, the γ crystallin scaffold performed in ribosome display. The ribosome displays PCR-product yield and the specificity of the obtained PCR-product signals were dependent on the γ crystallin derivative used in the experiment.

4.13.2 Ribosome display with error prone PCR generated γ crystallin libraries

The next aim was to perform an affinity maturation of both γ crystallin constructs. The strategy was to diversify the “first-generation” γ crystallin constructs and to evolve “second generation” ErbB2 and ErbB3 binding-proteins, which should reveal potentially improved receptor binding-affinities.

Thereby the evolutionary principle should maintain the *de novo* binding-function of the “first generation” constructs and further amino acid substitutions should be generated apart from the *de novo* binding site. Since these amino acid positions theoretically could have been located in both γ crystallin domains as well as in the inter-domain linker peptide, the complete DNA sequence was subjected to a random mutagenesis approach by the means of an error prone PCR (Cadwell *et al.* 1994).

Five ribosome display cycles were performed (see fig. 30). The erbB2- and erbB3/IgG₁FC-chimeras were alternately presented on protein A and protein G coated MT-plates to deplete derivatives with affinities versus protein A or protein G. Unspecific IgG₁-FC binders were removed by the incubation of the stopped translation mixtures with IgG₁FC-coated protein G magnetic beads.

In the first and fourth display cycle the templates were subjected to error prone PCR-steps to introduce diversity into the sequences. Background signals versus the presented IgG₁FC protein were observed after each error prone PCR-step. Here, unfavourable mutations led to aggregation-prone background, which was reduced by further cycling. Step-wise intensified washing from 10 min to 1 h should increase the selection-force on the constructs.

DNA sequencing of subcloned constructs was performed after the first (5 constructs each), third and fifth ribosome display cycle (20 constructs each). 89 % of the 12/A5-2 and 64 % of the 13/B11-2 derivatives revealed interpretable sequence-information (see fig. 31 and fig. 32).

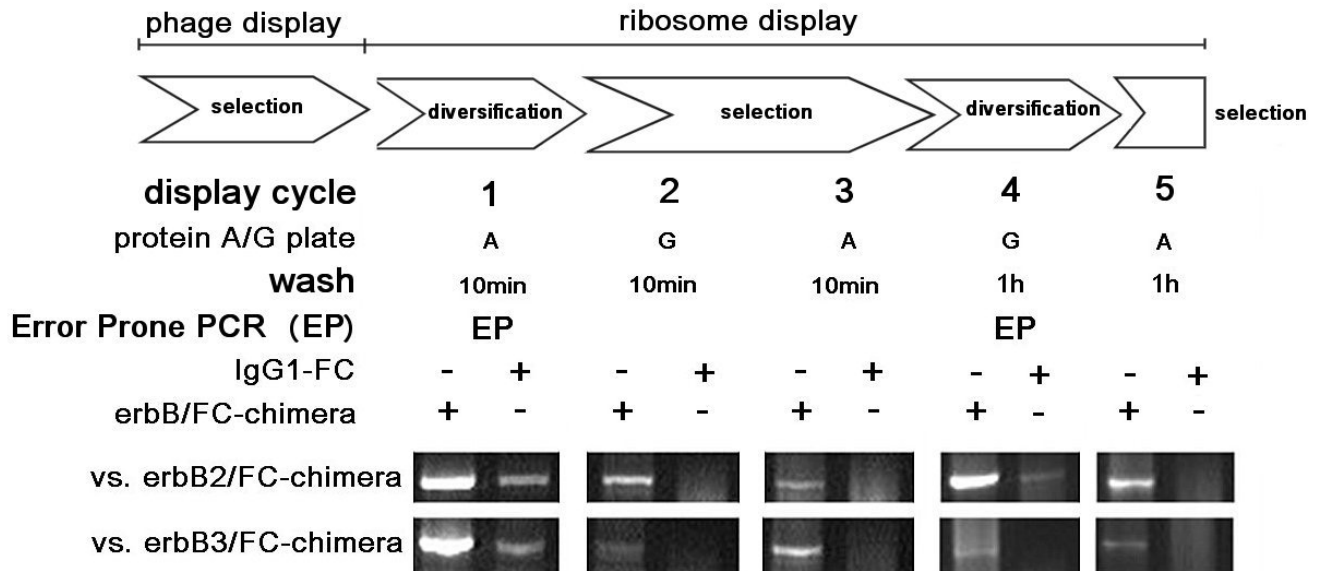


Fig. 30: 5 ribosome display cycles were performed with both γ crystallin derivatives. Outcuts from 1 % EtBr-stained agarose gels with the obtained PCR-products are presented. The receptor-chimeras were alternated presented on protein A and protein G coated MTP-plates. In the first and fourth cycle an Error-Prone PCR (EP) introduced further diversity. Washing was prolonged in the fourth and fifth cycle to 1h. As a background control the IgG₁-FC protein of the receptor-chimeras was used.

6 sequences of the 13/B11-2 and 12/A5-2 derivatives reciprocally occurred among the sequenced constructs. Possibly this was caused by a cross-contamination. These sequences were excluded from further evaluation so that 64 interpretable sequences remained.

The “second generation” derivatives contained up to 8 functional amino acid mutations. In average the 12/A5-2 derivatives contained 3.4 mutations per construct. The 13/B11-2 derivatives contained 2.8 mutations per construct.

After the fifth display cycle 17 % of the 12/A5-2 constructs and 0 % of the 13/B11-2 constructs revealed a mutation in the initial *de novo* binding site. After the fifth display cycle 0 % of the 12/A5-2 and 10 % of the 13/B11-2 constructs retained a “first generation” sequence. This obviously correlated with the basic affinity of the “first generation” constructs. The higher the initial affinity of the constructs was, the less mutations were obtained after the fifth display cycle.

4.13.3 Evolution of new sequence motives in γ crystallin

Optimally ribosome display selects a pool of sequence-similar constructs with ligand-specific binding features (Mattheakis *et al.* 1994; Hanes *et al.* 1997; Lamla *et al.* 2003). In this study ribosome display had selected γ crystallin derivatives featuring sequence similarities, too. The most dominant sequence-item was obtained after the fifth display cycle, were 32 % of the 12/A5-2 derivatives revealed a characteristic amino acid pattern located in the N-terminal domain (see fig. 33). An amino acid sequence alignment revealed the consensus sequence information D21E, N24H and G60A. Three of seven constructs contained the replacement Y16C. All these positions did not belong to the *de novo* binding site of the outgoing constructs. In general, newly evolved amino acid patterns mainly occurred in the N-terminal domain of the crystallin derivatives.

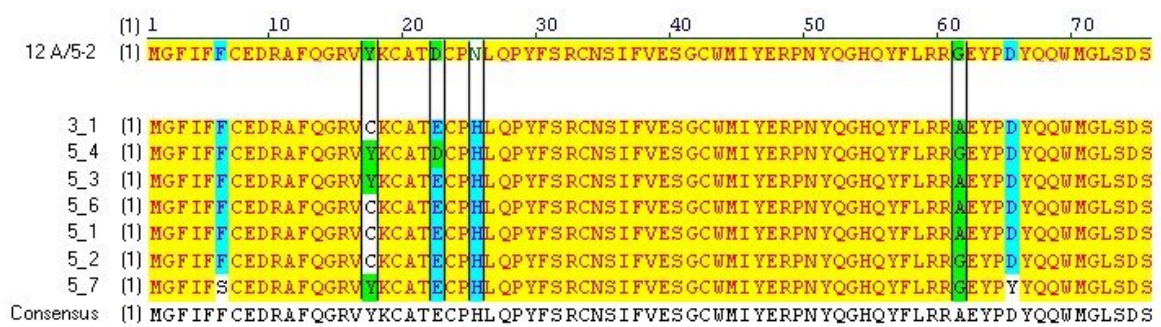


Fig. 33: Exemplary, the N-terminal γ crystallin domains of 7 constructs derived from the 12/A5-2 sequence are shown. The sequence motive resembled a pool of 32 % of the sequences, obtained after the fifth ribosome display cycle. Alignment and consensus formation revealed the amino acid replacements D21E, N24H and G60A. These positions did not belong to the *de novo* binding-site of 12/A5-2.

The erbB3-recognizing 13/B11-2 derivatives from the fifth display cycle did not reveal repeating new amino acid motives. Constructs carrying the G15D, A17I, T19G amino acid replacements, which occurred after the first and third display cycle, were not retained after the fifth cycle (see fig. 32).

4.13.4 Expression and Purification of γ crystallin derivatives

The “first generation” and “second generation” γ crystallin constructs were assembled into Linear Expression Elements. The AviTag peptide was C-terminally fused to the constructs. The LEEs were *in vitro* transcribed and translated and enzymatically monobiotinylated. Western blotting with subsequent detection of biotinylated protein by HRP-conjugate revealed, that all constructs were precipitated (see fig. 34). Addition of GroE supplement or protease inhibitor did not affect this (no data shown). In the soluble portion of the expression reactions a biotinylated protein fragment was detected. This fragment was also detected by a γ crystallin specific monoclonal antibody-HRP conjugate. The fragment could be immobilized on a BIAcore SA-chip and was subjected to SPR analysis. No binding-activity versus the erbB2 or erbB3 ectodomains was detectable (no data shown).

The Western blot further showed, that the C-terminally hexahistidine-tagged “first generation” constructs 12/A5-2 and 13/B11-2 could be expressed as soluble proteins in *E.coli* cells. C-terminally hexahistidine-tagged crystallin derivatives were also not expressible as soluble proteins in the cell-free system (no data shown).

It was presumed that the *E.coli* expression system could be used for the production of soluble “second generation” derivatives. After subcloning into the vector pET20bplus 14 constructs were selected for the expression as C-terminally hexahistidine-fused proteins in *E.coli* BL21 Codon plus cells. 5 constructs could be expressed. The soluble portion of each construct was purified using IMAC-chromatography. The purified constructs were dialysed versus PBS-ME buffer and subsequently centrifuged. Supernatant and pellet of each construct were PAGE-resolved (see fig. 34). All purified crystallins (at 21 kDa) revealed precipitation to different extent. This indicated a reduced conformational stability of the γ crystallin derivatives. Unidentified protein-bands of higher molecular weight were detectable, too.

The protein concentration of the soluble portion of each derivative was spectrometrically quantified at: 25/3: 1.9 μ M; 46/5: 2.6 μ M; 24/3: 0.8 μ M, 6/5: 1 μ M, 14/5: 1.2 μ M. When compared to the 13/B11-2 derivatives (25/3,46/5), the 12/A5-2 derivatives (24/3, 6/5, 14/5) revealed significantly lower protein yields.

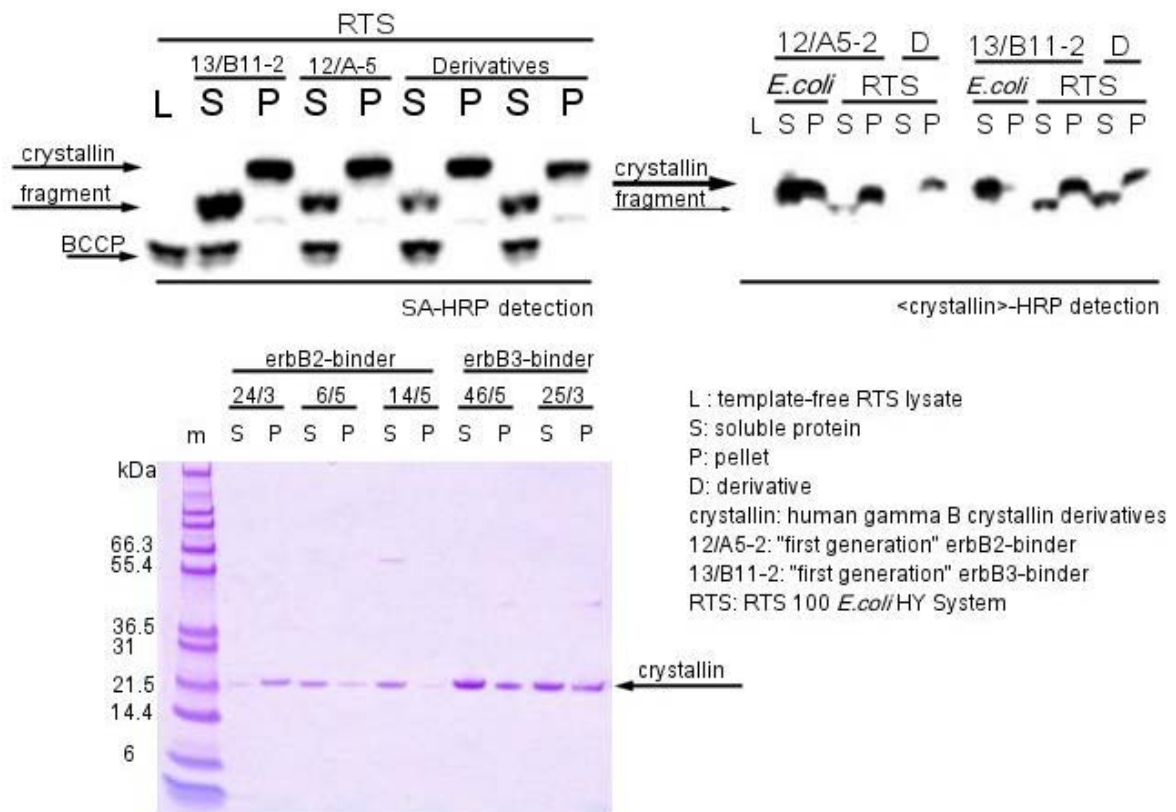


Fig. 34: Above left: Cell-free expressed and biotinylated γ crystallin-AviTag constructs were detected by SA-HRP conjugate after Western blotting. With the exception of a soluble fragment, all constructs were insoluble. Above right: Cell-free and in *E.coli* expressed γ crystallin constructs were detected after Western-blotting using a protein-specific antibody-HRP conjugate. In contrast to the cell-free expressed constructs, the expression in *E.coli* revealed a soluble protein portion. Below: 4-20 % Bis-Tris coomassie-stained gel with the soluble (S) and insoluble (P) fraction of γ crystallin derivatives after dialysis (marked with an arrow at 21.5 kDa). Three erbB2-binders and two erbB3-binders were expressed and purified.

The amino acid sequences of the purified constructs are referred (see fig. 35). The single mutated derivatives 25/3 and 46/5 contained no amino acid mutation in the C-terminal γ crystallin domain. The construct 6_5 contained the replacement N24H, which was found in the presented sequence similarity-pattern (see fig. 33).

4.13.5 Binding properties of selected γ crystallin derivatives

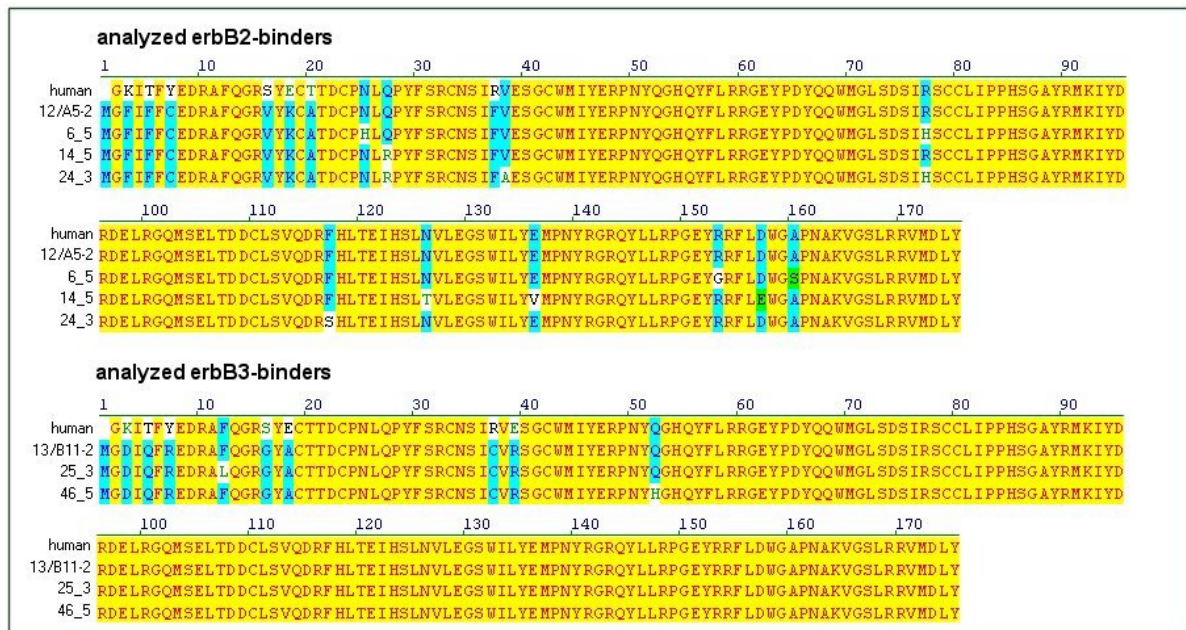


Fig. 35: Amino acid sequences of 5 in *E.coli* expressed and purified constructs. The erbB3-binders revealed only single additional amino acid replacements in the N-terminal domain. The erbB2-binders revealed 4 additional amino acid replacements, each.

In order to obtain information about the binding properties of the purified constructs a γ crystallin specific ELISA was performed (see fig. 36). The binding-behavior of the γ crystallin derivatives versus the erbB2/FC- and erbB3/FC-chimeras was examined. IgG₁-FC protein and BSA was used as a background control. All constructs showed target-binding activity. When being compared to the IgG₁-FC background signal, with the exception of the erbB2-binder 14/5, all signals were beyond a signal to noise ratio (S/N) of 3.

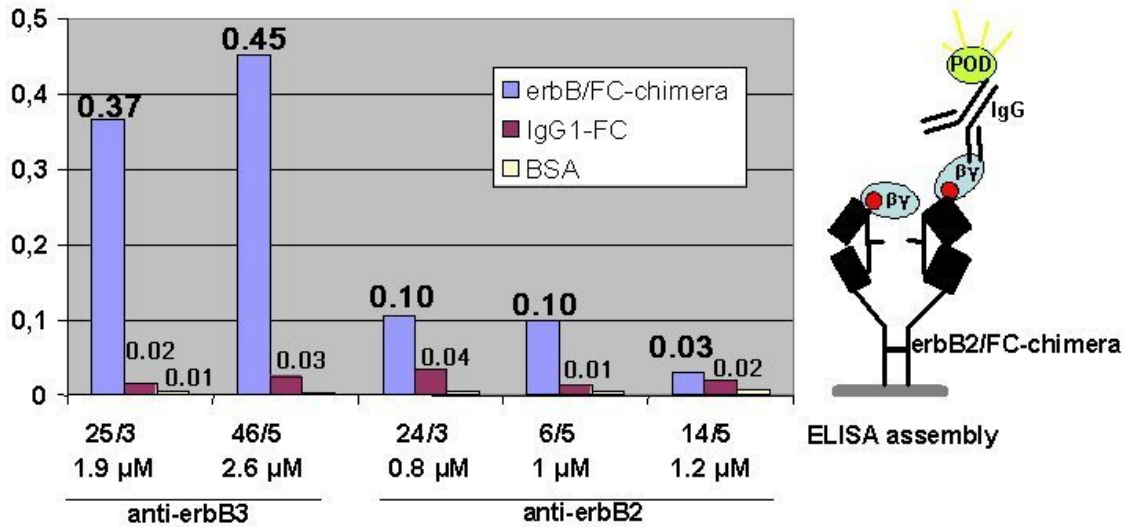


Fig. 36: ELISA with 5 human γ crystallin derivatives to determine the binding behavior versus the proteins erbB2/IgG1FC-, erbB3/IgG1FC-chimera, BSA and human IgG₁FC. The ELISA assembly is shown at the right side of the diagram.

The concentration-dependent binding-behavior of the crystallin derivatives was analyzed (see fig. 37). Two exemplary diagrams of the constructs 25/3 and 24/3 are presented, showing a concentration-dependent receptor binding-behavior. From the ELISA data, no information about the receptor affinities of these constructs could be obtained. Due to the low amount of the obtained purified derivatives and their tendency to precipitate it was not possible to concentrate the derivatives in order to achieve a signal-saturation in the ELISA. Thus no equilibrium constant could be determined. Biacore SPR measurements of the purified constructs revealed no binding activity, too (no data shown).

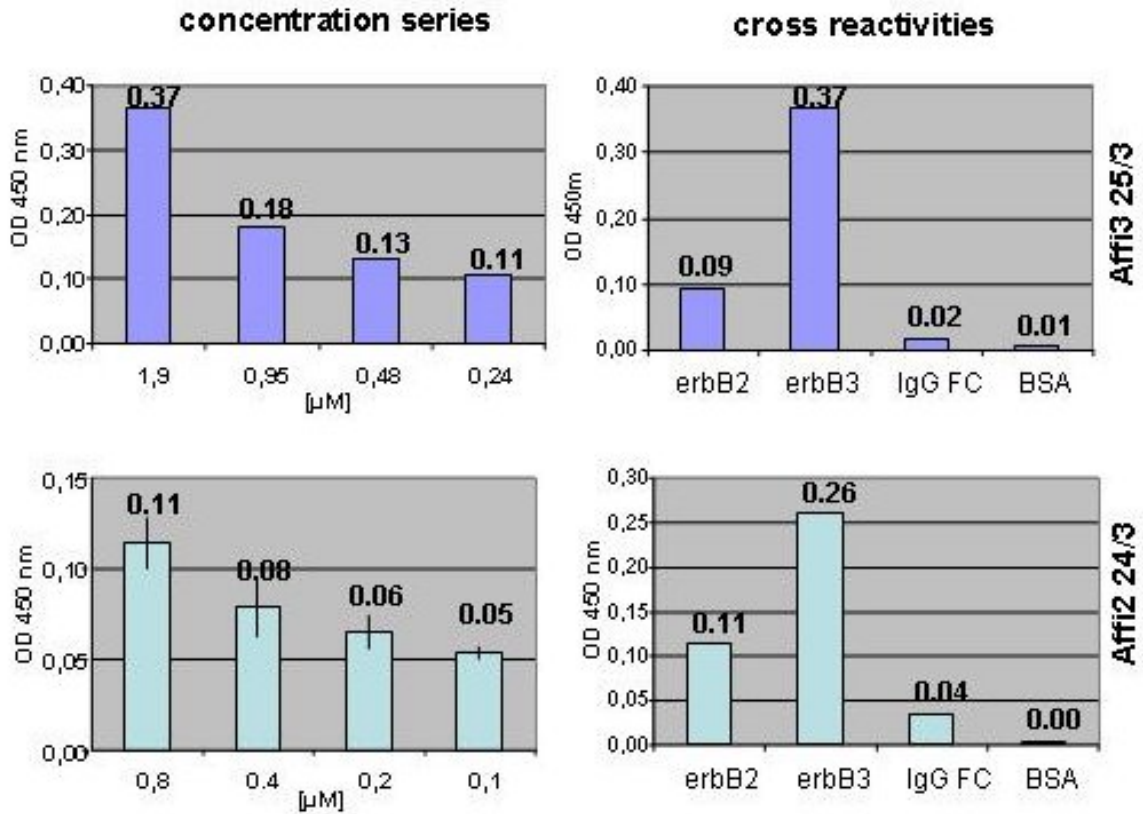


Fig. 37: Left: Exemplary two ELISAs revealing the concentration dependent binding of the construct 25/3 and 24/3 towards the erbB3/FC- and erbB2/FC-chimeras. Right: ELISA detected binding of the derivatives 25/3 and 24/3 towards the erbB2/FC- and erbB3/FC chimera, IgG1-FC and BSA. A strong cross-reactivity of the erbB2-binder 24/3 towards the erbB3/Fc-chimera was detected.

The reciprocal target binding behavior of the constructs was analyzed (see fig. 37). The genuine erbB3-binding signal of the 13/B11-2 derivative 25/3 was 4-times higher than the erbB2 derived signal. The cross binding to BSA and IgG₁-FC was negligible. The erbB2-binding derivative 24/3 showed a 2.4-times higher cross binding towards the erbB3 receptor than to its genuine target erbB2. Reciprocal binding of the erbB2-binders 6/5 and 14/5 versus the erbB3-receptor was observed (no data shown). Due to the reciprocal binding properties of these constructs a γ crystallin-based diagnostic-tool, which should be able to specifically recognize and differentiate between the erbB2 and erbB3 receptor ectodomains, could not be realized using these derivatives.

4.13.6 Consequences of the two domain character of γ crystallin

The error prone PCR had also introduced non-functional mutations. 41 % of all sequenced γ crystallin derivatives revealed a DNA-frame shift, which produced in 90 % a stop-codon at the amino acid position 93 (see fig. 38). This amino acid position is located after the N-terminal domain in the inter-domain peptide linker region of γ crystallin.

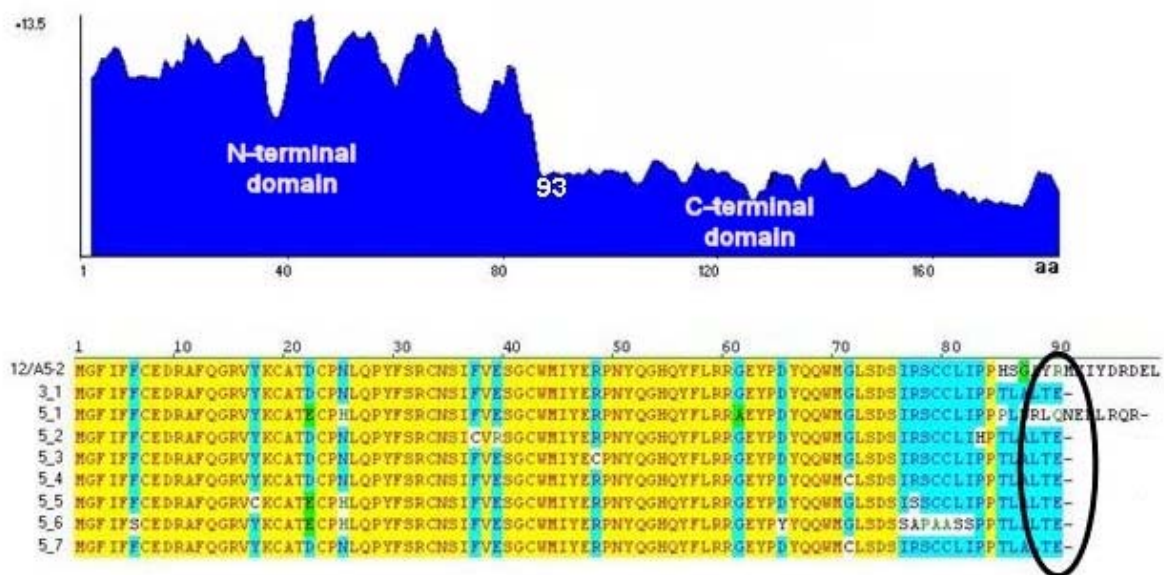


Fig. 38: *Above*: Absolute amino acid similarity calculation from 44 sequenced erbB2-recognizing γ crystallin derivatives (Vector NTI). Due to DNA frame shifts after amino acid position 93 the similarity index strongly declines. *Below*: DNA-sequencing of all γ crystallin derivatives revealed a typical pool of constructs, which contained a stop-codon after the N-terminal γ crystallin-domain. The amino acid motive ALTE was first recovered after the third ribosome display cycle (construct 3_1) and was found enriched after the fifth cycle (58 % of all construct). 12/A5-2: first generation construct; 3_1 to 5_7 sequenced constructs ending with a stop-codon after the motive ALTE- or RQR-.

During the ribosome display protocol the translation was stopped on ice by Camp-inhibition of the ribosomal peptidyltransferase activity. The ribosomes must have been arrested before they had encountered a stop-codon. Otherwise, the ternary complexes would have been dissociated by the binding of the release factors and the regeneration factor and no information would have been recovered from these constructs (Grentzmann *et al.* 1998; Karimi *et al.* 1999; Nakamura *et al.* 2003).

44 full-length sequences of the erbB2-binding 12/A5-2 derivatives from the first, third and fifth display cycle were aligned and the absolute amino acid similarity was calculated (see fig. 38).

The calculation revealed a strong decline of the sequence similarity index at the position 93. After the fifth display cycle 58 % of the sequenced 12/A5-2 derivatives revealed a stop-codon (see fig. 38) at the position 93. Typically a DNA frame-shift occurred after Pro84, which induced the stop-codon downstream at the position 93. A rare codon calculation (GCG) of the γ crystallin DNA sequences revealed that two prolines at the positions 83 and 84 were encoded by the rare *E.coli* proline codon CCC. This indicated that the translation was attenuated at these positions and more ribosomes were attenuated at this position when the translation reaction was stopped. Since the *de novo* binding patch primarily enabled the target binding of the displayed constructs, the selective pressure was primarily targeted on the presentation of a binding-active N-terminal fragment, as these constructs were found enriched (58 %) after the fifth display cycle. From these results it was concluded that mostly the N-terminal γ crystallin domain or a binding active N-terminal fragment had been selected by ribosome display. To test this thesis one ribosome display cycle was performed with the performing 13/B11-2 γ crystallin construct versus its erbB3/IgG1FC-chimera target.

The experiment differed from the preceding ones by the omission of the ribosome display spacer "NoStalling" (see fig.39). The C-terminal γ crystallin domain should not be completely displayed and should overtake the function of a display spacer. The ribosome display experiment yielded a specific PCR-product. The background PCR-product signal of the spacer-less ribosome display construct was slightly increased when compared to the spacer-fused construct.

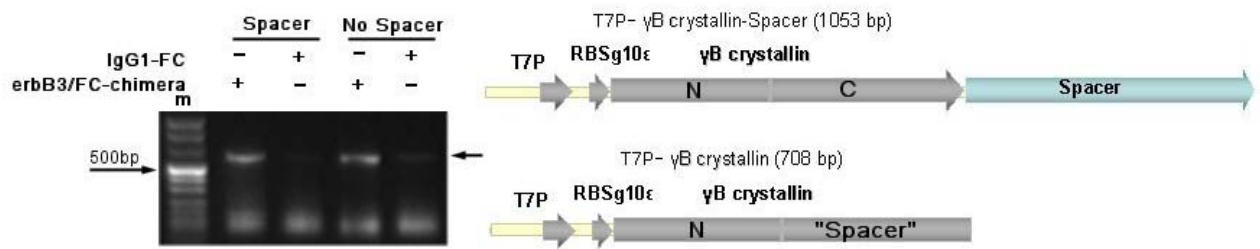


Fig. 39: 1% EtBr-stained agarose gels with γ crystallin PCR-products after one Ribosome display cycle. The γ crystallin derivative 13/B11-2 was fused to the “No Stalling” ribosome display spacer and was subjected to one ribosome display cycle versus the erbB3 target (Spacer). In a second experiment the spacer was omitted and the C-terminal domain of the γ crystallin performed as a spacer (“Spacer”). Both ribosome display constructs revealed a specific PCR-product at 550 bp. The background signal of the truncated construct was only slightly increased.

This result indicated that the N-terminal fragment of the γ crystallin construct could be independently displayed from the C-terminal domain. The C-terminal γ crystallin domain performed as a display spacer. This also indicated that the C-terminal domain was excluded from the forces of selection.

4.14 Engineering the hemopexin-like scaffold as a *de novo* binding-protein

Two criteria seem to characterize an applicable protein-scaffold: First, the protein should belong to a family, which reveals a well defined hydrophobic core that is structurally closely related among its individual members (Skerra 2000). Second, the protein should possess a spatially separated and functionally independent accessible active site or binding pocket, which does not contribute to the intrinsic core-stability (Predki *et al.* 1996). In ideal, this protein-family is involved in the recognition of multiple, non-related targets.

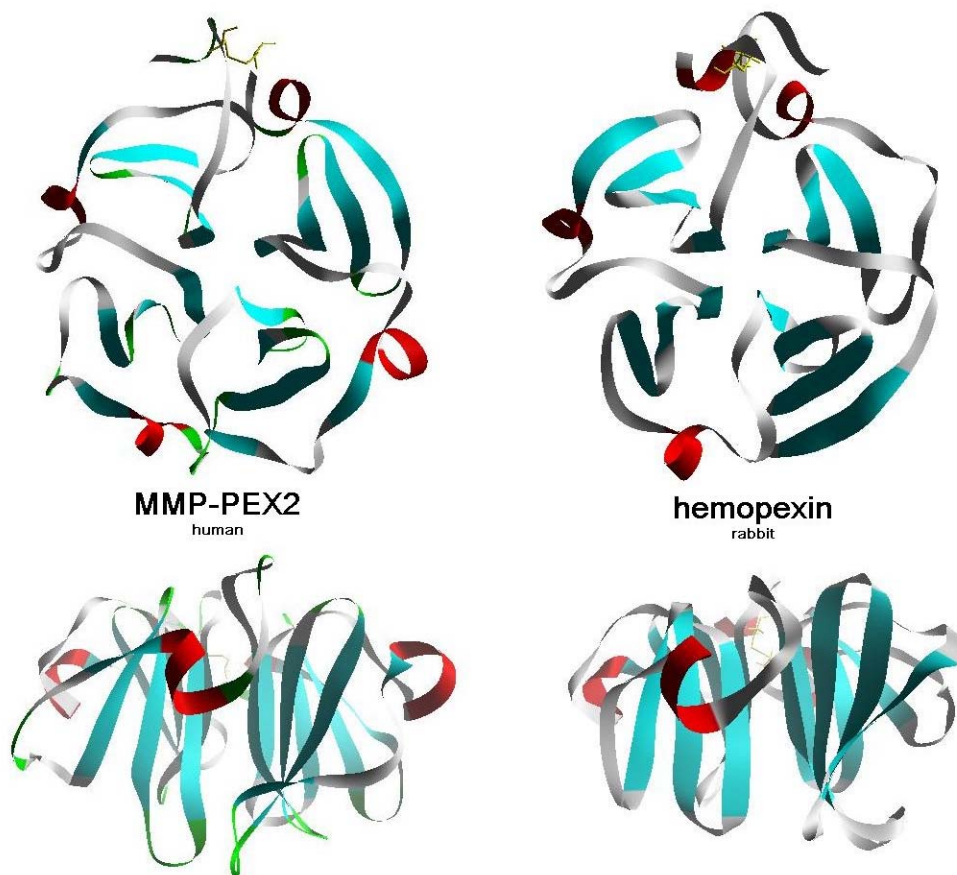


Fig. 40: The C-terminal, hemopexin-like domain of the human MMP2, PEX2 was elucidated for its suitability to perform as a template-protein scaffold in a library and screening approach using ribosome display. The hemopexin-fold (PEX) is a four-bladed, propeller-like, β -sheet scaffold, which is named after hemopexin, the human heme-binding plasma protein, because of its relation in structure. In the hemopexin-like fold the first blade is connected to the fourth blade via a disulfide bond. The proteins are schematically figured as ribbon diagrams based on X-ray data from *left*: (Gomis-Ruth *et al.* 1996) and *right*: (Paoli *et al.* 1999).

The hemopexin-like protein scaffold fulfills these criteria (see fig.40). In human beings there are 24 known Matrix Metalloproteinases (MMPs) (Egeblad *et al.* 2002). Twenty of them contain a hemopexin-like domain (PEX) at their C-terminus (Bode 1995; Gomis-Ruth *et al.* 1996). The scaffold carries its name because of the close structural relation to the heme-binding plasma protein hemopexin (Faber *et al.* 1995).

The hemopexin-like protein domain offers a high structural homology among its protein family. High structural equivalence of the hemopexin-domains of MMP-1, MMP-2 and MMP-13 was reported (Gomis-Ruth *et al.* 1996). The predominantly hydrophobic interaction between the adjacent and perpendicularly oriented beta-sheets provides most of the required structural stability (Gomis-Ruth *et al.* 1996; Fulop *et al.* 1999).

4.14.1 Stability of the PEX2 protein

Since the common functional property of the hemopexin-like scaffold is to participate in quite specific, but different protein-protein and protein-ligand interactions, the hemopexin-like framework permits a high versatility for molecular recognition (Bode 1995). For example in its central tunnel PEX2 binds ions like Ca^{2+} , Na^+ ; Cl^- (Libson *et al.* 1995; Gohlke *et al.* 1996). Further binding sites exist, which facilitate the interaction with fibronectin, TIMP-1/2, integrins and heparin (Wallon *et al.* 1997) (Willenbrock *et al.* 1993) (Brooks *et al.* 1998) (Bode 1995). It was to examine, whether the PEX-domain could be engineered as a multi-purpose binding protein. As a representative of the PEX-domain family, the amino acid sequence Pro466 to Cys660 of MMP-PEX2, the 21 kDa C-terminal domain of gelatinase A was taken as a model protein (Gohlke *et al.* 1996).

A fundamental question was if the PEX2-scaffold offers adequate properties to be used in engineering approaches and display strategies. In contrast to the 5 to 8 bladed beta-propeller structures the ring-closure in the hemopexin-like domain is facilitated by a disulfide-bond, which connects the first with the fourth blade. The contribution of this single disulfide bond to the overall scaffold-stability was examined by DSC-experiments. DSC-measurements of the apparent temperature transitions of PEX2 under different buffer conditions were performed (see fig. 41). All PEX2 temperature-transitions were irreversible. 2.5 mg/ml native PEX2 in PBS buffer with 1 mM CaCl_2 referred the highest transition temperature of $61.2\text{ }^\circ\text{C} \pm 1^\circ\text{C}$. Reduction of the disulfide bond by 1 mM DDT reduced the transition temperature to $56.9^\circ\text{C} \pm 1^\circ\text{C}$.

The reduction of the disulfide bond with subsequent alkylation of the sulfhydryl-groups revealed a transition temperature of $57.2\text{ }^{\circ}\text{C} \pm 1^{\circ}\text{C}$. The temperature transitions revealed that the disulfide bond significantly contributes to the thermal stability of PEX2. The central divalent Ca^{2+} -ion in the tunnel of the PEX2-protein also contributes to the stability of the protein, since supplementation of native PEX2 in PBS with 1 mM EDTA revealed a reduced transition temperature of $56.4^{\circ}\text{C} \pm 1^{\circ}\text{C}$.

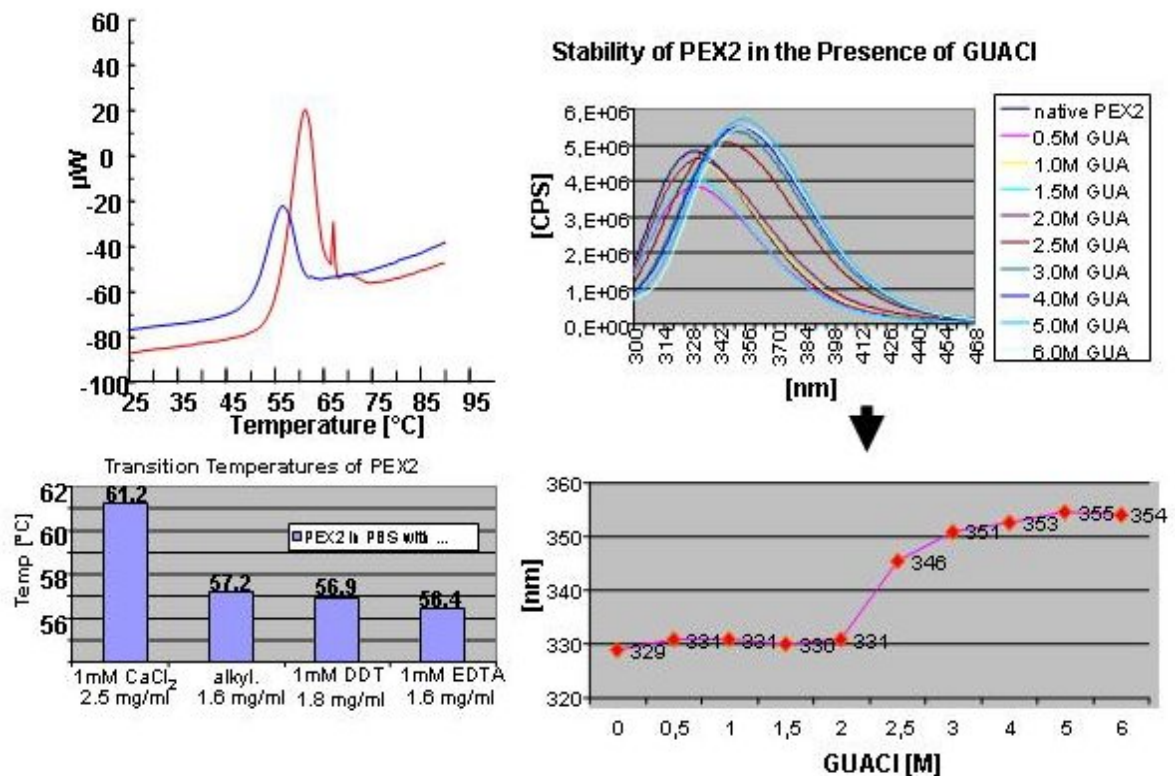


Fig. 41: *Left*: DSC-thermogram with two exemplary melting curves of 2.5 mg/ml native PEX2 in PBS with 1 mM CaCl_2 (red) and 1.6 mg/ml native PEX2 in PBS with 1mM EDTA (blue). Transition temperatures measured under different buffer-conditions are visualized in a column-plot. *Right*: Fluorescence emission shifts from stepwise-denatured PEX2 revealed stability of PEX2 up to 2 M GuaCl.

The intrinsic fluorescence emission shift of native (328 nm) to theoretically unfolded (355 nm) PEX2 was determined (see fig. 41). The protein was subjected to concentration series of GuaCl. PEX2 was stable up to 2 M GuaCl and was theoretically unfolded at 3 M GuaCl. The DSC- and the fluorescence emission-shift measurements under denaturing conditions revealed that PEX2 offered enough stability for being used in subsequent engineering approaches.

4.14.2 Identification of variable amino acid positions in hemopexin-like fold

The use of protein-databases like SMART (Schultz *et al.* 1998; Letunic *et al.* 2002) were recently used to compare homologous sequences and protein-folds in order to identify non-conserved, and thus theoretically randomizable amino acid positions in suitable protein frameworks (Binz *et al.* 2003; Forrer *et al.* 2004).

To identify potentially randomizable amino acid positions in the PEX2 fold, a similar approach was performed using the SMART database. Amino acid positions should be identified in the PEX2 protein, which might be randomizable without affecting the proteins structure-functional conformation and stability. From the SMART database 60 PEX-domains from 22 Matrix Metalloproteinases from different species were aligned with the Pretty bioinformatics tool (GCG) using the scoring matrix blosum 62 (see fig. 42). The number of different amino acids per position was counted in order to compile an amino acid diversity index.

```
MM02_human; PEX2_rat; PEX2mouse; PEX2_rabbit; Pex2_chick, MM01_Bovin,  
MM01_HORSE, MM01_human, MM01_PIG, MM03_human, MM03_MOUSE,  
MM03_RABIT, MM03_RAT, MM08_human, MM08_MOUSE, MM08_RAT,  
MM10_human, MM10_MOUSE, MM12_human, MM12_MOUSE, MM12_RABIT,  
MM12_RAT, MM13_BOVIN, MM13_HORSE, MM13_human, MM13_RABIT,  
MM20_BOVIN, MM20_human, MM20_MOUSE, MM20_PIG, MMP18_XENLA,  
MM16_RAT, MM09_BOVIN, MM19_human, MM09_CANFA, MM09_human,  
MM09_MOUSE, MM11_human, MM11_MOUSE, MM14_human, MM14_mouse,  
MM14_PIG, MM14_RABIT, MM14_RAT, MM15_human, MM15_MOUSE,  
MM16_human, MM16_MOUSE, MM17_human, MM17_MOUSE, MM19_MOUSE,  
MM24_human, MM24_MOUSE, MM24_RAT, MM25_human, MM28_human,  
VTNC_human, VTNC_MOUSE, VTNC_PIG, VTNC_RABIT.
```

Fig 42: 60 hemopexin-like protein domains from the SMART-database listed up in data-bank code. The sequences were used to generate an alignment.

Fig. 43: The amino acid consensus-sequence of 60 PEX-domains (Position). The PEX2 sequence is listed up in one-letter code (Sequence). Gaps in the consensus are marked by a hyphen (-). For every position the number of different amino acids and gaps are given. The diversity index is given for different amino acids per position (AA diversity). The maximum possible number is 21 (20 aa + 1 gap). A low diversity indicates a high conservation. A high diversity is supposed to indicate flexibility at this position. The red lines mark a high diversity index.

A	C	D	E	F	G	H	I	K	L	M	N	P	Q	R	S	T	V	W	Y	-	Position	AA diversity	Sequence	A	C	D	E	F	G	H	I	K	L	M	N	P	Q	R	S	T	V	W	Y	-	Position	AA diversity	Sequence				
0	3	2	2	0	0	0	0	1	0	0	40	0	0	3	0	0	0	0	0	1	1	6	P	0	0	46	0	0	1	1	0	0	0	0	0	0	2	5	3	0	2	0	0	0	110	7	D				
3	0	16	10	0	0	2	0	0	5	0	0	14	2	1	0	1	4	1	0	0	0	1	2	11	E	42	0	0	0	0	0	8	0	0	0	0	0	0	0	1	4	5	0	0	0	0	111	5	A		
6	0	0	0	1	3	0	19	6	5	3	1	4	0	4	0	0	6	0	1	0	1	3	12	I	51	0	0	0	0	1	1	0	0	1	0	0	2	0	2	0	0	2	0	0	0	112	7	A			
0	88	0	0	0	0	0	0	0	0	0	0	0	0	0	0	0	0	0	0	0	1	4	2	C	0	0	0	2	8	2	0	9	0	17	0	0	0	0	2	0	0	0	0	0	0	113	7	F			
0	0	22	0	0	0	2	0	4	0	0	0	0	0	5	1	0	0	0	0	0	26	5	5	K	0	0	0	13	0	7	0	2	0	0	5	3	0	6	14	0	0	5	0	0	0	114	9	N			
0	0	0	0	0	2	0	1	3	0	3	13	8	0	0	12	0	0	0	0	0	20	6	7	Q	0	0	0	5	5	0	0	1	0	5	0	0	0	2	2	3	0	0	23	3	0	115	11	K			
4	0	19	3	0	1	3	0	4	0	0	4	0	0	0	15	2	4	0	0	0	1	7	10	D	2	0	0	17	0	3	0	0	11	0	5	3	9	2	4	4	0	0	0	0	0	0	116	10	S		
5	0	2	2	0	14	0	5	0	22	0	0	0	0	4	2	1	0	0	0	1	8	10	I	0	0	13	8	0	3	2	4	3	0	21	2	3	5	0	1	0	0	0	0	0	117	13	K				
0	0	1	0	1	0	2	3	1	1	0	13	0	0	2	19	5	11	0	0	0	1	9	11	V	1	0	0	1	0	0	4	3	0	15	2	4	3	10	6	0	0	9	118	11	N						
0	0	2	0	53	0	0	0	0	4	0	0	0	0	0	0	0	0	0	0	0	1	10	3	F	0	0	0	0	0	0	0	0	1	0	0	0	0	0	0	0	0	0	0	0	0	119	2	.			
2	0	47	3	0	0	0	0	0	0	0	7	0	0	0	0	0	0	0	0	0	1	11	4	D	0	0	0	0	0	0	0	0	0	0	0	0	0	0	0	0	2	0	0	0	0	0	0	120	1	.	
35	0	0	0	5	3	0	0	0	0	2	0	0	0	0	1	13	0	0	0	0	1	12	6	G	0	0	2	0	0	27	1	0	9	0	0	1	0	8	5	0	0	0	0	1	0	0	0	121	8	K	
1	0	0	3	0	0	21	0	3	1	0	0	0	0	0	1	28	0	0	0	1	13	7	I	0	0	0	0	0	2	0	46	0	0	0	0	0	0	0	0	0	0	0	0	0	0	0	122	3	K		
28	0	0	0	0	0	0	0	0	2	0	0	0	0	0	8	21	0	0	0	0	1	14	4	A	1	0	1	0	0	0	0	0	2	1	0	1	1	0	1	44	8	0	0	0	0	0	123	9	T		
0	0	0	4	0	2	0	3	0	4	11	1	0	7	0	4	20	3	0	0	0	1	15	10	Q	0	0	0	4	0	0	1	0	12	0	0	0	0	0	4	0	0	0	39	0	0	0	124	5	V		
0	0	1	0	4	0	0	17	0	29	2	0	0	0	0	4	0	0	0	0	1	16	7	I	0	0	0	42	0	0	5	0	9	0	0	0	0	4	0	0	0	0	0	0	0	0	125	4	I			
0	0	0	0	9	1	0	0	0	0	0	0	0	3	45	0	0	0	0	0	0	1	17	4	R	1	0	0	0	55	0	0	0	0	0	0	0	0	0	0	0	0	0	0	0	0	0	126	4	F		
0	0	1	1	0	41	0	0	4	0	5	0	1	6	0	0	0	0	0	0	0	1	18	7	G	6	0	0	0	0	0	0	3	11	0	0	0	0	0	2	8	9	2	19	0	0	0	127	8	A		
1	0	3	45	0	0	5	3	0	0	0	0	2	1	0	0	0	0	0	0	1	19	7	E	7	0	6	6	0	32	0	1	0	3	0	0	1	1	0	0	3	0	0	0	0	0	128	9	G			
0	0	0	0	0	0	0	0	0	1	0	0	0	0	0	0	15	3	2	5	0	0	29	33	8	V	0	0	44	10	1	0	0	0	1	0	1	0	0	0	0	0	0	0	0	0	0	0	129	12	D	
2	0	0	0	0	0	0	14	0	13	0	0	0	0	0	0	7	6	3	0	0	1	21	8	I	0	0	2	5	0	2	1	0	19	4	0	0	0	1	10	13	3	0	0	0	0	0	130	10	K		
0	0	0	3	26	0	3	1	0	13	7	0	0	0	0	0	0	0	0	0	6	1	22	7	F	0	4	0	0	0	0	0	0	3	0	0	0	0	0	0	0	0	5	2	38	0	0	0	131	6	F	
2	0	2	0	32	0	0	5	0	3	0	1	0	0	0	0	14	0	0	0	1	23	7	F	0	0	0	0	4	0	0	0	0	0	0	0	0	0	0	0	0	0	0	0	0	0	0	0	132	3	W	
0	0	0	0	56	0	0	3	0	0	0	0	0	0	0	0	0	0	0	0	1	24	2	F	0	0	0	0	0	0	0	0	1	0	0	0	0	0	0	2	44	12	0	1	0	0	0	133	5	R		
0	0	0	3	0	0	0	0	53	0	0	0	0	0	2	0	1	0	0	0	1	25	4	K	0	0	0	0	19	0	0	0	1	0	0	0	0	0	4	0	0	4	0	0	23	4	0	0	134	5	Y	
3	0	57	8	0	0	0	3	0	0	0	0	0	0	0	0	0	0	0	0	1	26	5	D	1	0	38	4	0	0	2	0	0	0	0	12	0	0	0	0	0	0	0	0	0	0	0	0	135	6	N	
0	0	2	0	6	0	0	4	3	0	2	0	2	36	2	0	0	2	0	0	1	27	9	R	9	0	0	6	4	0	0	0	0	0	0	0	0	0	0	0	0	0	0	0	0	0	0	0	0	136	7	E
0	0	0	20	0	4	4	3	0	0	0	0	0	0	0	0	15	10	1	0	1	28	7	F	1	0	1	15	0	1	2	0	8	2	0	1	0	0	2	9	3	6	5	0	4	0	0	0	137	14	V	
0	0	0	41	0	0	4	0	1	1	0	0	0	0	0	4	0	8	0	1	29	6	I	4	0	0	2	3	0	0	16	3	3	5	0	2	11	3	8	0	0	0	0	0	0	0	0	138	11	K		
0	0	0	0	0	0	0	0	4	0	0	0	0	0	0	55	0	0	0	1	30	2	W	1	0	3	0	0	4	0	10	4	0	1	1	15	2	1	0	0	0	0	0	0	0	0	0	0	139	9	K	
0	0	0	1	0	3	0	0	1	1	0	0	0	0	48	0	2	0	3	0	1	31	7	R	8	0	0	0	1	4	2	1	11	2	3	0	0	0	2	5	11	7	3	0	0	0	0	140	13	K		
0	0	0	3	0	0	1	8	13	0	0	0	0	0	13	8	13	0	0	1	32	7	T	1	0	2	0	0	3	0	0	1	35	0	0	0	0	0	0	4	12	0	0	0	0	0	0	141	8	M		
0	0	0	0	0	0	0	0	1	0	0	0	0	5	15	3	2	5	0	0	29	33	8	V	0	0	44	10	1	0	0	0	1	0	1	0	0	0	0	0	0	0	0	0	0	0	0	0	142	6	D	
0	0	0	2	0	0	0	0	1	0	0	0	1	0	2	0	0	0	0	0	0	53	34	5	.	4	0	0	0	0	0	0	9	1	0	5	30	2	0	8	0	0	0	0	0	0	0	0	143	8	P	
1	0	2	0	0	4	11	1	1	2	0	15	0	0	0	8	4	5	0	0	6	35	11	T	3	0	8	6	0	30	0	0	0	0	0	1	2	2	3	1	0	0	0	4	0	0	0	144	10	G		
1	0	0	0	4	6	0	1	4	0	13	20	4	4	2	0	0	0	0	0	1	36	10	P	0	0	2	1	11	0	0	0	0	0	0	0	0	0	0	4	1	2	0	39	0	0	0	145	7	F		
0	0	3	1	2	7	2	0	1	5	0	0	0	0	15	17	3	0	0	2	1	37	12	R	2	0	4	0	0	0	0	0	0	0	0	0	0	0	5	2	0	0	0	0	0	0	0	146	4	P		
2	0	5	0	0	3	0	1	1	9	2	2	1	3	4	7	2	13	0	0	1	38	15	D	2	0	0	0	0	1	0	1	35	0	0	0	0	0	14	1	2	0	0	4	0	0	0	147	8	K		
0	0	0	5	0	0	5	4	8	1	12	6	5	4	2	7	0	0	0																																	

The amino acid diversity calculation revealed amino acid positions with a low diversity-index (see fig. 43). This resembled a high conservation like the position Nr. 4 (C469), which was found conserved in 56 from 60 PEX sequences. The cystein residue Nr. 210 in PEX2 (C660) was found conserved in all PEX sequences.

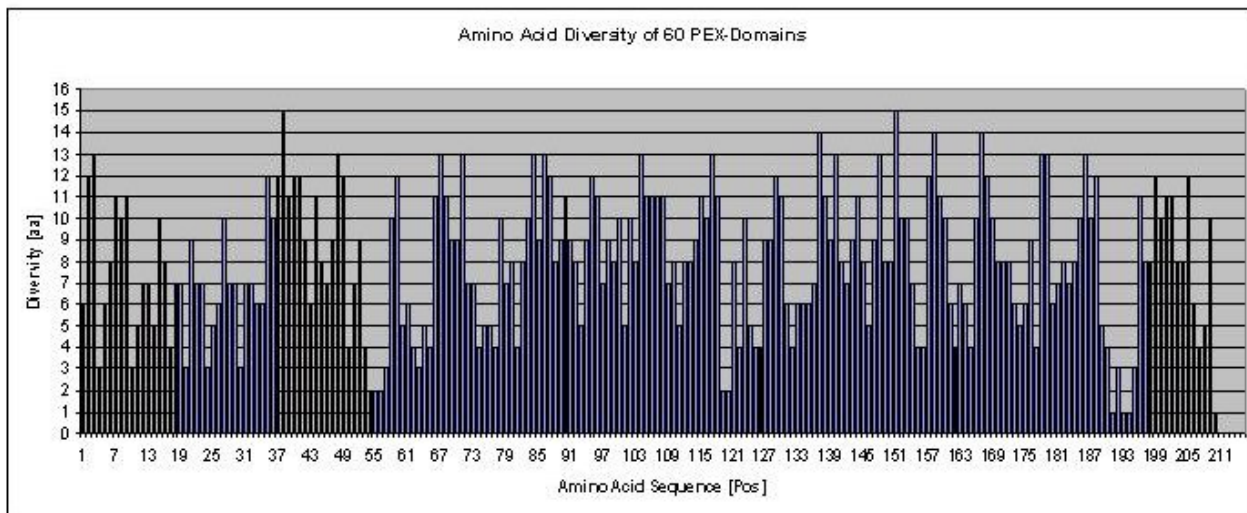


Fig. 44: The plot illustrates fig.43. The number of amino acid-counts is plotted versus the consensus sequence. The maximum diversity index was 15 (e.g. Asp38).

This demonstrated the importance of the conserved cysteins in the hemopexin-like scaffold. Positions with a high diversity-index were also detected. In the PEX2 ribbon plot all amino acids (see fig. 45) with a greater diversity than 10 were marked in green. In the compact disc-like fold of PEX2 the fourth outermost strand of the beta-sheet blade is connected by a long loop to the innermost strand of the next blade.

The analysis revealed, that these loop regions exposed a high variability and spatially brought together several surface exposed amino acids from other blade connecting loops. The results also suggested not using the interior surface of the tunnel for randomization experiments. The inner three beta-sheets of each blade were also "forbidden", because they resembled a high conservation and contributed to the core-stability of the PEX2 protein. Thus, solvent-exposed amino acids, which do not contribute to the hydrophobic core stability of the protein, which revealed a sufficient high diversity number and hence a low conservation, were in the focus of interest for a potential mutagenesis approach.

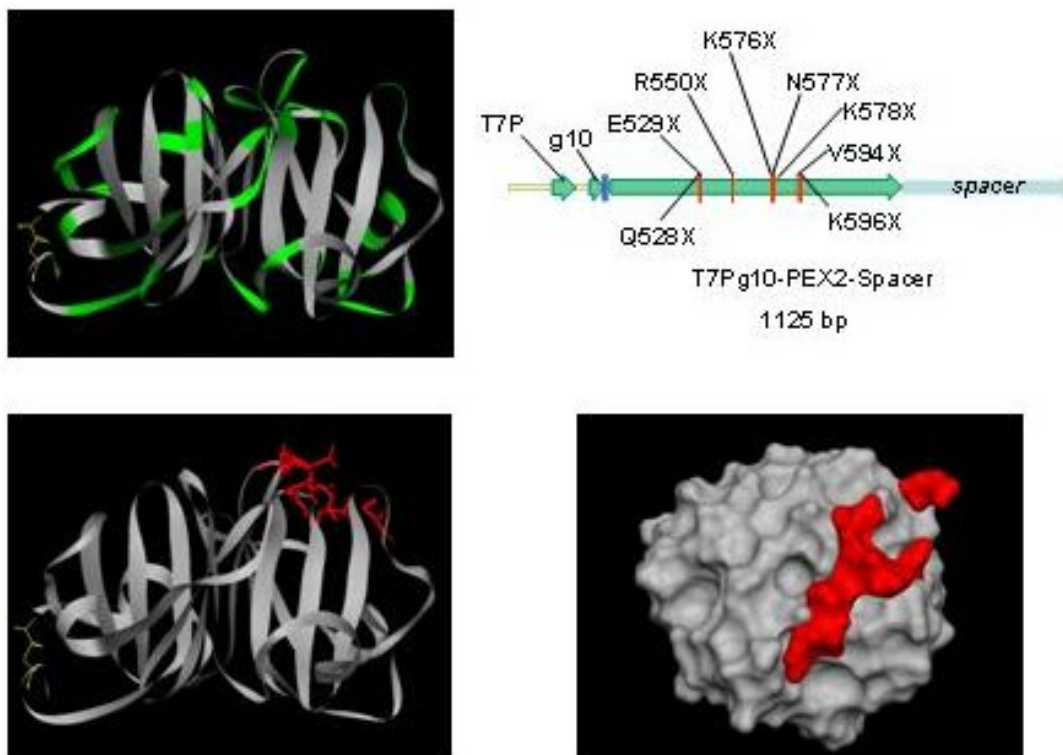


Fig. 45: Left: Ribbon diagrams of PEX2. Positions marked in green resemble a diversity index beyond 10. 8 amino acids shown as red sticks were randomized. Right: The electron surface density map of PEX2 shows this approach. A flexible surface, marked in red should be generated. The PEX2 ribosome display library DNA construct is schematically drawn. The 8 randomized positions are indicated.

4.14.3 Ribosome Display of wild type PEX2 versus TIMP2

The next aim was to establish an appropriate display strategy in order to select PEX2 binding proteins from a library of protein mutants (see fig. 45). Therefore the wild type PEX2 protein was tested for its ability to work in a ribosome display selection. One ribosome display cycle was performed with the wild type PEX2 DNA sequence, which was fused to the “NoStalling” display spacer. The display cycle was performed like it was established with the mini-BP4/IGF-I model (see 4.12). The natural PEX2 binding partner, TIMP2, was presented as a biotinylated ligand in a streptavidin coated MT-plate. The wild type PEX2 construct (585 bp) was retained after one ribosome display cycle versus TIMP2. No background PCR-product signal was obtained.

Using ribosome display it could be shown that PEX2 could be displayed in its TIMP-2 binding-active conformation, despite PEX2 was still being tethered to the ribosome via the “NoStalling” spacer. At the same time this experiment proved, that ribosome display was an appropriate method to exploit the PEX2 scaffold in display approaches.

4.14.4 Approach to engineer PEX2 as a binding protein

In a first library approach, 8 amino acid positions were randomized (see fig. 45). Amino acids with a diversity index between 8 and 14 were chosen, from which 7 formed a fork-shaped 914 Å² surface around the central PEX2 tunnel. One further randomized position was located in the position Arg550. The randomized surface takes 13.8 % of the proteins water exposed 6596 Å² surface and comprised the blades two and three.

The PEX2 positions Gln528, Glu529; Arg550; Lys576, Asn577, Lys578, Val594 and Lys596 were randomized. The library was generated by template free PCR synthesis as described under paragraph 3.21.13. The linear DNA-template was cloned into the vector pUC18. The quality of the library was confirmed by sequencing of 10 DNA constructs (no data shown). A ribosome display template was assembled by the modules T7P-g10ε-ATG, the PEX2 library and the Ribosome Display Spacer “No Stalling” (see 3.23.3.).

A prerequisite for a suitable protein scaffold is its capability to stably fold in its active conformation, even under conditions where it has to carry the burden of multiple substituted amino acids. This can be examined by targeting the library versus a known protein-binding partner.

The PEX2 library was displayed to recognize the TIMP2 protein ligand (see fig. 46). A specific PCR-product at 600 bp was obtained. By-products at 150 bp and a background PEX2 PCR-signal were detected, too. DNA sequencing revealed that specific PEX2 derivatives with TIMP2 binding activity were retained from the PEX2 library (no data shown).

The randomized PEX2-library was still able to recognize its TIMP2 binding partner in a ribosome display approach. This indicated that the structure-function of the scaffold was maintained despite the scaffold was multiple mutated.

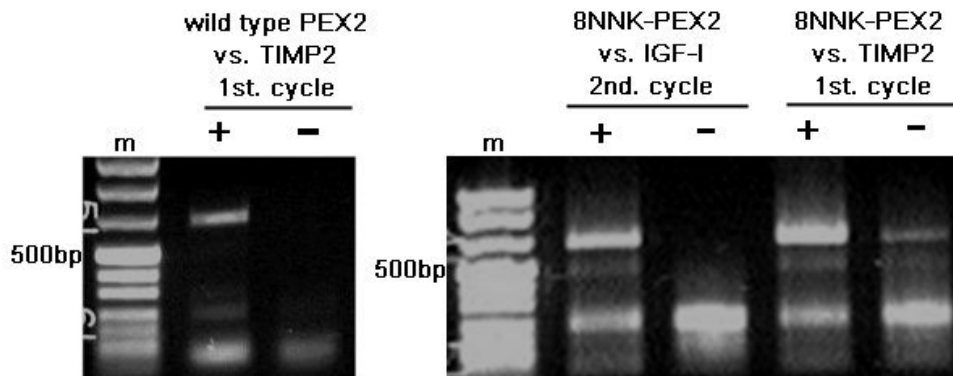


Fig. 46: 1% EtBr-stained agarose-gels. Left: After one ribosome display cycle with wild-type PEX2 versus its natural binding partner TIMP2 a specific PCR-product (600 bp) was obtained. Right: After one display cycle, the PEX2 library recognized the PEX2 binding partner TIMP2. After two display cycles a specific PCR-product versus the target protein IGF-I was obtained.

In a third experiment the non-PEX2 binder IGF-I was plate-presented as a biotinylated ligand. After the second ribosome display cycle with the PEX2 library a visible PCR-product signal was retained (see fig. 46). No background signal was detectable. This suggested that the library was also suited for the selection of binding proteins versus non-related target proteins.

5 Discussion

5.1 Advantages of a high throughput cell-free protein production and analysis

In this study it could be demonstrated that a parallel cell-free protein production and protein-interaction analysis of various gene-products is possible using the coupled transcription and translation as a platform technology.

The establishment of the cell-free *in situ* enzymatic monobiotinylation of fusion proteins permitted the rapid supply of SPR protein-protein interaction analyses with functional active proteins (see 3.22.1). It was also possible to directly capture biotinylated proteins on SA-coated sensor chips from dialyzed crude extracts (see 4.6). In principle it was not necessary to purify the recombinant proteins prior to their immobilization and analysis, since the SA-coated sensor-surface was able to perform as a highly selective affinity matrix for biotinylated proteins.

Conventional immobilization methods, like the chemical biotinylation require labourous protein purification prior to their modification. Biotin is randomly coupled to the ϵ -amino group of surface accessible lysins in the protein (Bayer *et al.* 1990). But even if proteins are being biotinylated in a 1:1 stoichiometry, proteins can loose their activity due to the modification of lysins located nearby or in the active site of a protein. Moreover, after the immobilization of such a protein, the active site might get inaccessible for interaction partners (Schräml *et al.* 2002). Another reason for the loss of activity can be the harsh reaction conditions (e.g. pH value) required for a chemical biotinylation, which might be detrimental for the solubility or the active conformation of the protein. The rapid cell-free production of enzymatically monobiotinylated proteins bypassed these obstacles, since the major advantage of the enzymatic monobiotinylation is the maintenance of the ligands binding activity after its oriented immobilization (Schräml *et al.* 2002).

The coexpression of BirA took the advantage offered by a cell-free system to simultaneously express more than one protein at once (Elbaz *et al.* 2004). Despite a supplementation of the system with separately expressed and purified BirA enzyme is possible (Schräml *et al.* 2002) it was circumvented in this case. The addition of only a small amount of BirA DNA-template hardly diluted the overall concentration of the standard RTS components and did not affect the optimized translation parameters of the system.

Furthermore the enzymatic biotinylation was suited for the sensitive detection of biotinylated proteins, especially when no protein-specific antibody was available, like it was the case with the mini-BP4 constructs (see 4.5). The SA-HRP conjugate detected biotinylated proteins, but BCCP, the only naturally occurring biotinylated protein in *E.coli* was not detectable under native conditions. BCCP binds to streptavidin only in a denatured or proteolytically cleaved configuration (John E. Cronan 1990). BCCP could only be detected after Western blotting under denatured conditions. This qualified native slot blotting for the fast process-accompanied monitoring of the cell-free protein expression of monobiotinylated fusion proteins.

For a rapid protein production and analysis system it would be desirable to express and immobilize fusion proteins directly on a micro-chip surface (Tabuchi *et al.* 2002; Tohru Natsume *et al.* 2002; Angenendt *et al.* 2004), accompanied by the SPR-interaction analysis. Here difficulties with the handling of BAP-fused proteins arise, because free biotin from the enzymatic biotinylation reaction saturate the streptavidin surface, before sufficient ligand-protein is captured on the chip surface. Up to now streptavidin binding peptides like the SBP-tag or the *nano*-tag are no better alternative to immobilize fusion proteins on wild type streptavidin functionalized surfaces (Keefe *et al.* 2001; Lamla *et al.* 2004). These peptides reveal nanomolar affinities towards wild type streptavidin, which is too low for a stable long-term ligand presentation during SPR measurements.

The production of BAP-fusion proteins in a high throughput manner requires the efficient removal of free biotin prior to their immobilization. Small-scale ultrafiltration and dialysis are tedious and manual approaches, which are difficult to automate. The advantage of the robot-assisted bead-chromatography of the fusion proteins via the hexahistidine peptide was the efficient removal of free biotin as well as of *E.coli* background protein (see 4.7). The consecutive on-chip immobilization via the biotinylated C-terminal AviTag peptide furthermore guaranteed the on-chip presentation of solely correct in frame protein constructs.

5.2 The mini-BP4 kinetics in their scientific context

The human IGFBP-family is well known to form high affinity complexes with IGF-I /-II (Clemmons 1997). In this study it was shown, that site directed single amino acid replacements could modulate the interaction of mini-BP4 towards IGF-I. Hedging reported SPR measurements with full length IGFBP-3 versus the IGF-I/-II protein-

binding partners. The kinetic data was determined by a two-site interaction model (Heding *et al.* 1996), because the C-terminus of full length IGF-BPs is reported to additionally contribute to the IGF-I/II interaction. This is particularly resembled by a 10- to 200-fold enhanced IGF-affinity of full length IGF-BPs in contrast to their C-terminally truncated IGF-binding domains (Wang *et al.* 1988; Zapf *et al.* 1990; Chernašek *et al.* 1995; Hashimoto *et al.* 1997). In our SPR analyses the Langmuir binding model was applied, because the mini-BP4 binding domain was supposed not to have a second IGF-I binding site (see 4.8).

The SPR measurements revealed an IGF-I affinity of wild type mini-BP4 of $K_D = 32$ nM (see 4.8). Kalus found, that the homologous mini-BP5 revealed a similar IGF-I affinity of $K_D = 37$ nM (Kalus *et al.* 1998). Interestingly, the affinity of the mini-BP5/IGF-I interaction resulted from an extremely fast k_{on} -rate beyond the instruments resolution, but the IGF-I/mini-BP5 complex revealed a surprisingly low stability ($k_{off} = 0.19$ s⁻¹). In contrast, the interaction analysis of IGF-I with wild type mini-BP4 revealed a significantly improved dissociation-rate ($k_{off} = 0.00157$ s⁻¹, see 4.8). The complex stability of miniBP4/IGF-I was 120-fold more stable than the mini-BP5/IGF-I complex. The improved stability of the miniBP4/IGF-I complex is therefore a striking feature to test mini-BP4 in pharmaceutical inhibition assays, where a prolonged inhibition of the IGF-IGFR interaction is of a high demand.

Since only small amounts of recombinant mini-BP4 were obtained from the cell-free synthesis, the SPR analysis was also an excellent method to determine the optimal pre-treatment of the expressed proteins to achieve the highest ligand binding activity. As expected the IGF-binding of mini-BP4 was totally dependent on the oxidation of its cysteins to form disulfide-bonds (see 4.6 and 4.12).

The disulfide-bonding pattern of the analyzed mini-BP4 constructs should not be afflicted by the amino acid substitutions. Nevertheless it cannot be excluded that changes in the tertiary structure, wrong disulfide bonding, the disruption of folding or an increased aggregation tendency occurred due to these amino acid exchanges. This might be the case, why 11 muteins revealed a changed (“complex”) kinetic binding behavior (see 4.8 and 4.12). No binary binding model according to Langmuirs rule could be fitted to these obtained SPR data. Possibly the amino acid replacements resulted in an unspecific and non-stoichiometric IGF-I binding. To circumvent these obstacles a valuable approach was the determination of the constructs principal activity and IGF-I complex stability.

Among the mutants showing an improved IGF-I complex stability, the mutant V49F mini-BP4 revealed the highest IGF-I complex stability, which was 2.8-fold more stable than the wild type (see 4.8; 4.12). In the homologous mini-BP5, Val49 is buried in a hydrophobic pocket, in which it makes a direct hydrophobic contact with the protruding Phe16 of IGF-I (Zeslawski *et al.* 2001) (see 2.6; 4.5). In a similar way, V49F mini-BP4 might fill a hydrophobic cavity by its bulky aromatic side chain. The hydrophobic interface to IGF-I was possibly enlarged, which might explain the observed improvement of the IGF-I complex stability. The more bulky V49F might also have sterically interfered during its IGF-I association, since a 9-fold decreased k_{on} -rate of V49F mini-BP4 was determined.

In general the mutated constructs either deviated from the wild type kinetic behavior in their association- or in their dissociation-rate. In fact, all substitutions reduced the IGF-I binding affinity of the mini-BP4 mutants between 2- to 12-fold.

The 2-fold reduced affinity of K68Q mini-BP4 contributes to the observation that the IGF-affinities of IGFBP-1, -2 and -6 (K68Q; K68L, K68A) were also found to be reduced ones (see 4.8). (Bach *et al.* 1993; Hobba *et al.* 1996; Durham *et al.* 1997; Jansson *et al.* 1997). In mini-BP5 this substitution is supposed to decrease the IGF-I affinity by the abolishment of a proposed electrostatic interaction with Glu6 of IGF-I.

In a mutagenesis study done by Imai (Imai *et al.* 2000), where the full length IGFBP-5 and -3 was mutated at K68N, P69Q, L70Q, L73Q and L74N, this also resulted in a 100- to 1000-fold reduction of the IGF-I binding activity. Here, all 5 residues were replaced at once by neutral amino acids. Since our approach did not exchange all relevant residues at once, obviously such drastically reduced IGF-I affinities were not observed.

6 mini-BP4 mutants were determined as inactive IGF-I binders in SPR analysis (see 4.8). Inactivation after immobilization should be excluded due to the described benefits of the oriented presentation of the constructs via the biotinylated AviTag peptide (see 5.1). It is more likely, that replacements were made, which destroyed crucial structure functions of the protein. For example, L70Y mini-BP4 was inactive, whereas the mutants L70W, L70M, L70I and L70F were active IGF-I binders (see 4.8). The same was shown with the inactive mutant L73Y, whereas the constructs L73W, L73M, L73I, L73F were all active binders. Obviously, the replacement of a leucine at the position 70 and 73 by a tyrosine negatively afflicted the structure-functional properties of mini-BP4.

However, a more detailed explanation of the changed IGF-binding behaviors of the tested mutants would require structural information from future X-ray or NMR-measurements.

5.3 Regulatory peptides destabilize a ribosome display construct

The production of stable complexes, consisting from mRNA, the ribosome and the displayed and cotranslationally folded polypeptide is a prerequisite for a successful performance of the ribosome display technology. There are several reports about efforts either to circumvent the need for these complexes or to further stabilize them (Zhou *et al.* 2002) (Wilson *et al.* 2001) (Sawata *et al.* 2001; Griffiths A. D. *et al.* 2003; Sawata *et al.* 2003). It was our approach to examine the impact of regulatory peptides on the stability of these complexes.

Our results indicated that the SecM peptide sequence in a display spacer is mainly responsible for the expression of C-terminally truncated ribosome display protein constructs (see 4.11). Surprisingly, the “Stalling” display spacer strongly induced the tmRNA mediated protein degradation. Just recently it was reported that the SecM peptide is not only responsible for an arrest of translation, but it also induces the cleavage of the mRNA near the ribosome A-site (Sunohara *et al.* 2004).

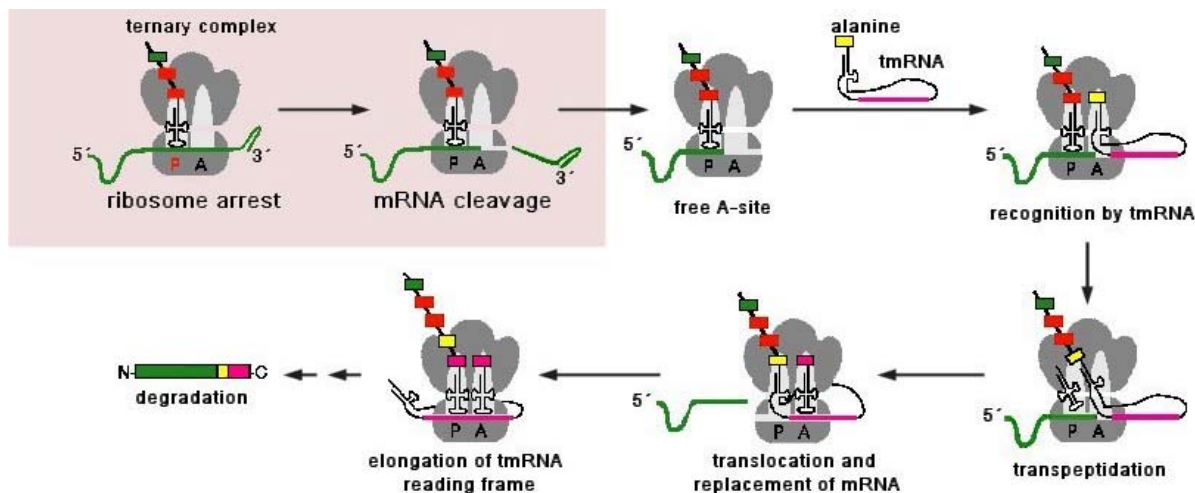


Fig. 47: The models of Sunohara (grey background) and Keiler explain a reduced PCR-product yield after a ribosome display cycle using nascent regulatory peptides in the display spacer.

Due to this mechanism the ribosome A-site becomes free from sense-mRNA and the tmRNA mediated protein degradation mechanism is induced (see fig. 47). Furthermore Sunohara found, that the SecM translation arrest sequence induces ribosome stalling even when the peptide is present in SecM unrelated sequences (see 4.11). These findings are totally conforming to our results. Truncated ribosome

display constructs were obtained. A cleavage of the mRNA downstream of the SecM sequence liberated the ribosome A-site and the nascent polypeptide was again prone to degradation. The stabilizing hairpin structure at the 3'-end of the mRNA possibly was cleaved off. The exonucleolytic mRNA digestion was fostered and the ribosome display yield decreased. Furthermore, the "Stalling" spacer displayed mini-BP4 by a shorter amino acid chain. The length of the display spacer correlates with the ribosome displays PCR-product yields (Hanes *et al.* 1997; Hanes *et al.* 1999). These processes reduced the amount of functional complexes and therefore reduced the ribosome displays PCR-product yield.

All in all, regulatory peptides are rather disadvantageous for ribosome display. Stalling sequences are responsible for a reduction of functional mRNA as well as of functionally displayed polypeptide. The regulatory peptides therefore had the contrary effect of what was to be achieved, namely to stabilize ternary complexes and to increase the PCR-product yield. For the present our findings suggest that a ribosome display spacer should anyway avoid translation-attenuating sequences. It remains to be tested if other regulatory nascent peptides, like from *cmlA*, *catA112/221*, *tnaC* from the tryptophan operon or the *ermC*-system also induce ribosomal mRNA cleavage and subsequent tmRNA recruitment.

Despite the fact that the "Nostalling" construct was a conventional nonstop-codon mRNA sequence, which also should induce tmRNA recruitment, the expression-yield was surprisingly not influenced by tmRNA recruitment (see 4.11). This is in contrast to present data (Hanes *et al.* 1997). The palindromic 3'-end mRNA hairpin protected the construct against exonucleolytic digestion (Yoshizawa *et al.* 1994) and possibly against tmRNA recruitment, too.

5.4 Selection of mini-BP4 mutants featuring IGF-I affinity

The established ribosome display protocol was successfully performed with a mini-BP4 library, which was site directed randomized at three distinct amino acid positions (see 4.12). The mini-BP4 library comprised 8000 mini-BP4 mutants. According to the potential of the ribosome display technology this resembled a small library. Successful ribosome display peptide selection procedures can comprise up to 10^{14} members (Lamla *et al.* 2003) (Wilson *et al.* 2001). Here, the library size correlated with the proteins ability to be displayed as a cotranslationally folded and correctly oxydized polypeptide. Three randomized amino acid positions in mini-BP4 resembled 6 % of the proteins sequence. Experiments with mini-BP4 libraries, which were

randomized at five and nine amino acid positions revealed no results. Obviously the cotranslational folding and a correct disulfide bonding was no more possible using these libraries.

A prescreening by ribosome display was a fairly well alternative to a tedious sequential production and analysis of mini-BP4 mutants (see 4.12). Met74 is unique in IGFBP-4 and was found replaced by Leu74, which is conserved in 50 % of all human IGFBPs (see 4.5). In the homologous mini-BP5, Leu74 is a key determinant for the hydrophobic interaction with IGF-I/II (Kalus *et al.* 1998). Obviously, the position 74 was exerted with the most selective pressure to restore the structure-functional demands to maintain the hydrophobic character of the mini-BP4/IGF-I interaction. These results also reflect a close relationship between mini-BP5 and mini-BP4 and emphasize the importance of this amino acid position for the IGF-I interaction.

Surprisingly, the best binding mutein deviated from the consensus-model revealing the mutation M74P (see 4.12). In the homologous mini-BP5 the position 74 is located in an alpha helix. A proline at this position might have severe consequences on the secondary structure formation in this region of mini-BP4. It would be interesting to elucidate the impact on the secondary structure formation of mini-BP4 in future X-ray or NMR analyses.

From the selection process mini-BP4 mutants were retained, which revealed no consensus formation at the positions R53 and Pro62 (see 4.12). Obviously no selective pressure was exerted onto these amino acids. Although both positions are highly conserved in nearly all human IGFBPs, they seem to be of less importance for the IGF-I binding of the mini-BP4-domain.

As expected, constructs with lacking or additional cysteins were inactive (see 4.12). This again underlines the importance of the cysteins and their correct disulfide bonding in the mini-BP4 topology.

To conclude, the mini-BP4/IGF-I interaction performed a “horizontal evolution” during ribosome display. During the selection cycles, the previous function of the binding-domain was restored by mutated constructs offering an IGF-binding affinity similar to the wild type (see 4.12). Interestingly, a similar IGF-affinity was retained with a mutated mini-BP4 construct, but no wild type construct was recovered from the ribosome display approach. This obviously reflects the altered *in vitro* selection conditions in contrast to the conditions in nature.

Of course it cannot be excluded that other library approaches than the tested ones could have evolved mini-BP4 constructs revealing higher IGF-I affinities. The present

results seem to confirm that the IGF-I/mini-BP4 interaction is of an extraordinary specificity. The protein-protein interaction is “tailored by evolution”. In a physiological context this is reflected by the essential roles of IGFBPs in growth and development, in tissue differentiation as well as in cell survival and cell proliferation (Stewart *et al.* 1996).

5.5 γ crystallin-specific results of ribosome display

Cell-free protein synthesis and its specified application ribosome display is an ideal platform for the selection of proteins to which *de novo* binding functions are assigned. The human γ crystallin was tested for the first time to perform as a site directed randomized protein scaffold in ribosome display. The 13/B11-2 construct was successfully displayed versus the erbB3 receptor ectodomain, whereas the 12/A5-2 derivative did not reproducibly perform in the recognition of the erbB2 ectodomain (see 4.13; 4.13.1). This might correlate with the observation, that the 13/B11-2 derivative was expressed as a soluble protein in *E.coli*, whereas the 12/A5-2 derivative showed significant precipitation (see 4.13.4). The cotranslational folding of 12/A5-2, a prerequisite for a successful ribosome display, was obviously restricted. Nevertheless, in order to perform an affinity maturation with the “first generation” constructs, additional diversity was introduced into the derivatives (see 4.13.2). Obviously erbB3 constructs, which upmost maintained their initial binding site were retained, since no better alternative had been generated in the error-prone pool of the “second generation constructs”. Contrarily, the erbB2 binding construct still provided opportunity for mutations, because the constructs lower initial affinity and maybe even stability obviously permitted alternatives to the initial construct.

There are reports that repeated cycles of ribosome display select constructs, which facilitate the core-binding function of a protein binding domain (Keefe *et al.* 2001; Wilson *et al.* 2001). The obtained results are conform to the proposed sequential and independent folding-kinetics of the γ crystallin domains (Rudolph *et al.* 1990). The N-terminal domain folds significantly faster and offers more stability than the C-terminal domain (Mayr *et al.* 1997). For the bovine γ crystallin it was reported that due to variations in the codon-frequency and possibly due to unfavourable mRNA secondary structures, the translation pauses especially in the inter-domain linker-peptide region and in the C-terminal domain. This provides a delay in the translation allowing the correct folding of the N-terminal domain (Komar *et al.* 1995). It was also reported

(Rudolph *et al.* 1990) that a stable bovine γ crystallin intermediate was isolated, where the N-terminal domain maintains its conformational stability and fold, whereas the C-terminal domain remains unfolded giving rise to a stable “molten globule” intermediate (Kuwajima 1989; Pande *et al.* 1998). In the same study limited proteolysis of the respective intermediate revealed a stable N-terminal domain-fragment ending with Phe88 at the C-terminus. This intermediate and the *in vitro* proteolytically cleaved intermediate are analogous to the γ crystallin constructs, which were enriched by ribosome display after the fifth display cycle (see fig. 38).

Obviously, the ribosomes were attenuated and finally arrested in the linker region and the display was performed with these constructs. An adequate selection on receptor binding could be solely subjected to the N-terminally presented polypeptide chain. Indeed, a significant amount of derivatives contained DNA frame shifts and stop codons after the N-terminal γ crystallin domain (see 4.13.3 and 4.13.6). Furthermore, the inter-domain translation delay suggests that even in frame C-terminal sequences were not properly selected for their stability, fold or binding-specificity. The theory that the C-terminal domain might only have assisted to the N-terminal domain by performing as a display spacer was confirmed by the experiment, in which the ribosome display spacer was simply omitted (see 4.13.6). It could be demonstrated, that the C-terminal domain was able to present the protruded N-terminal domain as a receptor binding active fragment.

Optimizing the codon usage and/or the mRNA secondary structure might eliminate translation-attenuating effects, but it remains to be tested, whether this approach might be disadvantageous for the overall folding kinetic of the scaffold.

5.6 Future display strategies using the γ crystallin scaffold

The present data suggest considering only modifications in the N-terminal γ crystallin domain. Indeed, new amino acid patterns particularly evolved in the N-terminal domain, especially in the erbB2 receptor recognizing constructs (see 4.13.3). Optimally ribosome display selects a pool of sequence-similar binding proteins (Mattheakis *et al.* 1996; Hanes *et al.* 1998; Lamla *et al.* 2003; Lamla *et al.* 2004). The additionally found γ crystallin amino acid replacements at the position D21E, N24H and G60A did not belong to the assigned *de novo* binding site of the 12/A5-2 construct. Unfortunately, no derivatives could be expressed and purified, which contained all three (D21E, N24H, G60A) substitutions. The replacements D21E and

G60A are conservative substitutions, whereas N24H is a non-conservative one (Bordo *et al.* 1991). The positions 21 and 60 are in proximity to the components of the *de novo* binding site 19, 38 and 36 (see fig.48) and might have contributed to the specific requirements of the erbB2 binding of the construct, thus fostering the adaptation to changed structure-function requirements of the *de novo* binding patch. After the fifth ribosome display cycle the N24H mutation was found in 30 % of all erbB-2 binders. This position is in a spatial distance of the *de novo* binding patch and might be used as a further randomizable position in future library construction approaches.

Since in the present approach the C-terminal domain was obviously excluded from the forces of selection, mutations in the C-terminal domain might have led to a destabilization of the full-length protein in subsequent expression and purification approaches. From 14 constructs to be expressed in *E.coli* only five could be expressed and purified (see 4.13.4). This also reflects the drawback of ribosome display to transfer the *in vitro* evolved polypeptides into the scale of *in vitro* and *in vivo* expression conditions. After a prescreening by ribosome display, future selection-approaches might finish with a phage display selection under harsh *in vivo* conditions to obtain *in vivo* applicable constructs.

Using this approach, a γ crystallin library with 8 or more randomized positions could be used more efficiently than in a mere phage display approach, where the library size is limited by the transformation efficacy of the cells.

The automated *in vitro* protein production and purification system could not be established with the γ crystallin derivatives, because the cell-free expression of C-terminally AviTag-fused constructs invariably revealed insoluble protein pellet (see 4.13.4). N-terminal peptide tagging of the constructs seemed to be disadvantageous for the binding activity of the constructs, because the fused peptide tag might have negatively interfered with the assigned *de novo* binding site in the N-terminal domain. In the ELISA experiments a cross-reactivity of the erbB2-binders versus the erbB3 receptor ectodomain was detected (see 4.13.5). A potential γ crystallin-based diagnostic tool, which should be able to differentiate between the erbB2 and erbB3 receptor ectodomains would afford it to re-launch the selection process with a native library. The selection procedure should then be accompanied by reciprocal receptor blocking as it was successfully demonstrated with IgG₁FC protein and BSA. Here only negligible background signals were observed.

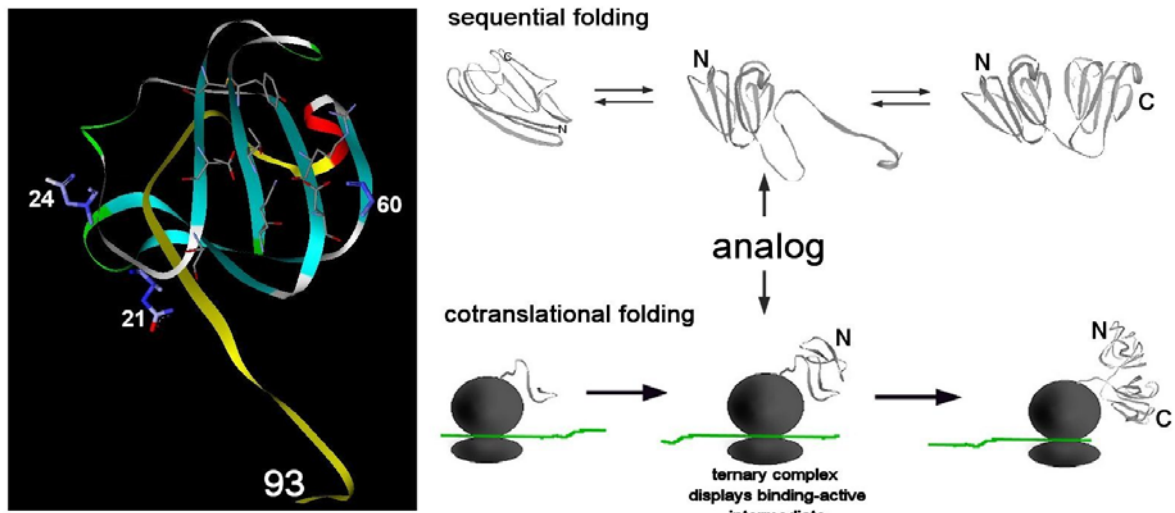


Fig. 48: The independent and sequential folding of γ crystallin has its analogy in the cotranslational folding process. A future approach should use the C-terminal γ crystallin domain as a display spacer. It seems also possible to perform ribosome display with a truncated construct up to the position 93. The yellow marked ribbon would then be used as a display spacer. The positions 21, 24, and 60 might be interesting positions for a further mutagenesis approaches.

Future ribosome display approaches should circumvent the handicaps derived from the two-domain character of the γ crystallin scaffold and ribosome display should specifically target the N-terminal domain. The C-terminal domain should perform as a display spacer (see 4.13.6). Moreover, it should be even possible to truncate the construct up to position 93, as these were the shortest constructs identified in the present approach. This construct would only exhibit the first greek-key motive comprising the primary binding site. Very interestingly the display of a binding active single greek-key motive would resemble the proposed evolutionary ancestor of the γ crystallin scaffold (D'Alessio 2002). The yellow marked sequence (see fig. 48) would then be used as a minimum 26 aa spacer (68 aa – 93 aa). After several display cycles the engineered N-terminal domain would be fused to a wild type C-terminal domain and further screening for stable binders could be performed.

5.7 PEX2 as a general source for affinity reagents?

Since the γ crystallin could not be transferred into the automated cell-free protein production and analysis scale another protein family was investigated to perform as a potential general source of affinity reagents. During the establishment of the *in situ*

cell-free enzymatic biotinylation it was shown that PEX2 could be soluble expressed and biotinylated in a prokaryotic cell-free system (see 4.4). The protein could be successfully presented in its active configuration during the SPR analysis towards its natural binding partner TIMP2. In a recent work we also reported that PEX2 was expressed as soluble and biotinylated protein *in vivo* (Schräml *et al.* 2002). PEX2 derived biotinylated affinity reagents would offer the advantage to immobilize these PEX2 derivatives on diverse SA-coated surfaces, enabling high throughput and microchip assays.

In order to identify potentially randomizable amino acid positions in the structural topology of the PEX2 domain the diversity index calculation from 60 PEX domains was a valuable tool (see 4.14.2). It is also not surprising, that positions revealing a high diversity index are also responsible for the differentiation of the structural features and functions of the PEX-domain members (Bode 1995).

It was shown, that PEX2 is able to fold in a cotranslational manner, which makes this protein to an ideal scaffold to be used in a ribosome display selection procedure (see 4.14.3). The randomized PEX2 scaffold still recognized its natural binding partner TIMP2. Obviously the protein takes in its binding active configuration, despite carrying randomized amino acid positions and it is still possible to select TIMP2 binding active derivatives from the library.

Of course, the presented approach is just one possible combination of different potentially randomizable amino acids in the PEX2 sequence. In this approach, a connected surface was chosen to assign a potential *de novo* binding site into the PEX2 scaffold (see 4.14.2). Depending on the topology and the shape of the molecular target to be recognized other library strategies should be tested in future approaches. The amino acids in the outermost strand of the first N-terminal blade of the PEX2 scaffold reveal a high diversity index, too, and thus seem to be suitable for randomization. Further amino acids to be randomized might be located in the surface exposed strand of the third PEX2-blade. This might be a useful strategy, when it is to recognize molecular targets offering a concave surface topology. The diversity index calculation also revealed gaps in the consensus formation. These gaps indicate that additional amino acids might be inserted into the PEX2 sequence. The PEX2 scaffold might then be used as a carrier for functional peptide motives.

Future approaches might generate a two-domain fusion-protein from two PEX2 binding-domains in order to use the avidity-effect to increase the overall affinity (Deyev *et al.* 2003). Since in MMPs the C-terminal hemopexin-like domains are linked

to the MMP protein via a flexible linker, a non protease-sensitive spacer could be used to genetically fuse two PEX-domains via their exposed N- and C-termini. This must be feasible, since the human plasma protein hemopexin itself is also a dimeric protein (Tolosano *et al.* 2002; Baker *et al.* 2003).

It remains to be tested, whether it is possible to select high-affinity binders from such PEX-libraries. The basic ratio and a first practical conversion could be presented in this study. This might be a basis for future investigations in this field using the hemopexin-like domain family as a scaffold protein to generate multi purpose affinity reagents in an automated cell-free protein production assembly line.

6 Curriculum vitae

Persönliche Daten

Name Michael Albin Schräml
Geboren 08.07.1974
Stand verheiratet
Nationalität Deutsch
Geburtsort München

Ausbildung

1985 - 1995 Gymnasium Fürstenried West, München
Abschluss allgemeine Hochschulreife

1995-1996 Wehrdienst 3. Gebirgsjägerbataillon Bad Reichenhall

1996-2001 Fachhochschule Weihenstephan Studiengang Biotechnologie

2001 Diplomarbeit bei der Roche Diagnostics GmbH, Penzberg
Abteilung pharmazeutische Biochemie
*„Klonierung, in vivo/in vitro Expression und Reinigung von
Fusionsproteinen für den Einsatz in der Affinitätsbiosensorik“*
Diplomarbeitenote: 1.0

7/2001-3/2004 Promotion in der Pharmaforschung der Roche Diagnostics GmbH,
Penzberg Abteilung pharmazeutische Biochemie unter der Anleitung
von Herrn Dr. Martin Lanzendörfer und betreut von Herrn Prof. Dr.
Rainer Rudolph von der Martin-Luther-Universität Halle-Wittenberg.
*“In vitro protein engineering approaches for the development of
biochemical, diagnostic and therapeutic tools”*

Penzberg, den 17.06.2004

7 Publications

Schräml M., Ambrosius D., Lanzendörfer M. (2003). „Rapid Generation of Protein Variants and Subsequent Analysis by Surface Plasmon Resonance”. in Cell-Free Protein Expression. J. R. Swartz. ISBN 3-540-05041-8 Springer Verlag. 1: 223.

Schräml M., Ambrosius D., Lanzendörfer M. (2003). "Automated Generation and Surface Plasmon Resonance Analysis of Protein Constructs." Biochemica 2: 1-4.

Schräml M., Ambrosius D., Lanzendörfer M.. (2003). "Automated Generation and Biacore analysis of protein constructs." Biacore Journal 3: 8-11.

Schräml M., Ambrosius D., Lanzendörfer M. (2003). "Rapid generation of protein variants and subsequent analysis by Surface Plasmon Resonance." RTS Application Manual for Cell-free Protein Expression 1: 99-104.

Schräml M., Ambrosius D., Stracke J., Lanzendörfer M.. (2002). "Sequence Specific Biotinylation and Purification of proteins expressed in the RTS 500 System". Cell-Free Translation Systems. A. S. Spirin. ISBN 3-540-42050-9, Springer Verlag. 1: 235-246.

Uttenthaler E., Schräml M., Mandel J., Drost S. (2001)
„Ultrasensitive quartz crystal microbalance sensors for detection of M13-Phages in liquids." Biosensors and Bioelectronics 16(9-12): 735-43.

patent application

“Method for an *in vitro* sequence specific biotinylation of polypeptides” (2002)
Application No./Patent No. 02021322.9-2404

8 References

- Abo, T., T. Inada, et al. (2000). "SsrA-mediated tagging and proteolysis of LacI and its role in the regulation of lac operon." Embo J **19**(14): 3762-9.
- Alimov, A. P., A. Khmel'nitsky, et al. (2000). "Cell-free synthesis and affinity isolation of proteins on a nanomole scale." Biotechniques **28**(2): 338-44.
- Angenendt, P., L. Nyarsik, et al. (2004). "Cell-free protein expression and functional assay in nanowell chip format." Anal Chem **76**(7): 1844-9.
- Bach, L. A., S. Hsieh, et al. (1993). "Binding of mutants of human insulin-like growth factor II to insulin-like growth factor binding proteins 1-6." J Biol Chem **268**(13): 9246-54.
- Baker, H. M., B. F. Anderson, et al. (2003). "Dealing with iron: common structural principles in proteins that transport iron and heme." Proc Natl Acad Sci U S A **100**(7): 3579-83.
- Barik, S. (1996). "Site-directed mutagenesis in vitro by megaprimer PCR." Methods Mol Biol **57**: 203-15.
- Barik, S. (2002). "Megaprimer PCR." Methods Mol Biol **192**: 189-96.
- Bayer, E. A. and M. Wilchek (1990). "Protein biotinylation." Methods Enzymol **184**: 138-60.
- Beckett, D., E. Kovaleva, et al. (1999). "A minimal peptide substrate in biotin holoenzyme synthetase-catalyzed biotinylation." Protein Sci **8**(4): 921-9.
- Benson, D. A., I. Karsch-Mizrachi, et al. (2004). "GenBank: update." Nucleic Acids Res **32**: 23-26.
- Binz, H. K., M. T. Stumpp, et al. (2003). "Designing repeat proteins: well-expressed, soluble and stable proteins from combinatorial libraries of consensus ankyrin repeat proteins." J Mol Biol **332**(2): 489-503.
- Birnboim, H. C. and J. Doly (1979). "A rapid alkaline extraction procedure for screening recombinant plasmid DNA." Nucleic Acids Res **7**(6): 1513-23.
- Bode, W. (1995). "A helping hand for collagenases: the haemopexin-like domain." Structure **3**(6): 527-30.
- Bordo, D. and P. Argos (1991). "Suggestions for "safe" residue substitutions in site-directed mutagenesis." J Mol Biol **217**(4): 721-9.
- Brodsky, L. I., A. L. Drachev, et al. (1991). "The package of programs for sequence analysis: GeneBee." Biopolymery i Kletka **7**(1): 10-14.
- Brooks, P. C., S. Silletti, et al. (1998). "Disruption of angiogenesis by PEX, a noncatalytic metalloproteinase fragment with integrin binding activity." Cell **92**(3): 391-400.
- Budisa, N., P. P. Pal, et al. (2004). "Probing the role of tryptophans in Aequorea victoria green fluorescent proteins with an expanded genetic code." Biol Chem **385**(2): 191-202.
- Byun, D., S. Mohan, et al. (2001). "Localization of the IGF binding domain and evaluation of the role of cysteine residues in IGF binding in IGF binding protein-4." J Endocrinol **169**(1): 135-43.
- Cadwell, R. C. and G. F. Joyce (1994). "Mutagenic PCR." PCR Methods Appl **3**(6): S136-40.
- Chen, H. Z. and G. Zubay (1983). "Prokaryotic coupled transcription-translation." Methods Enzymol **101**: 674-90.
- Chernausk, S. D., C. E. Smith, et al. (1995). "Proteolytic cleavage of insulin-like growth factor binding protein 4 (IGFBP-4). Localization of cleavage site to non-homologous region of native IGFBP-4." J Biol Chem **270**(19): 11377-82.
- Cho H., Mason K., et al. (2003). "Structure of the extracellular region of HER2 alone and in complex with the Herceptine Fab." Nature **42**(13): 756-759.
- Clemmons, D. R. (1997). "Insulin-like growth factor binding proteins and their role in controlling IGF actions." Cytokine Growth Factor Rev. **8**: 45-62.
- Cohen, S. N., A. C. Chang, et al. (1972). "Nonchromosomal antibiotic resistance in bacteria: genetic transformation of Escherichia coli by R-factor DNA." Proc Natl Acad Sci U S A **69**(8): 2110-4.

- D'Alessio, G. (2002). "The Evolution of monomeric and oligomeric betagamma-type crystallins Facts and hypothesis." Eur J Biochem **269**: 3122-3130.
- D'Aquila, R. T., L. J. Bechtel, et al. (1991). "Maximizing sensitivity and specificity of PCR by pre-amplification heating." Nucleic Acids Res **19**(13): 3749.
- Deyev, S. M., R. Waibel, et al. (2003). "Design of multivalent complexes using the barnase*barstar module." Nat Biotechnol **21**(12): 1486-92.
- Dong-Myung Kim and J. R. Swartz (2000). "Regeneration of Adenosine Triphosphate Glycolytic Intermediates for Cell-Free Protein Synthesis." Biotechnology and Bioengineering **74**(August 20).
- Durham, S. K., S. Mohan, et al. (1997). "Bioactivity of a 29-kilodalton insulin-like growth factor binding protein-3 fragment present in excess in chronic renal failure serum." Pediatr Res **42**(3): 335-41.
- Duszenko, M., X. Kang, et al. (1999). "In vitro translation in a cell-free system from *Trypanosoma brucei* yields glycosylated and glycosylphosphatidylinositol-anchored proteins." Eur J Biochem **266**(3): 789-97.
- Edelhoch, H. (1967). "Spectroscopic determination of tryptophan and tyrosine in proteins." Biochemistry **6**(7): 1948-54.
- Egeblad, M. and Z. Werb (2002). "New functions for the matrix metalloproteinases in cancer progression." Nat Rev Cancer **2**(3): 161-74.
- Elbaz, Y., S. Steiner-Mordoch, et al. (2004). "In vitro synthesis of fully functional EmrE, a multidrug transporter, and study of its oligomeric state." Proc Natl Acad Sci U S A **101**(6): 1519-24.
- Faber, H. R., C. R. Groom, et al. (1995). "1.8 Å crystal structure of the C-terminal domain of rabbit serum haemopexin." Structure **3**(6): 551-9.
- Fall (1979). "Analysis of microbial biotin proteins." Methods Enzymology **62**: 390-398.
- Fiedler, U. and R. Rudolph (2001). Fabrication of beta-pleated sheet proteins with specific binding properties. AU, BR, CA, CN, CZ, HU, IL, JP, KR, NO, PL, RU, SK, US, ZA: 26.
- Forrer, P., H. K. Binz, et al. (2004). "Consensus design of repeat proteins." Chembiochem **5**(2): 183-9.
- Fulop, V. and D. T. Jones (1999). "Beta propellers: structural rigidity and functional diversity." Curr Opin Struct Biol **9**(6): 715-21.
- Garrity, P. A. and B. J. Wold (1992). "Effects of different DNA polymerases in ligation-mediated PCR: enhanced genomic sequencing and in vivo footprinting." Proc Natl Acad Sci U S A **89**(3): 1021-5.
- Gohlke, U., F. X. Gomis-Ruth, et al. (1996). "The C-terminal (haemopexin-like) domain structure of human gelatinase A (MMP2): structural implications for its function." FEBS Lett **378**(2): 126-30.
- Gomis-Ruth, F. X., U. Gohlke, et al. (1996). "The helping hand of collagenase-3 (MMP-13): 2.7 Å crystal structure of its C-terminal haemopexin-like domain." J Mol Biol **264**(3): 556-66.
- Granzow, R. and R. Reed (1992). "Interactions in the fourth dimension." Biotechnology (N Y) **10**(4): 390-3.
- Gravel, P. and O. Golaz (1987). "Protein Blotting by Semidry Methods". The Protein Protocols Handbook. J. M. Walker, Humana Press Inc., Totowa.
- Grentzmann, G., P. J. Kelly, et al. (1998). "Release factor RF-3 GTPase activity acts in disassembly of the ribosome termination complex." Rna **4**(8): 973-83.
- Griffiths A. D. and T. D. S. (2003). "Directed evolution of an extremely fast phosphotriesterase by an in vitro compartmentalization." The EMBO Journal **22**(1): 24-35.
- Gussow, D. and T. Clackson (1989). "Direct clone characterization from plaques and colonies by the polymerase chain reaction." Nucleic Acids Res **17**(10): 4000.

- Hanahan, D. (1983). "Studies on transformation of Escherichia coli with plasmids." J Mol Biol **166**(4): 557-80.
- Hanes, J., L. Jermutus, et al. (1999). "Comparison of Escherichia coli and rabbit reticulocyte ribosome display systems." FEBS Lett **450**(1-2): 105-10.
- Hanes, J., L. Jermutus, et al. (1998). "Ribosome display efficiently selects and evolves high-affinity antibodies in vitro from immune libraries." Proc Natl Acad Sci U S A **95**(24): 14130-5.
- Hanes, J. and A. Pluckthun (1997). "In vitro selection and evolution of functional proteins by using ribosome display." Proc Natl Acad Sci U S A **94**(10): 4937-42.
- Hartl, F. U. and M. Hayer-Hartl (2002). "Molecular chaperones in the cytosol: from nascent chain to folded protein." Science **295**(5561): 1852-8.
- Hartvig, L. and J. Christiansen (1996). "Intrinsic termination of T7 RNA polymerase mediated by either RNA or DNA." Embo J **15**(17): 4767-74.
- Hashimoto, R., M. Ono, et al. (1997). "Binding sites and binding properties of binary and ternary complexes of insulin-like growth factor-II (IGF-II), IGF-binding protein-3, and acid-labile subunit." J Biol Chem **272**(44): 27936-42.
- Hayes, C. S. and R. T. Sauer (2003). "Cleavage of the A site mRNA codon during ribosome pausing provides a mechanism for translational quality control." Mol Cell **12**(4): 903-11.
- He, M. and M. J. Taussig (1997). "Antibody-ribosome-mRNA (ARM) complexes as efficient selection particles for in vitro display and evolution of antibody combining sites." Nucleic Acids Res **25**(24): 5132-4.
- Heding, A., R. Gill, et al. (1996). "Biosensor measurement of the binding of insulin-like growth factors I and II and their analogues to the insulin-like growth factor-binding proteins." J. Biol. Chem. **271**(June 14): 13948-13952.
- Henkel, T. and P. A. Baeuerle (1993). "Functional analysis of mutated cDNA clones by direct use of PCR products in in vitro transcription/translation reactions." Anal Biochem **214**(1): 351-2.
- Ho, S. N., H. D. Hunt, et al. (1989). "Site-directed mutagenesis by overlap extension using the polymerase chain reaction." Gene **77**(1): 51-9.
- Hobba, G. D., B. E. Forbes, et al. (1996). "The insulin-like growth factor (IGF) binding site of bovine insulin-like growth factor binding protein-2 (bIGFBP-2) probed by iodination." J Biol Chem **271**(48): 30529-36.
- Horton, R. M., H. D. Hunt, et al. (1989). "Engineering hybrid genes without the use of restriction enzymes: gene splicing by overlap extension." Gene **77**(1): 61-8.
- Imai, Y., A. Moralez, et al. (2000). "Substitutions for hydrophobic amino acids in the N-terminal domains of IGFBP-3 and -5 markedly reduce IGF-I binding and alter their biologic actions." J Biol Chem **275**(24): 18188-94.
- Jaenicke, R. (1994). "Eye-lens proteins: structure, superstructure, stability, genetics." Naturwissenschaften **81**(10): 423-9.
- Jaenicke, R. (1996). "Stability and folding of ultrastable proteins: eye lens crystallins and enzymes from thermophiles." Faseb J **10**(1): 84-92.
- Jansson, M., M. Uhlen, et al. (1997). "Structural changes in insulin-like growth factor (IGF) I mutant proteins affecting binding kinetic rates to IGF binding protein 1 and IGF-I receptor." Biochemistry **36**(14): 4108-17.
- Jewett, M. C. and J. R. Swartz (2004). "Rapid expression and purification of 100 nmol quantities of active protein using cell-free protein synthesis." Biotechnol Prog **20**(1): 102-9.
- John E. Cronan, J. (1990). "Biotination of proteins in vivo." The Journal of Biotlogical Chemistry **265**, No.18(Issue of June 25): 10327-10333.
- Kain, K. C., P. A. Orlandi, et al. (1991). "Universal promoter for gene expression without cloning: expression-PCR." Biotechniques **10**(3): 366-74.

- Kalus, W., M. Zweckstetter, et al. (1998). "Structure of the IGF-binding domain of the insulin-like growth factor-binding protein-5 (IGFBP-5): implications for IGF and IGF-I receptor interactions." *Embo J* **17**(22): 6558-72.
- Karimi, R., M. Y. Pavlov, et al. (1999). "Novel roles for classical factors at the interface between translation termination and initiation." *Mol Cell* **3**(5): 601-9.
- Karzai, A. W., E. D. Roche, et al. (2000). "The SsrA-SmpB system for protein tagging, directed degradation and ribosome rescue." *Nat Struct Biol* **7**(6): 449-55.
- Karzai, A. W., M. M. Susskind, et al. (1999). "SmpB, a unique RNA-binding protein essential for the peptide-tagging activity of SsrA (tmRNA)." *Embo J* **18**(13): 3793-9.
- Keefe, A. D., D. S. Wilson, et al. (2001). "One-step purification of recombinant proteins using a nanomolar-affinity streptavidin-binding peptide, the SBP-Tag." *Protein Expr Purif* **23**(3): 440-6.
- Keiler, K. C., P. R. Waller, et al. (1996). "Role of a peptide tagging system in degradation of proteins synthesized from damaged messenger RNA." *Science* **271**(5251): 990-3.
- Khandwala, H. M., I. E. McCutcheon, et al. (2000). "The effects of insulin-like growth factors on tumorigenesis and neoplastic growth." *Endocr Rev* **21**(3): 215-44.
- Kigawa, T. and S. Yokoyama (1991). "A continuous cell-free protein synthesis system for coupled transcription-translation." *J Biochem (Tokyo)* **110**(2): 166-8.
- Kim, D. M. and J. R. Swartz (2004). "Efficient production of a bioactive, multiple disulfide-bonded protein using modified extracts of Escherichia coli." *Biotechnol Bioeng* **85**(2): 122-9.
- Klammt, C., F. Lohr, et al. (2004). "High level cell-free expression and specific labeling of integral membrane proteins." *Eur J Biochem* **271**(3): 568-80.
- Komar, A. A. and R. Jaenicke (1995). "Kinetics of translation of gamma B crystallin and its circularly permuted variant in an in vitro cell-free system: possible relations to codon distribution and protein folding." *FEBS Lett* **376**(3): 195-8.
- Kuwajima, K. (1989). "The molten globule state as a clue for understanding the folding and cooperativity of globular-protein structure." *Proteins* **6**(2): 87-103.
- Lamla, T. and V. A. Erdmann (2003). "Searching sequence space for high-affinity binding peptides using ribosome display." *J Mol Biol* **329**(2): 381-8.
- Lamla, T. and V. A. Erdmann (2004). "The Nano-tag, a streptavidin-binding peptide for the purification and detection of recombinant proteins." *Protein Expr Purif* **33**(1): 39-47.
- Landale, E. C., D. D. Strong, et al. (1995). "Sequence comparison and predicted structure for the four exon-encoded regions of human insulin-like growth factor binding protein 4." *Growth Factors* **12**(4): 245-50.
- Letunic, I., L. Goodstadt, et al. (2002). "Recent improvements to the SMART domain-based sequence annotation resource." *Nucleic Acids Res* **30**(1): 242-4.
- Libson, A. M., A. G. Gittis, et al. (1995). "Crystal structure of the haemopexin-like C-terminal domain of gelatinase A." *Nat Struct Biol* **2**(11): 938-42.
- Lovett, P. S. and E. J. Rogers (1996). "Ribosome regulation by the nascent peptide." *Microbiol Rev* **60**(2): 366-85.
- Martemyanov, K. A., A. S. Spirin, et al. (1997). "Direct expression of PCR products in a cell-free transcription/translation system: synthesis of antibacterial peptide cecropin." *FEBS Lett* **414**(2): 268-70.
- Mattheakis, L. C., R. R. Bhatt, et al. (1994). "An in vitro polysome display system for identifying ligands from very large peptide libraries." *Proc Natl Acad Sci U S A* **91**(19): 9022-6.
- Mattheakis, L. C., J. M. Dias, et al. (1996). "Cell-free synthesis of peptide libraries displayed on polysomes." *Methods Enzymol* **267**: 195-207.
- Mayr, E. M., R. Jaenicke, et al. (1997). "The domains in gammaB-crystallin: identical fold-different stabilities." *J Mol Biol* **269**(2): 260-9.

- Miyakoshi, N., C. Richman, et al. (1999). "Effects of recombinant insulin-like growth factor-binding protein-4 on bone formation parameters in mice." Endocrinology **140**(12): 5719-28.
- Mohan, S., D. J. Baylink, et al. (1996). "Insulin-like growth factor (IGF)-binding proteins in serum--do they have additional roles besides modulating the endocrine IGF actions?" J Clin Endocrinol Metab **81**(11): 3817-20.
- Mullis, K. B. and F. A. Faloon (1987). "Specific synthesis of DNA in vitro via a polymerase-catalyzed chain reaction." Methods Enzymol **155**: 335-50.
- Najmudin, S., V. Nalini, et al. (1993). "Structure of the bovine eye lens protein gamma-B(gamma-II)crystallin at 1.47 Angström." Acta Crystallogr D Biol Crystallogr **49**: 223.
- Nakamura, Y. and K. Ito (2003). "Making sense of mimic in translation termination." Trends Biochem Sci **28**(2): 99-105.
- Nakano, H., T. Shinbata, et al. (1999). "Efficient coupled transcription/translation from PCR template by a hollow-fiber membrane bioreactor." Biotechnol Bioeng **64**(2): 194-9.
- Nakatogawa, H. and K. Ito (2002). "The ribosomal exit tunnel functions as a discriminating gate." Cell **108**(5): 629-36.
- Napolitano, E. W., H. O. Villar, et al. (1996). "Glubodies: randomized libraries of glutathione transferase enzymes." Chem Biol **3**(5): 359-67.
- Neumann, G. M. and L. A. Bach (1999). "The N-terminal disulfide linkages of human insulin-like growth factor-binding protein-6 (hIGFBP-6) and hIGFBP-1 are different as determined by mass spectrometry." J Biol Chem **274**(21): 14587-94.
- Nord, K., E. Gunneriusson, et al. (1997). "Binding proteins selected from combinatorial libraries of an alpha-helical bacterial receptor domain." Nat Biotechnol **15**(8): 772-7.
- Pande, V. S. and D. S. Rokhsar (1998). "Is the molten globule a third phase of proteins?" Proc Natl Acad Sci U S A **95**(4): 1490-4.
- Paoli, M., B. F. Anderson, et al. (1999). "Crystal structure of hemopexin reveals a novel high-affinity heme site formed between two beta-propeller domains." Nat Struct Biol **6**(10): 926-31.
- Per-Ake, N. and A. Skerra (2004). "Binding proteins from alternative scaffolds." Journal of Immunological Methods **290**: 3-28.
- Predki, P. F., V. Agrawal, et al. (1996). "Amino-acid substitutions in a surface turn modulate protein stability." Nat Struct Biol **3**(1): 54-8.
- Qin, X., D. D. Strong, et al. (1998). "Structure-function analysis of the human insulin-like growth factor binding protein-4." J Biol Chem **273**(36): 23509-16.
- Reddy, D. V., B. C. Shenoy, et al. (2000). "High resolution solution structure of the 1.3S subunit of transcarboxylase from *Propionibacterium shermanii*." Biochemistry **39**(10): 2509-16.
- Royall, E., K. E. Woolaway, et al. (2004). "The Rhopalosiphum padi virus 5' internal ribosome entry site is functional in *Spodoptera frugiperda* 21 cells and in their cell-free lysates: implications for the baculovirus expression system." J Gen Virol **85**(Pt 6): 1565-9.
- Rudolph, R., R. Siebendritt, et al. (1990). "Folding of an all-beta protein: independent domain folding in gamma II-crystallin from calf eye lens." Proc Natl Acad Sci U S A **87**(12): 4625-9.
- Sambrook, J. and D. W. Russell (2001). MolecularCloning. Cold Spring Harbor, NY, USA, Cold Spring Harbor Laboratory Press.
- Sang Soo Lee and C. Kang (1991). "A DNA Bending at Early Region of Phage T7 Gene 10 Analyzed by Wedge Angels." Korean Biochemistry Journal **24**: 673-679.
- Sanger, F., S. Nicklen, et al. (1977). "DNA sequencing with chain-terminating inhibitors." Proc Natl Acad Sci U S A **74**(12): 5463-7.
- Sawasaki, T., T. Ogasawara, et al. (2002). "A cell-free protein synthesis system for high-throughput proteomics." Proc Natl Acad Sci U S A **99**(23): 14652-7.

- Sawata, S. Y. and K. Taira (2001). "Development of an advanced polysome display system dependent on a specific protein-RNA motif interaction." Nucleic Acids Res Suppl(1): 99-100.
- Sawata, S. Y. and K. Taira (2003). "Modified peptide selection in vitro by introduction of a protein-RNA interaction." Protein Eng **16**(12): 1115-24.
- Schatz, P. J. (1993). "Use of peptide libraries to map the substrate specificity of a peptide-modifying enzyme: a 13 residue consensus peptide specifies biotinylation in *Escherichia coli*." Biotechnology (N Y) **11**(10): 1138-43.
- Schräml, M., D. Ambrosius, et al. (2002). Sequence Specific Biotinylation and Purification of proteins expressed in the RTS 500 System. Cell-Free Translation Systems. A. S. Spirin. ISBN 3-540-42050-9, Springer Verlag. **1**: 235-246.
- Schultz, J., F. Milpetz, et al. (1998). "SMART, a simple modular architecture research tool: identification of signaling domains." Proc Natl Acad Sci U S A **95**(11): 5857-64.
- Shuldiner, A. R., K. Tanner, et al. (1991). "Ligase-free subcloning: a versatile method to subclone polymerase chain reaction (PCR) products in a single day." Anal Biochem **194**(1): 9-15.
- Sitaraman, K., D. Esposito, et al. (2004). "A novel cell-free protein synthesis system." J Biotechnol **110**(3): 257-63.
- Skerra, A. (2000). "Engineered protein scaffolds for molecular recognition." J Mol Recognit **13**(4): 167-87.
- Skerra, A. (2001). "Anticalins': a new class of engineered ligand-binding proteins with antibody-like properties." J Biotechnol **74**(4): 257-75.
- Smith, G. P. and V. A. Petrenko (1997). "Phage Display." Chem Rev **97**(2): 391-410.
- Spirin, A. S., V. I. Baranov, et al. (1988). "A continuous cell-free translation system capable of producing polypeptides in high yield." Science **242**: 1162-1164.
- Stewart, C. E. and P. Rotwein (1996). "Growth, differentiation, and survival: multiple physiological functions for insulin-like growth factors." Physiol Rev **76**(4): 1005-26.
- Stiege, W. and V. A. Erdmann (1995). "The potentials of the in vitro protein biosynthesis system." Journal of Biotechnology **41**: 81-90.
- Sunohara, T., K. Jojima, et al. (2004). "Ribosome stalling during translation elongation induces cleavage of mRNA being translated in *Escherichia coli*." J Biol Chem **279**(15): 15368-75.
- Suzuki, T., T. Iwasaki, et al. (2002). "Sulfolobus tokodaii sp. nov. (f. Sulfolobus sp. strain 7), a new member of the genus Sulfolobus isolated from Beppu Hot Springs, Japan." Extremophiles **6**(1): 39-44.
- Sykes, K. F. and S. A. Johnston (1999). "Linear expression elements: a rapid, in vivo, method to screen for gene functions." Nat Biotechnol **17**(4): 355-9.
- Tabuchi, M., M. Hino, et al. (2002). "Cell-free protein synthesis on a microchip." Proteomics **2**(4): 430-5.
- Thomas, P. S. (1980). "Hybridization of denatured RNA and small DNA fragments transferred to nitrocellulose." Proc Natl Acad Sci U S A **77**(9): 5201-5.
- Tohru Natsume, Masato Taoka, et al. (2002). "Rapid analysis of protein interactions: On-chip micropurification of recombinant protein expressed in *Escherichia Coli*." Proteomics **2**: 1247-1253.
- Tolosano, E. and F. Altruda (2002). "Hemopexin: structure, function, and regulation." DNA Cell Biol **21**(4): 297-306.
- Verhaegen, M. and T. K. Christopoulos (2002). "Bacterial expression of in vivo-biotinylated aequorin for direct application to bioluminometric hybridization assays." Anal Biochem **306**(2): 314-22.
- Vogelstein, B. and D. Gillespie (1979). "Preparative and analytical purification of DNA from agarose." Proc Natl Acad Sci U S A **76**(2): 615-9.

- Wallon, U. M. and C. M. Overall (1997). "The hemopexin-like domain (C domain) of human gelatinase A (matrix metalloproteinase-2) requires Ca²⁺ for fibronectin and heparin binding. Binding properties of recombinant gelatinase A C domain to extracellular matrix and basement membrane components." J Biol Chem **272**(11): 7473-81.
- Wang, J. F., B. Hampton, et al. (1988). "Isolation of a biologically active fragment from the carboxy terminus of the fetal rat binding protein for insulin-like growth factors." Biochem Biophys Res Commun **157**(2): 718-26.
- Warburg, O. and W. Christian (1941). "Isolierung und Kristallisation des Gärungsferments Enolase." Biochemische Zeitung **310**(384 - 421).
- Wetterau, L. A., M. G. Moore, et al. (1999). "Novel aspects of the insulin-like growth factor binding proteins." Mol Genet Metab **68**(2): 161-81.
- Willenbrock, F., T. Crabbe, et al. (1993). "The activity of the tissue inhibitors of metalloproteinases is regulated by C-terminal domain interactions: a kinetic analysis of the inhibition of gelatinase A." Biochemistry **32**(16): 4330-7.
- Wilson, D. S., A. D. Keefe, et al. (2001). "The use of mRNA display to select high-affinity protein-binding peptides." Proc Natl Acad Sci U S A **98**(7): 3750-5.
- Wilson, K. P., L. M. Shewchuk, et al. (1992). "Escherichia coli biotin holoenzyme synthetase/bio repressor crystal structure delineates the biotin- and DNA-binding domains." Proc Natl Acad Sci U S A **89**(19): 9257-61.
- Yoshizawa, S., Y. Ueda, et al. (1994). "Nuclease resistance of an extraordinary thermostabile mini-hairpin DNA-fragment, d(GCGAAGC) and its application to in vitro protein synthesis." Nucleic Acids Res **22**(12): 2217-2221.
- Zapf, J., M. Kiefer, et al. (1990). "Isolation from adult human serum of four insulin-like growth factor (IGF) binding proteins and molecular cloning of one of them that is increased by IGF I administration and in extrapancreatic tumor hypoglycemia." J Biol Chem **265**(25): 14892-8.
- Zeslawski, W., H. G. Beisel, et al. (2001). "The interaction of insulin-like growth factor-I with the N-terminal domain of IGFBP-5." Embo J **20**(14): 3638-44.
- Zhou, J. M., S. Fujita, et al. (2002). "A novel strategy by the action of ricin that connects phenotype and genotype without loss of the diversity of libraries." J Am Chem Soc **124**(4): 538-43.
- Zubay, G. (1973). "In vitro synthesis of protein in microbial systems." Annu. Rev. Genet. **7**: 267-287.

9 Appendix

Mini-BP4 constructs

wild type mini-BP4 DNA-Sequence

5'-

GCGTTAGGCTTAGGTATGCCGTGTGGCGTGTATACCCACGTTGCGGATCGGG
CTTACGCTGCTATCCACCGCGTGGAGTGGAAAAACCGTTACACACCTTAATGCA
CGGCCAGGGTGTCTGTATGGAATTAGCGGAAATTGAAGCG-3'

Combinations of syntheses-oligonucleotides for the template-free PCR generation of the mini-BP4 gene constructs are referred. Each PCR additionally contained the terminal primers F1 5'-GCGTTAGGCTTAGGTATGCCG-3' and R1 5'-CGCTTCAATTTCCGCTAATTCC-3'.

Wild-type-miniBP4

name	Sequence 5'-3'
BP4_wtF1	GCGTTAGGCTTAGGTATGCCGTGTGGCGTGTATACCCC
BP4_wtF2	GCGGATCGGGCTTACGCTGCTATCCACCGCGTGGAGTGGAAAAACCGTTACACACC
BP4_wtR1	CGCTTCAATTTCCGCTAATTCCATACAGACACCCTGGCC
BP4_wtR2	CATACAGACACCCTGGCCGTGCATTAAGGTGTGTAACGGTTTTTCCACTCCACG
BP4_wtR3	GCAGCGTAAGCCCGATCCGCAACGTGGGGTATACACGCCACACGGCATACC

„3xNNK“-miniBP4 library

name	Sequence 5'-3'
BP4_wtF1	GCGTTAGGCTTAGGTATGCCGTGTGGCGTGTATACCCC
NNK-F2	5'-GCGGATCGGGCTTACGCTGCTATNNKCCGCGTGGAGTGGAAAAACCGTTACACACC-3'
NNK-R2	5'-CCATACAGACACCCTGGCCGTGMNNTAAGGTGTGTAACGGTTTTTCCACTCCACG-3'
NNK-R3	5'-GCAGCGTAAGCCCGATCCGCAACGTGGGGTATACACGCCACACGGCATACC-3'
BP4_wtR3	GCAGCGTAAGCCCGATCCGCAACGTGGGGTATACACGCCACACGGCATACC

V49L-miniBP4:

name	Sequence 5'-3'
BP4_V49LF1	GCGTTAGGCTTAGGTATGCCGTGTGGCCTCTATACCCC
BP4_wtF2	GCGGATCGGGCTTACGCTGCTATCCACCGCGTGGAGTGGAAAAACCGTTACACACC
BP4_wtR1	CGCTTCAATTTCCGCTAATTCCATACAGACACCCTGGCC
BP4_wtR2	CATACAGACACCCTGGCCGTGCATTAAGGTGTGTAACGGTTTTTCCACTCCACG
BP4_V49LR3	GCAGCGTAAGCCCGATCCGCAACGTGGGGTATAGAGGCCACACGGCATACC

V49I-miniBP4

name	Sequence 5'-3'
BP4_V49IF1	GCGTTAGGCTTAGGTATGCCGTGTGGCATTATACCCC
BP4_wtF2	GCGGATCGGGCTTACGCTGCTATCCACCGCGTGGAGTGGAAAAACCGTTACACACC
BP4_wtR1	CGCTTCAATTTCCGCTAATTCCATACAGACACCCTGGCC
BP4_wtR2	CATACAGACACCCTGGCCGTGCATTAAGGTGTGTAACGGTTTTTCCACTCCACG
BP4_V49IR3	GCAGCGTAAGCCCGATCCGCAACGTGGGGTATAAATGCCACACGGCATACC

V49M-miniBP4

name	Sequence 5'-3'
BP4_V49MF1	GCGTTAGGCTTAGGTATGCCGTGTGGCATGTATACCCC
BP4_wtF2	GCGGATCGGGCTTACGCTGCTATCCACCGCGTGGAGTGGAAAAACCGTTACACACC
BP4_wtR1	CGCTTCAATTTCCGCTAATTCATACAGACACCCTGGCC
BP4_wtR2	CATACAGACACCCTGGCCGTGCATTAAGGTGTGTAACGGTTTTTCCACTCCACG
BP4_V49MR3	GCAGCGTAAGCCCGATCCGCAACGTGGGGTATACATGCCACACGGCATACC

V49F-miniBP4

name	Sequence 5'-3'
BP4_V49FF1	GCGTTAGGCTTAGGTATGCCGTGTGGCTTCTATACCCC
BP4_wtF2	GCGGATCGGGCTTACGCTGCTATCCACCGCGTGGAGTGGAAAAACCGTTACACACC
BP4_wtR1	CGCTTCAATTTCCGCTAATTCATACAGACACCCTGGCC
BP4_wtR2	CATACAGACACCCTGGCCGTGCATTAAGGTGTGTAACGGTTTTTCCACTCCACG
BP4_V49FR3	GCAGCGTAAGCCCGATCCGCAACGTGGGGTATAGAAGCCACACGGCATACC

V49Y-miniBP4

name	Sequence 5'-3'
BP4_V49YF1	GCGTTAGGCTTAGGTATGCCGTGTGGCTATTATACCCC
BP4_wtF2	GCGGATCGGGCTTACGCTGCTATCCACCGCGTGGAGTGGAAAAACCGTTACACACC
BP4_wtR1	CGCTTCAATTTCCGCTAATTCATACAGACACCCTGGCC
BP4_wtR2	CATACAGACACCCTGGCCGTGCATTAAGGTGTGTAACGGTTTTTCCACTCCACG
BP4_V49YR3	GCAGCGTAAGCCCGATCCGCAACGTGGGGTATAATAGCCACACGGCATACC

V49W-miniBP4

name	Sequence 5'-3'
BP4_V49WF1	GCGTTAGGCTTAGGTATGCCGTGTGGCTGGTATACCCC
BP4_wtF2	GCGGATCGGGCTTACGCTGCTATCCACCGCGTGGAGTGGAAAAACCGTTACACACC
BP4_wtR1	CGCTTCAATTTCCGCTAATTCATACAGACACCCTGGCC
BP4_wtR2	CATACAGACACCCTGGCCGTGCATTAAGGTGTGTAACGGTTTTTCCACTCCACG
BP4_V49WR3	GCAGCGTAAGCCCGATCCGCAACGTGGGGTATACCAGCCACACGGCATACC

Y50R-miniBP4

name	Sequence 5'-3'
BP4_Y50RF1	GCGTTAGGCTTAGGTATGCCGTGTGGCGTTCGCACCCC
BP4_wtF2	GCGGATCGGGCTTACGCTGCTATCCACCGCGTGGAGTGGAAAAACCGTTACACACC
BP4_wtR1	CGCTTCAATTTCCGCTAATTCATACAGACACCCTGGCC
BP4_wtR2	CATACAGACACCCTGGCCGTGCATTAAGGTGTGTAACGGTTTTTCCACTCCACG
BP4_Y50RR3	GCAGCGTAAGCCCGATCCGCAACGTGGGGTGCAGACGCCACACGGCATACC

Y50K-miniBP4

name	Sequence 5'-3'
BP4_Y50KF1	GCGTTAGGCTTAGGTATGCCGTGTGGCGTTAAAACCCC
BP4_wtF2	GCGGATCGGGCTTACGCTGCTATCCACCGCGTGGAGTGGAAAAACCGTTACACACC
BP4_wtR1	CGCTTCAATTTCCGCTAATTCATACAGACACCCTGGCC
BP4_wtR2	CATACAGACACCCTGGCCGTGCATTAAGGTGTGTAACGGTTTTTCCACTCCACG
BP4_Y50KR3	GCAGCGTAAGCCCGATCCGCAACGTGGGGTTTTAACGCCACACGGCATACC

R53W-miniBP4

name	Sequence 5'-3'
BP4_wtF1	GCGTTAGGCTTAGGTATGCCGTGTGGCGTGTATACCCC
BP4_wtF2	GCGGATCGGGCTTACGCTGCTATCCACCGCGTGGAGTGGAAAAACCGTTACACACC
BP4_wtR1	CGCTTCAATTTCCGCTAATTCATACAGACACCCTGGCC
BP4_wtR2	CATACAGACACCCTGGCCGTGCATTAAGGTGTGTAACGGTTTTTCCACTCCACG
BP4_R53WR3	GCAGCGTAAGCCCGATCCGCAACGTGGGGTATACACGCCACACGGCATACC

R53Y-miniBP4

name	Sequence 5'-3'
BP4_wtF1	GCGTTAGGCTTAGGTATGCCGTGTGGCGTGTATACCCC
BP4_wtF2	GCGGATCGGGCTTACGCTGCTATCCACCGCGTGGAGTGGAAAAACCGTTACACACC
BP4_wtR1	CGCTTCAATTTCCGCTAATTCATACAGACACCCTGGCC
BP4_wtR2	CATACAGACACCCTGGCCGTGCATTAAGGTGTGTAACGGTTTTTCCACTCCACG
BP4_R53YR3	GCAGCGTAAGCCCGATCCGCGATATGGGGTATACACGCCACACGGCATACC

R53M-miniBP4

name	Sequence 5'-3'
BP4_wtF1	GCGTTAGGCTTAGGTATGCCGTGTGGCGTGTATACCCC
BP4_wtF2	GCGGATCGGGCTTACGCTGCTATCCACCGCGTGGAGTGGAAAAACCGTTACACACC
BP4_wtR1	CGCTTCAATTTCCGCTAATTCATACAGACACCCTGGCC
BP4_wtR2	CATACAGACACCCTGGCCGTGCATTAAGGTGTGTAACGGTTTTTCCACTCCACG
BP4_R53MR3	GCAGCGTAAGCCCGATCCGCGACATTGGGGTATACACGCCACACGGCATACC

R53F-miniBP4

name	Sequence 5'-3'
BP4_wtF1	GCGTTAGGCTTAGGTATGCCGTGTGGCGTGTATACCCC
BP4_wtF2	GCGGATCGGGCTTACGCTGCTATCCACCGCGTGGAGTGGAAAAACCGTTACACACC
BP4_wtR1	CGCTTCAATTTCCGCTAATTCATACAGACACCCTGGCC
BP4_wtR2	CATACAGACACCCTGGCCGTGCATTAAGGTGTGTAACGGTTTTTCCACTCCACG
BP4_R53FR3	GCAGCGTAAGCCCGATCCGCAAAATGGGGTATACACGCCACACGGCATACC

R53H-miniBP4

name	Sequence 5'-3'
BP4_wtF1	GCGTTAGGCTTAGGTATGCCGTGTGGCGTGTATACCCC
BP4_wtF2	GCGGATCGGGCTTACGCTGCTATCCACCGCGTGGAGTGGAAAAACCGTTACACACC
BP4_wtR1	CGCTTCAATTTCCGCTAATTCATACAGACACCCTGGCC
BP4_wtR2	CATACAGACACCCTGGCCGTGCATTAAGGTGTGTAACGGTTTTTCCACTCCACG
BP4_R53HR3	GCAGCGTAAGCCCGATCCGCAATGTGGGGTATACACGCCACACGGCATACC

Y61W-miniBP4

name	Sequence 5'-3'
BP4_wtF1	GCGTTAGGCTTAGGTATGCCGTGTGGCGTGTATACCCC
BP4_Y61WF2	GCGGATCGGGCTTACGCTGCTGCCCACCGCGTGGAGTGGAAAAACCGTTACACACC
BP4_wtR1	CGCTTCAATTTCCGCTAATTCATACAGACACCCTGGCC
BP4_wtR2	CATACAGACACCCTGGCCGTGCATTAAGGTGTGTAACGGTTTTTCCACTCCACG
BP4_wtR3	GCAGCGTAAGCCCGATCCGCAACGTGGGGTATACACGCCACACGGCATACC

Y61F-miniBP4

name	Sequence 5'-3'
BP4_wtF1	GCGTTAGGCTTAGGTATGCCGTGTGGCGTGTATACCCC
BP4_Y61FF2	GCGGATCGGGCTTACGCTGCTTCCCACCGCGTGGAGTGGAAAAACCGTTACACACC
BP4_wtR1	CGCTTCAATTTCCGCTAATTCATACAGACACCCTGGCC
BP4_wtR2	CATACAGACACCCTGGCCGTGCATTAAGGTGTGTAACGGTTTTTCCACTCCACG
BP4_wtR3	GCAGCGTAAGCCCGATCCGCAACGTGGGGTATACACGCCACACGGCATACC

K68Q-miniBP4

name	Sequence 5'-3'
BP4_wtF1	GCGTTAGGCTTAGGTATGCCGTGTGGCGTGTATACCCC
BP4_K68QF2	GCGGATCGGGCTTACGCTGCTATCCACCGCGTGGAGTGGAAACAACCGTTACACACC
BP4_wtR1	CGCTTCAATTTCCGCTAATTCATACAGACACCCTGGCC
BP4_K68QR2	CATACAGACACCCTGGCCGTGCATTAAGGTGTGTAACGGTTTCCACTCCACG
BP4_wtR3	GCAGCGTAAGCCCGATCCGCAACGTGGGGTATACACGCCACACGGCATACC

L70Y-miniBP4

name	Sequence 5'-3'
BP4_wtF1	GCGTTAGGCTTAGGTATGCCGTGTGGCGTGTATACCCC
BP4_L70YF2	GCGGATCGGGCTTACGCTGCTATCCACCGCGTGGAGTGGAAAAACCGTATCACACC
BP4_wtR1	CGCTTCAATTTCCGCTAATTCATACAGACACCCTGGCC
BP4_L70YR2	CATACAGACACCCTGGCCGTGCATTAAGGTGTGATACGGTTTTTCCACTCCACG
BP4_wtR3	GCAGCGTAAGCCCGATCCGCAACGTGGGGTATACACGCCACACGGCATACC

L70W-miniBP4

name	Sequence 5'-3'
BP4_wtF1	GCGTTAGGCTTAGGTATGCCGTGTGGCGTGTATACCCC
BP4_L70WF2	GCGGATCGGGCTTACGCTGCTATCCACCGCGTGGAGTGGAAAAACCGTGGCACACC
BP4_wtR1	CGCTTCAATTTCCGCTAATTCATACAGACACCCTGGCC
BP4_L70WR2	CATACAGACACCCTGGCCGTGCATTAAGGTGTGCCACGGTTTTTCCACTCCACG
BP4_wtR3	GCAGCGTAAGCCCGATCCGCAACGTGGGGTATACACGCCACACGGCATACC

L70M-miniBP4

name	Sequence 5'-3'
BP4_wtF1	GCGTTAGGCTTAGGTATGCCGTGTGGCGTGTATACCCC
BP4_L70MF2	GCGGATCGGGCTTACGCTGCTATCCACCGCGTGGAGTGGAAAAACCGATGCACACC
BP4_wtR1	CGCTTCAATTTCCGCTAATTCATACAGACACCCTGGCC
BP4_L70MR2	CATACAGACACCCTGGCCGTGCATTAAGGTGTGCATCGTTTTTCCACTCCACG
BP4_wtR3	GCAGCGTAAGCCCGATCCGCAACGTGGGGTATACACGCCACACGGCATACC

L70I-miniBP4

name	Sequence 5'-3'
BP4_wtF1	GCGTTAGGCTTAGGTATGCCGTGTGGCGTGTATACCCC
BP4_L70IF2	GCGGATCGGGCTTACGCTGCTATCCACCGCGTGGAGTGGAAAAACCGATTACACC
BP4_wtR1	CGCTTCAATTTCCGCTAATTCATACAGACACCCTGGCC
BP4_L70IR2	CATACAGACACCCTGGCCGTGCATTAAGGTGTGAATCGTTTTTCCACTCCACG
BP4_wtR3	GCAGCGTAAGCCCGATCCGCAACGTGGGGTATACACGCCACACGGCATACC

L70F-miniBP4

name	Sequence 5'-3'
BP4_wtF1	GCGTTAGGCTTAGGTATGCCGTGTGGCGTGTATACCCC
BP4_L70FF2	GCGGATCGGGCTTACGCTGCTATCCACCGCGTGGAGTGGAAAAACCGTTTACACC
BP4_wtR1	CGCTTCAATTTCCGCTAATTCATACAGACACCCTGGCC
BP4_L70FR2	CATACAGACACCCTGGCCGTGCATTAAGGTGTGAAACGGTTTTTCCACTCCACG
BP4_wtR3	GCAGCGTAAGCCCGATCCGCAACGTGGGGTATACACGCCACACGGCATACC

L73I-miniBP4

name	Sequence 5'-3'
BP4_wtF1	GCGTTAGGCTTAGGTATGCCGTGTGGCGTGTATACCCC
BP4_wtF2	GCGGATCGGGCTTACGCTGCTATCCACCGCGTGGAGTGGAAAAACCGTTACACC
BP4_wtR1	CGCTTCAATTTCCGCTAATTCATACAGACACCCTGGCC
BP4_L73IR2	CATACAGACACCCTGGCCGTGCATGATGGTGTGTAACGGTTTTTCCACTCCACG
BP4_wtR3	GCAGCGTAAGCCCGATCCGCAACGTGGGGTATACACGCCACACGGCATACC

L73W-miniBP4

name	Sequence 5'-3'
BP4_wtF1	GCGTTAGGCTTAGGTATGCCGTGTGGCGTGTATACCCC
BP4_wtF2	GCGGATCGGGCTTACGCTGCTATCCACCGCGTGGAGTGGAAAAACCGTTACACC
BP4_wtR1	CGCTTCAATTTCCGCTAATTCATACAGACACCCTGGCC
BP4_L73WR2	CATACAGACACCCTGGCCGTGCATCCAGGTGTGTAACGGTTTTTCCACTCCACG
BP4_wtR3	GCAGCGTAAGCCCGATCCGCAACGTGGGGTATACACGCCACACGGCATACC

L73M-miniBP4

name	Sequence 5'-3'
BP4_wtF1	GCGTTAGGCTTAGGTATGCCGTGTGGCGTGTATACCCC
BP4_wtF2	GCGGATCGGGCTTACGCTGCTATCCACCGCGTGGAGTGGAAAAACCGTTACACACC
BP4_wtR1	CGCTTCAATTTCCGCTAATTCATACAGACACCCTGGCC
BP4_L73MR2	CATACAGACACCCTGGCCGTGCATCATGGTGTGTAACGGTTTTTCCACTCCACG
BP4_wtR3	GCAGCGTAAGCCCGATCCGCAACGTGGGGTATACACGCCACACGGCATACC

L73F-miniBP4

name	Sequence 5'-3'
BP4_wtF1	GCGTTAGGCTTAGGTATGCCGTGTGGCGTGTATACCCC
BP4_wtF2	GCGGATCGGGCTTACGCTGCTATCCACCGCGTGGAGTGGAAAAACCGTTACACACC
BP4_wtR1	CGCTTCAATTTCCGCTAATTCATACAGACACCCTGGCC
BP4_L73FR2	CATACAGACACCCTGGCCGTGATAAAGGTGTGTAACGGTTTTTCCACTCCACG
BP4_wtR3	GCAGCGTAAGCCCGATCCGCAACGTGGGGTATACACGCCACACGGCATACC

M74Y-miniBP4

name	Sequence 5'-3'
BP4_wtF1	GCGTTAGGCTTAGGTATGCCGTGTGGCGTGTATACCCC
BP4_wtF2	GCGGATCGGGCTTACGCTGCTATCCACCGCGTGGAGTGGAAAAACCGTTACACACC
BP4_wtR1	CGCTTCAATTTCCGCTAATTCATACAGACACCCTGGCC
BP4_M74YR2	CATACAGACACCCTGGCCGTGATATAAGGTGTGTAACGGTTTTTCCACTCCACG
BP4_wtR3	GCAGCGTAAGCCCGATCCGCAACGTGGGGTATACACGCCACACGGCATACC

M74W-miniBP4

name	Sequence 5'-3'
BP4_wtF1	GCGTTAGGCTTAGGTATGCCGTGTGGCGTGTATACCCC
BP4_wtF2	GCGGATCGGGCTTACGCTGCTATCCACCGCGTGGAGTGGAAAAACCGTTACACACC
BP4_wtR1	CGCTTCAATTTCCGCTAATTCATACAGACACCCTGGCC
BP4_M74WR2	CATACAGACACCCTGGCCGTGCCATAAAGGTGTGTAACGGTTTTTCCACTCCACG
BP4_wtR3	GCAGCGTAAGCCCGATCCGCAACGTGGGGTATACACGCCACACGGCATACC

M74I-miniBP4

name	Sequence 5'-3'
BP4_wtF1	GCGTTAGGCTTAGGTATGCCGTGTGGCGTGTATACCCC
BP4_wtF2	GCGGATCGGGCTTACGCTGCTATCCACCGCGTGGAGTGGAAAAACCGTTACACACC
BP4_wtR1	CGCTTCAATTTCCGCTAATTCATACAGACACCCTGGCC
BP4_M74IR2	CATACAGACACCCTGGCCGTGAATTAAGGTGTGTAACGGTTTTTCCACTCCACG
BP4_wtR3	GCAGCGTAAGCCCGATCCGCAACGTGGGGTATACACGCCACACGGCATACC

M74F-miniBP4

name	Sequence 5'-3'
BP4_wtF1	GCGTTAGGCTTAGGTATGCCGTGTGGCGTGTATACCCC
BP4_wtF2	GCGGATCGGGCTTACGCTGCTATCCACCGCGTGGAGTGGAAAAACCGTTACACACC
BP4_wtR1	CGCTTCAATTTCCGCTAATTCATACAGACACCCTGGCC
BP4_M74FR2	CATACAGACACCCTGGCCGTGAAATAAGGTGTGTAACGGTTTTTCCACTCCACG
BP4_wtR3	GCAGCGTAAGCCCGATCCGCAACGTGGGGTATACACGCCACACGGCATACC

H75D-miniBP4

name	Sequence 5'-3'
BP4_wtF1	GCGTTAGGCTTAGGTATGCCGTGTGGCGTGTATACCCC
BP4_wtF2	GCGGATCGGGCTTACGCTGCTATCCACCGCGTGGAGTGGAAAAACCGTTACACACC
BP4_wtR1	CGCTTCAATTTCCGCTAATTCATACAGACACCCTGGCC
BP4_H75DR2	CATACAGACACCCTGGCCGTCCATTAAGGTGTGTAACGGTTTTTCCACTCCACG
BP4_wtR3	GCAGCGTAAGCCCGATCCGCAACGTGGGGTATACACGCCACACGGCATACC

DNA-Modules

Sequences marked in red, were used as primers for the production of the modules. The underlined red sequences were used as terminal primers in the second OEL-PCR for the amplification of the full length LEEs.

T7Pg10ε

5'-

GGTGATGTCGGCGATATAGGCGCCAGCAACCGCACCTGTGGCGCCGGTGATGCCGGCCACGATGCGTCCG
GCGTAGAGGATCGAGATCTCGATCCCGCGAAATTAATACGACTCACTATAGGGAGACCACAACGGTTTTCCCT
CTAGAAATAATTTTGTTTAACTTTAAGAAGGAGATATACATATG-3'

name	sequence
T7Pfor.	5'-GGTGATGTCGGCGATATAGGCGCCAGC-3'
T7Pprev.	5'-CATATGTATATCTCCTTCTTAAAGTTAAACAAAATTATTTC-3

T7PAviTagFXa

5'-

GGTGATGTCGGCGATATAGGCGCCAGCAACCGCACCTGTGGCGCCGGTGATGCCGGCCACGAT
GCGTCCGGCGTAGAGGATCGAGATCTCGATCCCGCGAAATTAATACGACTCACTATAGGGAGACC
ACAACGGTTTTCCCTCTAGAAATAATTTTGTTTAACTTTAAGAAGGAGATATACATATGGGTCTTAAT
GATATTTTTGAAGCTCAGAAAATCGAATGGCACGAAATCGAGGGTCGT-3'

name	sequence
T7Pfor.	5'-GGTGATGTCGGCGATATAGGCGCCAGC-3'
T7PAvXrev.	5'-ACGACCCTCGATTCGTGCCATTTCG-3'

T7P(his)6FXa

5'-

GGTGATGTCGGCGATATAGGCGCCAGCAACCGCACCTGTGGCGCCGGTGATGCCGGCCACGAT
GCGTCCGGCGTAGAGGATCGAGATCTCGATCCCGCGAAATTAATACGACTCACTATAGGGAGACC
ACAACGGTTTTCCCTCTAGAAATAATTTTGTTTAACTTTAAGAAGGAGATATACCATGTCTGGTTCTC
ATCATCATCATCATCATAGCAGCGGCATCGAAGTTCGT-3'

name	sequence
T7Pfor.	5'-GGTGATGTCGGCGATATAGGCGCCAGC-3'
T7Ph6Xrev.	5'-ACGACCTTCGATGCCGCTGCTATGATGAT -3'

T7T

5'-

TAGGAAGCTCAGAAAATCGAATGGCACGAATAATGAGCTCCCGGGAGCGCTTGG
AGCCACCCGCAGTTCGAAAAATAATAAGGGCCTCCCACTGACTGCTCTTCTGTCA
GTGGGCTACTCCTGGACTCGGCACCAGATTGCCTCATTTTTCTCCTCTGGCATTITG
TATAAATCCACCTTGACTGGGGAAATTCTCCTGGGGTCAGGTGGCACCAGCCTGG
ATCCGGCTGCTAACAAAGCCCGAAAGGAAGCTGAGTTGGCTGCTGCCACCGCTGA
GCAATAACTAGCATAACCCCTTGGGGCCTCTAAACGGGTCTTGAGGGGTTTTTGC
-3'

name	sequence
T7Tfor.	TAGGAAGCTCAGAAAATCGAATGGC
T7Trev.	GCAAAAACCCCTCAAGACCCGTTTAGAGG

FXaAviTagT7T

5'-

ATCGAGGGTCGTGGTCTGAACGACATCTTCGAAGCTCAGAAAATCGAATGGCACG
AATAATGAGCTCCCGGGAGCGCTTGGAGCCACCCGCAGTTCGAAAAATAATAAGG
GCCTCCACTGACTGCTCTTCTGTCAGTGGGCTACTCCTGGACTCGGCACCAGATT
GCCTCATTTTTCTCCTCTGGCATTGTGTATAAATCCACCTTGACTGGGGAAATTCTC
CTGGGGTCAGGTGGCACCAGCCTGGATCCGGCTGCTAACAAAGCCCGAAAGGAA
GCTGAGTTGGCTGCTGCCACCGCTGAGCAATAACTAGCATAACCCCTTGGGG**CCT**
CTAAACGGGTCTTGAGGGGTTTTTTCG-3'

name	sequence
XAvT7Tfor.	5'-ATCGAGGGTCGTGGTCTGAACGACATCTTCG-3'
XAvT7Trev.	5'-GCAAAAACCCCTCAAGACCCGTTTAGAGGCCCAAGGGTTATGCTAG-3'

FXa(his)6T7T

5'-

ATCGAAGGTCGTGGGGGGGGTTCTCATCATCATCATCATTAATAAAAGGGCG
AATTCCAGCACACTGGCGGCCGTTACTAGTGGATCCGGCTGCTAACAAAGCCCGA
AAGGAAGCTGAGTTGGCTGCTGCCACCGCTGAGCAATAACTAGCATAACCCCTTG
GGCCTCTAAA**CGGGTCTTGAGGGGTTTTTTCG**-3'

name	sequence
Xh6T7Tfor.	5'-ATCGAAGGTCGTGGGGGGGG-3'
Xh6T7Trev.	5'-GCAAAAACCCCTCAAGACCCG-3'

Ribosome Display spacer „Stalling“

5'-

GCTGGCTCTGGAGCTGGTGCAGGCTCTGGTGGTGGCGCAGGTTCTGGCGCTGGTG
CTGGTTCTGGCACTGGTGCTTCTCCGGCAGCTGTTCCGGCAGCGGTTCCAGCAGCG
GTGCCGGCAGCAGTTCCTGCTGCGGTGGGCGAAGGAGAAGGAGAAGGCGAGGGA
GAGGGCGAAGGATCAACAAGCAAGAACGCCGACAAGAAGAGCGAGTTCAGTACG
CCAGTTTGGATCTCGCAGGCACAGGGCATCCGTGCTGGTCCTCAGAGGCTTACAG
ACTACAAGGACGACGACGACAAATCCCAAATCAAACGAAAGGCCAGTCGAAAA
ACTGGGCCTTTCGATTT-3'

Ribosome Display Spacer „No Stalling“

5'-

GCTGGCTCTGGAGCTGGTGCAGGCTCTGGTGCTGGCGCAGGTTCTGGCGCTGGTG
CTGGTTCTGGCACTGGTGTCTTCTCCGGCAGCTGTTCCGGCAGCGGTTCCAGCAGCG
GTGCCGGCAGCAGTTCCTGCTGCGGTGGGCGAAGGAGAAGGAGAAGGCGAGGGA
GAGGGCGAAGGATACCCGTACGACGTACCGGACTACGCCGAAGGTGGTGGTGGC
TCCGAGCAGAAGCTCATCTCCGAAGAAGACCTGGAGGGTGGTGGTGGCTCCACAG
ACTACAAGGACGACGACGACAAATCCCAAATCAAACGAAAGGCCAGTCGAAAA
ACTGGGCCTTTCGATTT-3'

name	sequence
F1A	5'-GCTGGCTCTGGAGCTGGTGC-3'
R1A	5'-AAATCGAAAGGCCAGTTTTTCG-3'
F1	5'-GGCGCAGGTTCTGGCGCTGGTGTCTGGTCTGGCACTGGTGTCTTCTCCGGC-3'
F2	5'-CGGTTCCAGCAGCGGTGCCGGCAGCAGTTCCTGCTGCGGTGGGCGAAGG-3'
F3	5'-GCGAGGGAGAGGGCGAAGGATCAACAAGCAAGAACGCCGACAAGAAGAGC-3',
F4	5'-CAGTACGCCAGTTTGGATCTCGCAGGCACAGGGCATCCGTGCTGGTCCTCAGAGG-3',
stem	5'AAATCGAAAGGCCAGTTTTTCGACTGGGCCTTTCGTTTGATTTGGGATTTGTCGTCGTCGTCCTTGTA G3'
R1	5'-GGATTTGTCGTCGTCGTCCTTGTAGTCTGTAAGCCTCTGAGGACCAGCACGGATG-3'
R2	5'-GCGAGATCCAACTGGCGTACTGAACTCGCTCTTCTTGTCCGGCCTTCTTG-3'
R3	5'-CCTTCGCCCTCTCCCTCGCCTTCTCCTTCTCCTTCGCCACCAGCAGC-3'
R4	5'-GGCACCCTGCTGGAACCGTCCCGAAGCAGCTGCCGGAGAAGCACCAGTGCC-3'
R5	5'-GCGCCAGAACCTGCGCCAGCACCAGAGCCTGCACCAGCTCCAGAGCCAGC-3'
R1'	5'-GGATTTGTCGTCGTCGTCCTTGTAGTCTGTGGAGCCACCACCACCTCCAGG-3'
R2'	5'-GGAGATGAGCTTCTGCTCGGAGCCACCACCACCTTCGGCGTAGTCCGGTACG-3'
F3'	5'-GCGAGGGAGAGGGCGAAGGATACCCGTACGACGTACCGGACTACGCCGAAGG-3'
F4'	5'-GGCTCCGAGCAGAAGCTCATCTCCGAAGAAGACCTGGAGGGTGGTGGTGGC-3'
<i>EcoRI-forw</i>	5'-CCGGAATTCGCTGGCTCTGGAGCTGGTGC-3'
<i>XhoI-rev</i>	5'-CCGCTCGAGAAATCGAAAGGCCAGTTTTTCG-3'

DNA-sequence of the of the site-directed randomized PEX2 gene-library

5'-

ATGCCTGAAATCTGCAAACAGGATATCGTATTTGATGGCATCGCTCAGATCCGTG
GTGAGATCTTCTTCTTCAAGACCGGTTCAATTTGGCGGACTGTGACGCCACGTGAC
AAGCCCATGGGGCCCCTGCTGGTGGCCACATTCTGGCCTGAGCTCCCGGAAAAGA
TTGATGCGGTATACGAGGCCCCANNKNNKGAGAAAGCTGTGTTCTTTGCAGGGAA
TGAATACTGGATCTACTCAGCGAGCACCTTGGAGNNKGGTTATCCCAAACCACTG
ACTAGCCTCGGACTGCCCCCTGATGTTCAACGTGTGGATGCAGCCTTTAACTGGAG
CNNKNNKNNKAAGACATACATCTTCGCTGGCGACAAGTTCTGGAGGTACAACGA
GNNKAAGNNKAAAATGGACCCTGGCTTCCCAAGCTCATCGCAGATGCCTGGAA
TGCCATCCCCGATAACCTGGATGCCGTCGTGGACCTGCAGGGCGGGCGGTACAGC
TACTTCTTCAAGGGTGCCTATTACCTGAAGCTGGAGAACCAAAGTCTGAAGAGCG
TGAAGTTTGAAGCATCAAATCCGACTGGCTAGGCTGC-3'

name	Sequence
PEX2forw.	5'-ATGCCTGAAATCTGCAAA CAGG-3'
PEXR4	5'-CCTGCAAAGAACACAGCTTTCTCMNNMNNNTGGGGCCTCGTATACCGCATCAATC-3'
PEXF4	5'-GGACCCTGGCTTCCCCAAGCTCATCGCAGATGCCTGGAATGC-3'
PEX2rev.	5'-GGAGCTCGCTCGAGTCAGC-3'
PEXR1	5'-GAGCTTGGGGAAGCCAGGGTCCATTTMNNCTTMNNCTCGTTGTACCTCCAGAACTTGTC-3'
PEXR2	5'-GCCAGCGAAGATGTATGTCTTMNNMNNMNGCTCCAGTTAAAGGCTGCATCC-3'
PEXR3	5'-GGCAGTCCGAGGCTAGTCAGTGGTTTGGGATAACCMNNCTCCAAGGTGCTCGCTGAG-3'
PEXF1	5'-GAGAAAGCTGTGTTCTTTGCAGGGAATGAATACTGGATCTACTCAGCGAGCACCTTGGAG-3'
PEXF2	5'-CTGACTAGCCTCGGACTGCCCCCTGATGTTCAACGTGTGGATGCAGCCTTTAACTGGAGC-3'
PEXF3	5'-AAGACATACATCTTCGCTGGCGACAAGTTCTGGAGGTACAACGAG-3'
T7P_PEX2	5'-GTTTAACTTTAAGAAGGAGATATACATATGCCTGAAATCTGCAAACAGGATATCG-3'
PEX2_RD	5'-CCTGCACCAGCTCCAGAGCCAGCGCAGCCTAGCCAGTCGGATTGATGC-3'
T7Pforw.	5'-GGTGATGTCGGCGATATAGGCG-3'
R1A	5'-AAATCGAAAGGCCAGTTTTTCG-3'

Amino Acid Sequence of the site directed randomized PEX2-library

NH₂-

PEICKQDIVFDGIAQIRGEIFFFKDRFIWRTVTPRDKPMGPLLVATFWPELPEKIDAVYEAPXXEKAVFFA
GNEYWIYSASTLEXGYPKPLTSLGLPPDVQRVDAAFNWSXXXKTYIFAGDKFWRYNEXKXKMDPGFP
KLIADAWNAIPDNLDAVVDLQGGGHSYFFKGAYYKLENQSLKSVKFGSIKSDWLGC-COOH

DNA sequence of the γ crystallin construct 12/A5-2

5'-

ATGGGTTTTATCTTTTTCTGTGAAGACCGTGCTTTCCAGGGTCGTGTGTACAAGTGCCGACCGA
CTGCCGAACCTGCAGCCGTACTTCTCCCGTTGCAACTCCATCTTTGTTGAGTCCGTTGCTGGA
TGATCTACGAACGTCCGAACCTACCAGGGTCACCAGTACTTCTGCGGCGTGGGGAGTACCCCGA
CTACCAGCAATGGATGGGCCTCAGCGACTCCATCCGCTCCTGCTGCCTCATCCCCCCCCACTCTG
GCGTTACAGAATGAAGATCTACGACAGAGATGAATTGAGGGGACAAATGTCAGAGCTCACAGAC
GACTGTCTCTGTTCAGGACCGCTTCCACCTCACTGAAATTCCTCAATGTGCTGGAGGG
CAGCTGGATCCTCTATGAGATGCCCAACTACAGGGGGAGGCAGTATCTGCTGAGGCCGGGGGAG
TACAGGAGGTTTCTTGATTGGGGGGCTCCAAATGCCAAAGTTGGCTCTCTTAGACGAGTCATGGA
TTTGTAC-3'

Amino Acid sequence γ crystallin 12/A5-2

MGFIFFCEDRAFQGRVYKCATDCPNLQPYFSRCNSIEVESGCWMIYERPNYQGHQYFLRRGEYPDYQ
QWMGLSDSIRSCCLIPPHSGAYRMKIYDRDELRGQMSELTDDCLSVQDRFHLTEIHSNLVLEGSWILY
EMPNYRGRQYLLRPGEYRRFLDWGAPNAKVGSLRRVMDLY

DNA sequence of the γ crystallin construct 13/B11-2

5'-

ATGGGTGATATCTAGTTCCTGGAAGACCGTGCTTTCCAGGGTCGTGGGTACGCGT
GCACTACCGACTGCCCGAACCTGCAGCCGTACTTCTCCCGTTGCAACTCCATCTGT
GTTCTGTTCCGGTTGCTGGATGATCTACGAACGTCCGAACCTACCAGGGTCACCAGT
ACTTCTGCGGCGTGGGGAGTACCCCGACTACCAGCAATGGATGGGCCTCAGCGA
CTCCATCCGCTCCTGCTGCCTCATCCCCCCCCACTCTGGCGCTTACAGAATGAAGA
TCTACGACAGAGATGAATTGAGGGGACAAATGTCAGAGCTCACAGACGACTGTCT
CTCTGTTACAGGACCGCTTCCACCTCACTGAAATTCCTCAATGTGCTGGAGG
GCAGCTGGATCCTCTATGAGATGCCCAACTACAGGGGGAGGCAGTATCTGCTGAG
GCCGGGGGAGTACAGGAGGTTTCTTGATTGGGGGGCTCCAAATGCCAAAGTTGGC
TCTCTTAGACGAGTCATGGATTGTAC-3'

Amino Acid sequence γ crystallin 13/B11-2

MGDIQFREDRAFQGRGYACTTDCPNLQPYFSRCNSICVRS GCWMIYERP NYQGHQYF
LRRGEYPDYQQWMGLSDSIRSCCLIPPHSGAYRMKIYDRDELRGQMSELTDDCLSVQ
DRFHLTEIHSLNVLEGSWILYEMP NYRGRQYLLRPGEYRRFLDWGAPNAKV GSLRRV
MDLY